UNIVERSIDADE FEDERAL DE GOIÁS
INSTITUTO DE MATEMÁTICA E ESTATÍSTICA
PROGRAMA DE PÓS-GRADUAÇÃO EM MATEMÁTICA

YOVANI ADOLFO VILLANUEVA HERRERA

Global Dynamics of Inelastic and Center-Type Piecewise Smooth Vector Fields in $\mathbb{R}^2$ and $\mathbb{R}^3$

Goiânia
2022

UNIVERSIDADE FEDERAL DE GOIÁS
INSTITUTO DE MATEMÁTICA E ESTATÍSTICA

TERMO DE CIÊNCIA E DE AUTORIZAÇÃO (TECA) PARA DISPONIBILIZAR VERSÕES ELETRÔNICAS DE TESES

E DISSERTAÇÕES NA BIBLIOTECA DIGITAL DA UFG

Na qualidade de titular dos direitos de autor, autorizo a Universidade Federal de Goiás (UFG) a disponibilizar, gratuitamente, por meio da Biblioteca Digital de Teses e Dissertações (BDTD/UFG), regulamentada pela Resolução CEPEC nº 832/2007, sem ressarcimento dos direitos autorais, de acordo com a Lei 9.610/98, o documento conforme permissões assinaladas abaixo, para fins de leitura, impressão e/ou download, a título de divulgação da produção científica brasileira, a partir desta data.

O conteúdo das Teses e Dissertações disponibilizado na BDTD/UFG é de responsabilidade exclusiva do autor. Ao encaminhar o produto final, o autor(a) e o(a) orientador(a) firmam o compromisso de que o trabalho não contém nenhuma violação de quaisquer direitos autorais ou outro direito de terceiros.

1. Identificação do material bibliográfico

[ ] Dissertação [X] Tese [ ] Outro*:_____

*No caso de mestrado/doutorado profissional, indique o formato do Trabalho de Conclusão de Curso, permitido no documento de área, correspondente ao programa de pós-graduação, orientado pela legislação vigente da CAPES.

Exemplos: Estudo de caso ou Revisão sistemática ou outros formatos.

2. Nome completo do autor

Yovani Adolfo Villanueva Herrera

3. Título do trabalho

Global Dynamics of Inelastic and Center-Type Piecewise Smooth Vector Fields in R^2 e R^3

4. Informações de acesso ao documento (este campo deve ser preenchido pelo orientador)

Concorda com a liberação total do documento [X] SIM [ ] NÃO[1]

[1] Neste caso o documento será embargado por até um ano a partir da data de defesa. Após esse período, a possível disponibilização ocorrerá apenas mediante:
a) consulta ao(à) autor(a) e ao(à) orientador(a);
b) novo Termo de Ciência e de Autorização (TECA) assinado e inserido no arquivo da tese ou dissertação.
O documento não será disponibilizado durante o período de embargo.
Casos de embargo:
- Solicitação de registro de patente;
- Submissão de artigo em revista científica;
- Publicação como capítulo de livro;
- Publicação da dissertação/tese em livro.

Obs. Este termo deverá ser assinado no SEI pelo orientador e pelo autor.

Documento assinado eletronicamente por **Rodrigo Donizete Euzébio**, **Professor do Magistério Superior**, em 13/12/2022, às 09:09, conforme horário oficial de Brasília, com fundamento no § 3º do art. 4º do Decreto nº 10.543, de 13 de novembro de 2020.

Documento assinado eletronicamente por **Yovani Adolfo Villanueva Herrera**, **Discente**, em 15/12/2022, às 10:06, conforme horário oficial de Brasília, com fundamento no § 3º do art. 4º do Decreto nº 10.543, de 13 de novembro de 2020.

A autenticidade deste documento pode ser conferida no site https://sei.ufg.br/sei/controlador_externo.php?acao=documento_conferir&id_orgao_acesso_externo=0, informando o código verificador **3395711** e o código CRC **BC81010B**.

YOVANI ADOLFO VILLANUEVA HERRERA

Global Dynamics of Inelastic and Center-Type Piecewise Smooth Vector Fields in $\mathbb{R}^2$ and $\mathbb{R}^3$

Tese apresentada ao Programa de Pós–Graduação do Instituto de Matemática e Estatística da Universidade Federal de Goiás, como requisito parcial para obtenção do título de Doutor em Matemática.

Área de concentração: Sistemas Dinâmicos.

Orientador: Prof. Rodrigo Donizete Euzébio

Goiânia
2022

Ficha de identificação da obra elaborada pelo autor, através do
Programa de Geração Automática do Sistema de Bibliotecas da UFG.

Villanueva Herrera, Yovani Adolfo
Global Dynamics of Inelastic and Center-Type Piecewise Smooth Vector Fields in R2 and R3 [manuscrito] / Yovani Adolfo Villanueva Herrera. - 2022.
CLXIII, 163 f.: il.

Orientador: Prof. Dr. Rodrigo Donizete Euzébio.
Tese (Doutorado) - Universidade Federal de Goiás, Instituto de Matemática e Estatística (IME), Programa de Pós-Graduação em Matemática, Goiânia, 2022.
Bibliografia. Apêndice.
Inclui siglas, símbolos, gráfico, tabelas, algoritmos, lista de figuras, lista de tabelas.

1. Compactificação. 2. Ciclo Limite. 3. Singularidade. 4. Estabilidade Assintótica. 5. Campo vetorial de Filippov. I. Donizete Euzébio, Rodrigo, orient. II. Título.

CDU 517.938

UNIVERSIDADE FEDERAL DE GOIÁS

INSTITUTO DE MATEMÁTICA E ESTATÍSTICA

ATA DE DEFESA DE TESE

Ata nº **08** da sessão de Defesa de Tese de **Yovani Adolfo Villanueva Herrera,** que confere o título de Doutor em Matemática, **na área de concentração de Sistemas Dinâmicos.**

Ao nono dia do mês de dezembro do ano de dois mil e vinte e dois, a partir das nove horas, via Web videoconferência, realizou-se a sessão pública de Defesa de Tese intitulada **"Global Dynamics of Inelastic and Center-Type Piecewise Smooth Vector Fields in R^2 e R^3."** Os trabalhos foram instalados pelo Orientador e Presidente da banca, Professor Doutor **Rodrigo Donizete Euzébio - IME/UFG** com a participação dos demais membros da Banca Examinadora: Professor Doutor **Durval José Tonon - IME/UFG** - membro titular interno, Professor Doutor **Ewerton Rocha Vieira - UFG / Rutgers University (USA)** - membro titular externo, Professor Doutor **Luis Fernando de Osório Mello - IMC/UNIFEI** membro titular externo e o **Professor Doutor José Régis Azevedo Varão Filho - IMECC/UNICAMP**, membro titular externo. Durante a arguição os membros da banca **não fizeram** sugestão de alteração do título do trabalho. A Banca Examinadora reuniu-se em sessão secreta a fim de concluir o julgamento da Tese, tendo sido o candidato **APROVADO** pelos seus membros. Proclamados os resultados pelo Professor Doutor **Rodrigo Donizete Euzébio - IME/UFG**, Presidente da Banca Examinadora, foram encerrados os trabalhos e, para constar, lavrou-se a presente ata que é assinada pelos Membros da Banca Examinadora, ao nono dia do mês de dezembro do ano de dois mil e vinte e dois.

TÍTULO SUGERIDO PELA BANCA

Global Dynamics of Inelastic and Center-Type Piecewise Smooth Vector Fields in R^2 e R^3

Documento assinado eletronicamente por **Durval José Tonon**, **Professor do Magistério Superior**, em 09/12/2022, às 12:33, conforme horário oficial de Brasília, com fundamento no § 3º do art. 4º do Decreto nº 10.543, de 13 de novembro de 2020.

Documento assinado eletronicamente por **Luis Fernando de osório Mello**, **Usuário Externo**, em 09/12/2022, às 12:33, conforme horário oficial de Brasília, com fundamento no § 3º do art. 4º do Decreto nº 10.543, de 13 de novembro de 2020.

Documento assinado eletronicamente por **Ewerton Rocha Vieira**, **Professor do Magistério Superior**, em 09/12/2022, às 19:52, conforme horário oficial de Brasília, com fundamento no § 3º do art. 4º do Decreto nº 10.543, de 13 de novembro de 2020.

Documento assinado eletronicamente por **Rodrigo Donizete Euzébio**, **Professor do Magistério Superior**, em 13/12/2022, às 08:24, conforme horário oficial de Brasília, com fundamento no § 3º do art. 4º do Decreto nº 10.543, de 13 de novembro de 2020.

Documento assinado eletronicamente por **José Régis Azevedo Varão Filho**, **Usuário Externo**, em 13/12/2022, às 10:48, conforme horário oficial de Brasília, com fundamento no § 3º do art. 4º do Decreto nº 10.543, de 13 de novembro de 2020.

A autenticidade deste documento pode ser conferida no site https://sei.ufg.br/sei/controlador_externo.php?acao=documento_conferir&id_orgao_acesso_externo=0, informando o código verificador **3342755** e o código CRC **E8D8C602**.

Referência: Processo nº 23070.063095/2022-68 SEI nº 3342755

Dedicado a Dios, a mi mamá, a mi papá, a mi hermana, profesores y amigos.

Acknowledgments

- First to God for all the blessings and opportunities.
- To my mother Gladys Herrera Barbosa, who is now in heaven, and my father Jesus Emilio Villanueva Campos for the strength.
- To my sister Diana Marcela Villanueva Herrera and my nephews for their love and support.
- To my advisor Prof. Rodrigo Donizete Euzébio for his guidance and patience throughout this work.
- To Prof. Oscar Eduardo Martinez for all the help.
- To friends and colleagues who were part of these moments.
- To CAPES for the financial support received during the completion of the PhD, by PDSE-CAPES grant 88881. 624523/2021-01 and DS-CAPES 88882.386238/2019-01.

Mathematics is a part of physics. Physics is an experimental science, a part of natural science. Mathematics is the part of physics where experiments are cheap.

V. I. Arnold,
Paris on 7^{th}, March 1997.

Resumo

Villanueva Herrera, Yovani Adolfo. **Global Dynamics of Inelastic and Center-Type Piecewise Smooth Vector Fields in $\mathbb{R}^2$ and $\mathbb{R}^3$**. Goiânia, 2022. 163p. Tese de Doutorado . Programa de Pós-Graduação em Matemática, Instituto de Matemática e Estatística, Universidade Federal de Goiás.

Quase todas as análises qualitativas das EDOs são válidas apenas localmente. Neste trabalho realizamos primeiramente um estudo global, via compactificação, de campos vetoriais inelásticos não suaves em $\mathbb{R}^2$ dando as classes de estabilidade desses sistemas, classificando todas as regiões canônicas, com todas as curvas quadráticas como regiões de descontinuidade. Posteriormente aumentamos uma dimensão e analisamos esses campos vetoriais inelásticos agora em $\mathbb{R}^3$, separados pela esfera unitária, cobrindo uma descrição completa do campo vetorial na variedade de descontinuidade e o comportamento assintótico e de estabilidade dos campos vetoriais externos e internos, por meio de teoremas de classificação relacionados aos tipos de tangência e outras regiões canônicas. Por último mostramos o estudo sobre ciclos limite em campos vetoriais genéricos do tipo centro também em dimensão 3, dando o número máximo de ciclos, nos casos contínuos e descontínuos, com um e dois planos paralelos como regiões de descontinuidade. Obtemos resultados sobre conjuntos limite, estabilidade assintótica, comportamento no infinito e bifurcações.

Palavras–chave

Teoria de Contato, Compactificação, Ciclo Limite, Singularidade, Estabilidade Assintótica, Campo vetorial de Filippov

Abstract

Villanueva Herrera, Yovani Adolfo. **Global Dynamics of Inelastic and Center-Type Piecewise Vector Fields in $\mathbb{R}^2$ and $\mathbb{R}^3$**. Goiânia, 2022. 163p. PhD. Dissertation . Programa de Pós-Graduação em Matemática, Instituto de Matemática e Estatística, Universidade Federal de Goiás.

Almost all qualitative analysis of the ODEs are valid only locally. Because of that, in this work we first present a global study, via compactification, of non-smooth inelastic vector fields in $\mathbb{R}^2$ giving the stability classes of these systems, classifying all canonical regions, with all quadratic curves as discontinuity regions. Posteriorly, we increase one dimension and analyze these inelastic vector fields in $\mathbb{R}^3$, separated by the unit sphere, covering a complete description of the vector field in the discontinuity manifold and the asymptotic and stability behavior of the external and internal vector fields, through classification theorems related to the type of the tangency points and other canonical regions. Finally, we present a study on limit cycles in generic vector fields of center-type, also in dimension 3, giving the maximum number of cycles, in the continuous and discontinuous cases, with one and two parallel planes as discontinuity regions. We obtained results on limit sets, asymptotic stability, behavior at infinity and bifurcations.

Keywords

Contact Theory, Compactification, Limit cycle, Singularity, Asymptotic Stability, Filippov Vector Field.

Contents

List of Figures

List of Tables

List of Algorithms

CHAPTER 1

Introduction

The study of Piecewise Smooth Vector Fields (PSVF) has experienced a consistent advance in the past three decades mainly due to [26]. PSVF can be described by smooth vector fields defined over specific regions of the ambient space. On the boundary between the regions, called switching region, a new vector field may be defined using Filippov convention in [26].

Many articles on this topic develop a local or semi-local approach, see for instance [9, 58]. An interesting phenomenon that occurs frequently is the sliding motion, when the trajectories on both sides of the switching manifold slides over the manifold after the collision, and there remains until reaching the boundary of the sliding region. This phenomenon has been studied, for instance, on relay control systems and systems with dry friction. But, it is interesting to investigate the behavior of the trajectories both close and far away from the switching manifold.

Classifying global behavior is a fundamental goal in dynamical systems. The study of global aspects of certain phenomena and its behavior at the infinity is certainly an important aspect in the study of limit sets, global bifurcations and the existence of invariant sets non-detected by local theory. In particular, classification of global phase portraits in smooth dynamical systems is a prominent area of research even for planar polynomial differential systems, see [9, 43, 44, 72]. On the opposite direction, global phase portraits of non-smooth systems are barely found in the literature, even with its the advances in the last 30 years mainly due to [26] and recently [22]. PSVF can be described by classical systems of ODEs over specific regions of an ambient space, the boundary

between them being a discontinuity region where vector fields may be discontinuous.

Non-smooth systems are widely encountered in sciences as engineering, physics and biology, see for instance [14] and [38]. However, it is often assumed that discontinuity occurs over relatively simply regions without assuming any sliding motion on it. Nevertheless, the hypothesis that trajectories can slide over some region in a discontinuous fashion may bring several new phenomena along with an increasing number of phase portrait, local or global.

Inelastic non-smooth vector fields appear in problems involving some kind of suitable collisions, see for instance [7] and [73]. Our study is carried out for some generic class of non-smmoth systems inside the class of inelastic ones. By generic we mean some phenomena occurring for a residual set within the set of parameters of the considered inelastic non-smooth vector fields.

In Chapter 2, we review some fundamental results of Classical Ordinary Differential Equations and Piecewise Smooth Vector Fields.

In Chapters 3 and 4, we consider the behavior at the infinity of a specific kind of non-smooth vector fields in the plane with different curves as switching manifold, starting with straight lines. We study the relations between canonical regions and vector fields that we can find over the switching regions. The results for global and structural stability considering the tangency points, vector field over the swithching manifold, equilibrium and pseudo-equilibrium points at the finite part, equilibrium and pseudo-equilibrium points at the infinite are stated with details and considering the whole set of cases.

In the Chapter 4, we extend the last classification for conics and algebraic curves, getting other results and proving the existence of non-common limit sets, for instance a strange attractor that comes from an isolated periodic orbit.

In the Chapter 5, which had the collaboration of Prof. Ricardo Martins from the Estadual University of Campinas, we address the inelastic non-smooth vector fields in $\mathbb{R}^3$. Inelastic vector fields are widely used in mechanical models with collisions, see in [7, 73] for making predictions in non-perfectly inelastic impacts, where the contact has a delay after

collisions. We studied the relations between tangency points and vector fields that we can find over the sphere as switching region and in the exterior and interior regions. We present and prove the results for global stability considering every possible case.

Finally, the goal for the Chapter 6, which was made with Prof. Jaume Llibre from the Universitat Autònoma de Barcelona, is to study the continuous and discontinuous PSVF in $\mathbb{R}^3$, formed by linear vector fields similar to planar centers separated by one or two parallel planes. We call those "center-type" differential systems, which have two pure imaginary numbers and zero as eigenvalues. When these systems are separated by one plane, then these have no limit cycles. Also, if they are continuous separated by two planes, then generically there is no limit cycles. But when PSVF is separated by two parallel planes, we show that generically they can have at most four limit cycles, and that there exist such systems with four limit cycles [74]. The genericity here means that the statements hold in a residual set of the space of parameters associated to the differential system.

We recall that the same problem, but for PSVF in $\mathbb{R}^2$ formed by linear differential centers separated by two parallel straight lines, has at most one limit cycle [54]. In Appendix B, we show the algorithm that we used for finding the limit cycles in the continuous case.

CHAPTER 2

Preliminary

The following facts are very useful along this PhD dissertation.

2.1 Classical Differential Equations

In this section we state some important facts of the classical theory of ODE's, which can be found for instance in [68].

Let $M \subseteq \mathbb{R}^n$ be a manifold, a collection of tangent vectors $X(\mathbf{x}) \in T_{\mathbf{x}}M$, $\mathbf{x} = (x_1, \ldots, x_n) \in M$ defines a vector field of class C^k, $1 \leq k \leq \infty$, if and only if the function $\mathbf{x} \mapsto X(\mathbf{x})(f)$ is of class C^k for all $f \in C^\infty(M)$. To the set of vector fields over a manifold M of class C^k we will denote by $\mathfrak{X}^k(M)$. A point $\mathbf{x} = (x_1, \ldots, x_n) \in M$ is singular if $X(\mathbf{x}) = 0$, otherwise it is regular. To the vector field we associate the differential equation

$$\dot{\mathbf{x}} = X(\mathbf{x}).$$

The solutions of this equation is described by the classical theorem of existence and uniqueness and a detailed theory of its qualitative behavior.

The solutions of this equation are maps $\varphi : (a, b) \to M$ such that

$$\frac{d\varphi}{dt}(t) = X(\varphi(t)),$$

for all $t \in (a,b)$. They are also called trajectories or integral curves of X (or of the differential equation). If we consider an initial value problem, $\mathbf{x}(0) = \mathbf{x}_0$, we will get a maximal interval of existence of the solution $(a,b)_{x_0}$ and we define the flow of the differential equation as $\varphi_t(\mathbf{x}_0) = \varphi(t,\mathbf{x}_0)$. With this we can say the following:

Definition 2.1.1 *The set $\gamma_{\boldsymbol{x}} = \{\varphi(t,\boldsymbol{x}) | t \in (a,b)_{\boldsymbol{x}}\}$ is the orbit of X crossing the point $\boldsymbol{x}$.*

The set M equipped with the splitting in orbits of X is a phase portrait. We present a notion of equivalence between vector fields:

Definition 2.1.2 *Let X_1, X_2 be vector fields defined over $M_1, M_2 \subset \mathbb{R}^n$, respectively. They are topologically equivalent if there is a homeomorphism $h : M_1 \to M_2$ that carries orbits from X_1 onto orbits of X_2.*

With this we can give the definition of a structurally stable vector field, a very important concept that we will consider in the following two chapters.

Definition 2.1.3 *Let X be a vector field over a compact manifold M. X is structurally stable over M if there exists $\varepsilon > 0$ such that for all $Y \in C^1(M)$ with*

$$||X - Y||_1 < \varepsilon,$$

Y is topologically equivalent to X. If X does not satisfy the above, then it is structurally unstable.

If the vector field X depends on one parameter μ, and for $\mu = \mu_0$ the vector field is structurally unstable, then μ_0 is called bifurcation value. The following system is shown in [62, pag. 319] which can be solved as an equation of Bernoulli type.

Example 2.1.1 *Let*

$$X_\mu = \begin{cases} \dot{x} = -y + x[(x^2+y^2-1)^2 - \mu], \\ \dot{y} = x + y[(x^2+y^2-1)^2 - \mu]. \end{cases}$$

This system is equivalent to the following in polar coordinates:

$$X_\mu = \begin{cases} \dot{r} = r[(r^2-1)^2 - \mu], \\ \dot{\theta} = 1. \end{cases} \tag{2-1}$$

We will see that the system of equations (2-1) with $\mu = 0$ and $\mu \neq 0$ are not topologically equivalent (its phase portraits appear in Figures 2.1.1 e 2.1.2 respectively).

Let φ_t and ψ_t be their flows, respectively. Suppose there exists a homeomorphism $H : \mathbb{R}^2 \to \mathbb{R}^2$ and a continuous and strictly increasing real function $t(\tau)$ such that $\varphi_{t(\tau)} = H^{-1} \circ \psi_\tau \circ H$. We get:

$$\left|\lim_{t\to\infty} \varphi_t(\boldsymbol{x})\right| = \left|\lim_{t\to\infty} \left[1 + \left(\frac{1}{x_0^2} - 1\right) e^{-2t}\right]^{-1/2}\right| = 1, \; if \; \mu = 0, \; |\boldsymbol{x}| < 1.$$

$$\left|\lim_{t\to\infty} \psi_t(\boldsymbol{x})\right| = \infty, \; if \; \mu < 0, \; \forall \boldsymbol{x} \in \mathbb{R}^2.$$

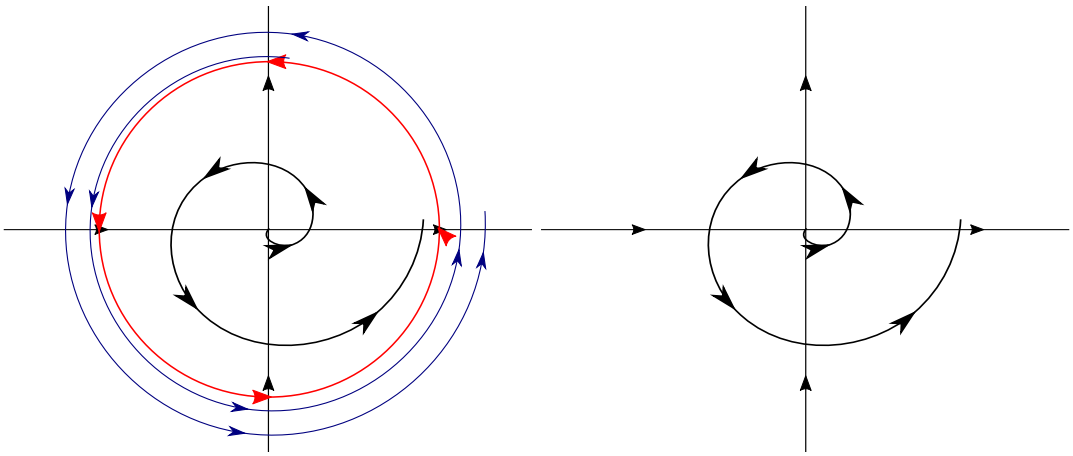

(.1) *Phase portrait of the system (2-1) with $\mu = 0$.* **(.2)** *Phase portrait of the system (2-1) with $\mu < 0$.*

Figure 2.1: *Example of a bifurcation value.*

But using the fact H^{-1} is increasing or decreasing then

$$\left|\lim_{t\to\infty} \varphi_t(\boldsymbol{x})\right| = \left|H^{-1} \lim_{\tau\to\infty} \psi_\tau(H(\boldsymbol{x}))\right| = \lim_{t\to\infty} |H^{-1}(t)| = \infty,$$

and this is a contradiction. So, system (2-1) with $\mu = 0$ is structurally unstable and it is a bifurcation value of the differential system.

We also define the sets α-limit and ω-limit of an orbit of a vector field $X : M \subset \mathbb{R}^n \to \mathbb{R}^n$ of class C^k, with M open, according to [68]. Let $\varphi(t) = \varphi(t, \mathbf{x})$ an integral curve of X passing through the point $\mathbf{x}$ defined in the maximal interval $I_{\mathbf{x}} = (\omega_-(\mathbf{x}), \omega_+(\mathbf{x}))$. If $\omega_+(\mathbf{x}) = \infty$ let:

$$\omega_{\mathbf{x}} = \{q \in M | \exists (t_n) \; with \; t_n \to \infty \; and \; \varphi(t_n) \to q, \; when \; n \to \infty\}. \tag{2-2}$$

If $\omega_-(\mathbf{x}) = -\infty$ let:

$$\alpha_{\mathbf{x}} = \{q \in M | \exists (t_n) \; with \; t_n \to -\infty \; and \; \varphi(t_n) \to q, \; when \; n \to \infty\}. \tag{2-3}$$

Now we present the Lyapunov criteria [68, pag. 272]:

Definition 2.1.4 *Let $\boldsymbol{x}_0 \in \mathbb{R}^n$ an equilibrium (singular) point of the system $\dot{\boldsymbol{x}} = X(\boldsymbol{x})$. A Lyapunov function for $\boldsymbol{x}_0$ is a differentiable function $f : M \subset \mathbb{R}^n \to \mathbb{R}$, defined in an open set U containing $\boldsymbol{x}_0$, such that:*

- *$f(\boldsymbol{x}_0) = 0$ and $f(\boldsymbol{x}) > 0$ for all $\boldsymbol{x} \neq \boldsymbol{x}_0$.*
- *$\dot{f}(\boldsymbol{x}) \leq 0$ in M, where $\dot{f}(\boldsymbol{x}) = \frac{d}{dt} f(\varphi_t(\boldsymbol{x}))|_{t=0}$ and $\varphi_t(\boldsymbol{x})$ is a solution of the system and also $\varphi_0(\boldsymbol{x}) = \boldsymbol{x}$.*

The Lyapunov function is strict if:

- *$\dot{f}(\boldsymbol{x}) < 0$ in $M \setminus \{\boldsymbol{x}_0\}$.*

Theorem 2.1.1 *Let $\boldsymbol{x}_0$ be a singular point of the differential system. If there exists a Lyapunov function for $\boldsymbol{x}_0$, then $\boldsymbol{x}_0$ is stable. If the function is also strict, then $\boldsymbol{x}_0$ is asymptotically stable.*

The important theorem for normal forms, is presented in [71, pag. 52].

Theorem 2.1.2 (Central Manifold) *Let $X = \sum_{i=1}^{n} f_i \frac{\partial}{\partial x_i}$ a vector field C^∞ in $\mathbb{R}^n$ with $X(0) = 0$. We assume that the Jacobian of X has c pure imaginary eigenvalues and let*

$l \in \mathbb{N}$. So there exists a C^l-manifold with dimension c, W^c, containing the origin and a neighborhood U of $0 \in \mathbb{R}^n$ such that for all $\boldsymbol{x} \in W^c \cap U$, $X(\boldsymbol{x})$ is tangent to W^c in $\boldsymbol{x}$. In addition, there exists $r \in \mathbb{N}$, $0 \leq r \leq n-c$, such that X is topologically equivalent to the vector field:

$$Y = \sum_{i=1}^{c} \bar{X}_i(y_1, \ldots, y_c) \frac{\partial}{\partial y_i} + \sum_{i=c+1}^{c+r} y_i \frac{\partial}{\partial y_i} - \sum_{i=c+r+1}^{n} y_i \frac{\partial}{\partial y_i}$$

where $(y_1, \ldots, y_c)$ are coordinates on the central manifold W^c and all the eigenvalues of $D_0\bar{X}$ are pure imaginary.

We present the Hartman-Grobman theorem which is an important tool to know the behavior of a nonlinear differential system near a singularity [62, pag. 120].

Theorem 2.1.3 (Hartman-Grobman Theorem) *Let $E \subset \mathbb{R}^n$ be a set containing the origin, a vector field X over E of class C^1 and φ_t the flow of the nonlinear system $\dot{\boldsymbol{x}} = X(\boldsymbol{x})$. Suppose that $X(0) = 0$ and the matrix $A = DX(0)$ has no eigenvalues with zero real part. So there exists a homeomorphism $H : U \to V$, where U and V are open sets containing the origin, such that for all $\boldsymbol{x}_0 \in U$ there exists an open interval $I_0 \subset \mathbb{R}$ containing the origin such that for all $\boldsymbol{x} \in U$ and $t \in I_0$, therefore*

$$H \circ \varphi_t(\boldsymbol{x}) = e^{At} H(\boldsymbol{x}).$$

Thus H takes nonlinear system orbits near the origin into linear vector field orbits near the origin, preserving time.

Another important and generalized theorem is the tubular flow theorem. [68, pag. 222].

Theorem 2.1.4 (Tubular Flow Theorem) *Let $\boldsymbol{x}$ be a non-singular point of the vector field $X : U \subset \mathbb{R}^n \to \mathbb{R}^n$ of class C^r and the homeomorphism $f : A \subset \mathbb{R}^{n-1} \to \Sigma \subset \mathbb{R}^n$ where A and U are open sets, f is transversal to $X(f(a))$ in a for all $a \in A$ (Σ is a transversal section) and $f(0) = \boldsymbol{x}$. Then there exists a neighborhood V of $\boldsymbol{x}$ in U and a diffeomorphism $h : V \to (-\varepsilon, \varepsilon) \times B$ of class C^r, where $\varepsilon > 0$ and B an open ball in $\mathbb{R}^{n-1}$ of center at the origin $0 = f^{-1}(\boldsymbol{x})$ such that:*

1. $h(\Sigma \cap V) = \{0\} \times B$,
2. *h is a topological equivalence between the vector field $X|_V$ and the constant one $Y : (-\varepsilon, \varepsilon) \times B \to \mathbb{R}^n$, $Y = (1, 0, \ldots, 0) \in \mathbb{R}^n$.*

And the Poincaré-Bendixson theorem that makes a classification of the ω-limit sets [68, pag. 248].

Theorem 2.1.5 (Poincaré-Bendixson Theorem) *Let $\varphi(t) = \varphi(t, \boldsymbol{x})$ an integral curve of X, a vector field C^r in the open set $M \subset \mathbb{R}^2$, which is the flow of $\dot{\boldsymbol{x}} = X(\boldsymbol{x})$ defined for all $t \geq 0$ and such that $\gamma_{\boldsymbol{x}}^+ = \{\varphi(t, \boldsymbol{x}) | t \geq 0\} \subset K \subset M$ where K is compact. Suppose that the vector field X has a finite number of singularities in M. Then we consider the following alternatives:*

1. *If $\omega_{\boldsymbol{x}}$ contains only regular points, then $\omega_{\boldsymbol{x}}$ is a periodic orbit.*
2. *If $\omega_{\boldsymbol{x}}$ contains regular and singular points, then $\omega_{\boldsymbol{x}}$ consists of a set of orbits, each of which tends to one of these singular points when $t \to \pm\infty$.*
3. *If $\omega_{\boldsymbol{x}}$ does not contain regular points, then $\omega_{\boldsymbol{x}}$ is a singular point.*

We present the Peixoto Theorem [60], a very important theorem in the theory of structural stability and dynamical systems.

Theorem 2.1.6 (Peixoto Theorem) *[61] Let X be a vector field over a differentiable manifold M compact of dimension 2. To be X structurally stable in M it is necessary and sufficient that the following conditions are satisfied:*

1. *The number of singular points and periodic orbits is finite and each of them is hyperbolic.*
2. *There are no connections between saddle points.*
3. *The α and ω-limit sets consist of singular points and/or periodic orbits.*

Furthermore, the set of structurally stable vector fields is an open and dense subset (C^r topology if M is orientable and C^1 topology when M is non-orientable) in the set of whole vector fields defined over M.

For finishing this section, we consider a very special canonical region using [62].

Definition 2.1.5 *A set $A \subset \mathbb{R}^n$ is positively invariant under a vector field X if $\varphi_X(A,t) \subset A$ for all $t \geq 0$.*

Definition 2.1.6 *A strange attractor A is a closed positively invariant set which contains:*

1. *A countable set of periodic orbits of arbitrarily large period.*
2. *An uncountable set of non-periodic motions.*
3. *A dense orbit.*

2.2 Piecewise Differential Systems

Following the Filippov rules introduced in [26] we first consider an open set $U \subset \mathbb{R}^m$ and the *discontinuity region* $\Sigma = f^{-1}(0)$, also called switching manifold, being 0 a regular value of a C^r smooth function $f : U \subset \mathbb{R}^m \to \mathbb{R}$, for $1 \leq r \leq \infty$. As usual a C^r vector field is a C^r function $X : U \to \mathbb{R}^m$.

Let $X_i \in \mathfrak{X}^r(\mathbb{R}^n)$ be arbitrary vector fields, with $i = 1,\ldots,m$, where m is the number of connected components D_i of $\mathbb{R}^n \setminus \Sigma$. We denote a Piecewise Smooth Vector Field (PSVF) in $\mathbb{R}^n$ by the m-tuple $N = (X_1,\ldots,X_m)$ where

$$N(\mathbf{x}) = X_i(\mathbf{x}), \quad \text{if } \mathbf{x} \in D_i. \tag{2-4}$$

We note that on the discontinuity region Σ the piecewise vector field N is bi-valuated.

Now we precisely define $N = (X,Y)$ over Σ. A point $\mathbf{x} \in \Sigma$ is of *crossing* type if the vector fields $X(\mathbf{x})$ and $Y(\mathbf{x})$ points through Σ. It is of *sliding* type if both $X(\mathbf{x})$ and $Y(\mathbf{x})$ points inward Σ and it is of *escaping* type if $X(\mathbf{x})$ and $Y(\mathbf{x})$ points outward Σ. In each situation we are assuming that the trajectories of X and Y are transversal to Σ. Otherwise we say that a point $\mathbf{x} \in \Sigma$ is a *tangency point* of X or Y.

An effective criterion for classifying points on the discontinuity region Σ can be established in terms of the Lie derivatives as follows. We define the Lie derivative at $\mathbf{x} \in \Sigma$

as

$$Xf(\mathbf{x}) = \langle \nabla f(\mathbf{x}), X(\mathbf{x}) \rangle \tag{2-5}$$

and for $k \geq 2$ we define $X^k f(\mathbf{x}) = \langle \nabla X^{k-1} f(\mathbf{x}), X(\mathbf{x}) \rangle$. The transversal points on Σ with respect to the vector fields X and Y are classified as follows:

- *Crossing region*: $\Sigma^c = \{\mathbf{x} \in \Sigma, (Xf(\mathbf{x})).(Yf(\mathbf{x})) > 0\}$, formed by crossing points.
- *Sliding region*: $\Sigma^s = \{\mathbf{x} \in \Sigma, Xf(\mathbf{x}) < 0 \text{ and } Yf(\mathbf{x}) > 0\}$, formed by sliding points.
- *Escaping region*: $\Sigma^e = \{\mathbf{x} \in \Sigma, Xf(\mathbf{x}) > 0 \text{ and } Yf(\mathbf{x}) < 0\}$, formed by escaping points.

We observe that tangency points of X and Y are now characterized by the conditions $X_i f(\mathbf{x}) = 0$, and divide those local regions. We denote the set of tangency points by Σ^t. We may also classify tangency points in terms of higher order Lie derivatives. Indeed, if $\mathbf{x} \in \Sigma$ is a tangency point satisfying $X^2 f(\mathbf{x}) \neq 0$ then we call $\mathbf{x}$ a *fold* tangency point. If $Xf(\mathbf{x}) = X^2 f(\mathbf{x}) = 0$ but $X^3 f(\mathbf{x}) \neq 0$ then $\mathbf{x}$ is called a *cusp* tangency point. Now we define an special kind of property with the Lie derivative (2-5).

2.2.1 Inelastic PSVF

Let $N = (X, Y)$ be a PSVF. We say that N is *generalized inelastic* over the switching manifold Σ if

$$Yf(\mathbf{x}) = -\lambda Xf(\mathbf{x}), \tag{2-6}$$

where $\lambda \in \mathbb{R}_+$. In particular, if $\lambda = 1$ we simply say that N is inelastic over Σ.

Definition 2.2.1 *Let $N = (X, Y)$ be a PSVF. We say that N is inelastic over the switching manifold Σ if $Yf(\boldsymbol{x}) = -Xf(\boldsymbol{x})$.*

Inelastic vector fields appear naturally in mechanic models (see [77]) and in reversible non-smooth models, for instance, to estimate contact forces and stick-slip transitions, see [73].

Remark 2.2.1 *Note that tangency points of X and Y coincide if N is inelastic. This configuration, although non-generic, allow us to perform a global approach once from the last equation no crossing points may occur.*
In the following, we will not consider the cases $X = -Y$ because of its triviality.

As commented before, we can induce a vector field on both $\Sigma^s \cup \Sigma^e$ which is called *Filippov vector field*. Following [26] and using the inelastic condition in Definition 2.2.1 we obtain

$$F(\mathbf{x}) = \frac{Yf(\mathbf{x})X(\mathbf{x}) - Xf(\mathbf{x})Y(\mathbf{x})}{Yf(\mathbf{x}) - Xf(\mathbf{x})} = \frac{X(\mathbf{x}) + Y(\mathbf{x})}{2}. \tag{2-7}$$

Any point $x^* \in \Sigma$ satisfying $F(x^*) = 0$ is called a pseudo-equilibrium point of the NSVF. As we will see later, pseudo-equilibrium points can also occur in the infinity.

Definition 2.2.2 *A global trajectory $\Gamma(t, \boldsymbol{x})$ of the PSVF (N) passing through $\boldsymbol{x}$ is the union of local trajectories $\sigma_i(t_i, \boldsymbol{x}_i)$ such that $\sigma_i(t_{i+1}, \boldsymbol{x}_i) = \sigma_{i+1}(t_{i+1}, \boldsymbol{x}_{i+1}) = \boldsymbol{x}_{i+1}$, where $t_i \to \infty$ as $i \to \infty$.*

$$\Gamma(t, \boldsymbol{x}) = \bigcup_{i \in \mathbb{Z}} \{\sigma_i(t, \boldsymbol{x}_i) \mid t_i < t < t_{i+1}\}.$$

Thus we can take the positive part of the trajectory $\Gamma^+(t, \boldsymbol{x})$ for $i \in \mathbb{N}$ and $t_i \geq 0$ and the negative one $\Gamma^-(t, \boldsymbol{x})$ with $-i \in \mathbb{N}$ and $t_i \leq 0$. We get the following options for the local trajectories:

(i) If $\boldsymbol{x} \in D_i$, then the trajectory through $\boldsymbol{x}$ in N is the same as in X_i until it reaches Σ or equilibrium points at the infinity.

(ii) If $\boldsymbol{x} \in \Sigma^s$, the trajectories of both vector fields will arrive and continue over the Filippov vector field in Σ.

(iii) If $\boldsymbol{x} \in \Sigma^e$, the trajectories of both vector fields will leave from the Filippov vector field in Σ.

(iv) If $\boldsymbol{x} \in \Sigma^c$, where the Filippov vector field is not defined, the trajectories through $\boldsymbol{x}$ of both vector fields will be concatenated directly to form the trajectory through the point in N.

2.2.2 Generic PSVF

Filippov's convention [26] allows to define of two kinds of limit cycles for the piecewise vector fields, the so-called *sliding limit cycles* and the *crossing limit cycles*. Sliding limit cycles contain *sliding points* on the line of discontinuity and *crossing limit cycles* contain only *crossing points*. In this context, we only consider crossing limit cycles, or simply *limit cycles*.

CHAPTER 3

Global Dynamics of Planar Piecewise Linear Inelastic Differential Systems having Straight Lines as Switching Manifolds

In this chapter we construct a global study of inelastic non-smooth systems in $\mathbb{R}^2$ separated by straight lines, covering a complete description of the vector field over the switching manifolds and the global behavior of the other vector fields in the connected components, through robust classification theorems related to the tangencies and Poincaré compactification. We obtain relevant results in the analysis of canonical regions and limit sets.

Firstly we are going to determine the discontinuity regions Σ of the PSVF (2-4), considering homogeneous linear vector fields. According to the normal forms shown in [6] there exists 9 possibilities for quadratic curves, but only six are in the real space, beyond the empty set, coincident lines, ellipse, hyperbola, parabola, and intersecting or parallel lines. In the following we start with the degenerate quadrics in $\mathbb{R}^2$, the lines. We consider the following switching manifolds:

$$\begin{aligned}
&\Sigma_1 = \{(x,y) \in \mathbb{R}^2 ; y + mx = 0\} = f_1^{-1}(0),\ f_1(x,y) = y - mx,\\
&\Sigma_2 = \{(x,y) \in \mathbb{R}^2 ; (y+x)^2 = 1\} = f_2^{-1}(0),\ f_2(x,y) = (y+x)^2 - 1,\\
&\Sigma_3 = \{(x,y) \in \mathbb{R}^2 ; (y+x)(y-x) = 0\} = f_3^{-1}(0),\ f_3(x,y) = (y+x)(y-x).
\end{aligned} \tag{3-1}$$

In particular $\Sigma_i = f_i^{-1}(0)$ where each $f_i(x,y) = a_i x^2 + 2b_i xy + c_i y^2 + 2d_i x + 2e_i y - g_i$ satisfies

$$\begin{vmatrix} a_i & b_i & d_i \\ b_i & c_i & e_i \\ d_i & e_i & g_i \end{vmatrix} = 0,$$

for suitable constants $a_i, \ldots, g_i$, $i = 1,2,3$. From now on we only write Σ instead of Σ_i if there is no confusion on the context.

Thus, we present the classical concept of Poincaré compactification and dynamics at the infinity. Using the classical theory described in [19, 44], we define the Poincaré Sphere $\mathbb{S}^2 \subset \mathbb{R}^3$ projecting over it the plane $z = 1$ containing the phase portrait of the differential system, through the intersection of the sphere and straight lines from the points in the plane to the origin of $\mathbb{R}^3$. Using the transformation $(u,v) = (\frac{y}{x}, \frac{1}{x})$ for the local charts U_1, U_2, U_3, V_1, V_2, V_3 at the infinity, see Figure 3.1, we obtain the expression for a generic vector field $X = A\mathbf{x} = (P(x,y), Q(x,y))$ in $\mathbb{S}^1 \cap (U_1 \cup V_1)$ and $\mathbb{S}^1 \cap (U_2 \cup V_2)$, respectively.

$$\begin{cases} \dot{u} = -a_{12}u^2 + (a_{22} - a_{11})u + a_{21}, \\ \dot{v} = -a_{12}uv - a_{11}v, \end{cases} \quad \begin{cases} \dot{u} = -a_{21}u^2 + (a_{11} - a_{22})u + a_{12}, \\ \dot{v} = -a_{21}uv - a_{22}v, \end{cases} \tag{3-2}$$

and in $\mathbb{S}^1 \cap (U_3 \cup V_3)$ is located the original differential system.

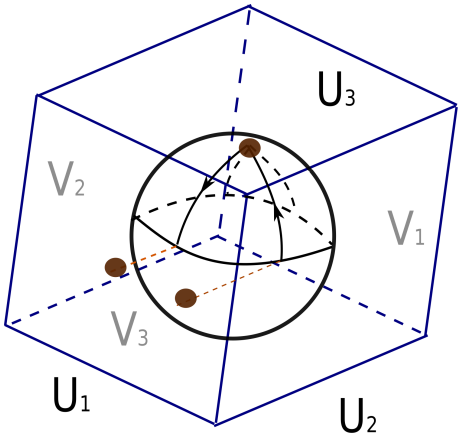

Figure 3.1: *Charts used in Poincaré Compactification.*

We define some especial points at the infinity in this discontinuous context. Some of them

we call fake, which take place in the cases $\Sigma = \Sigma_1$ and $\Sigma = \Sigma_2$, because these points do not share some characteristics of the classic ones but they resemble them in some sense.

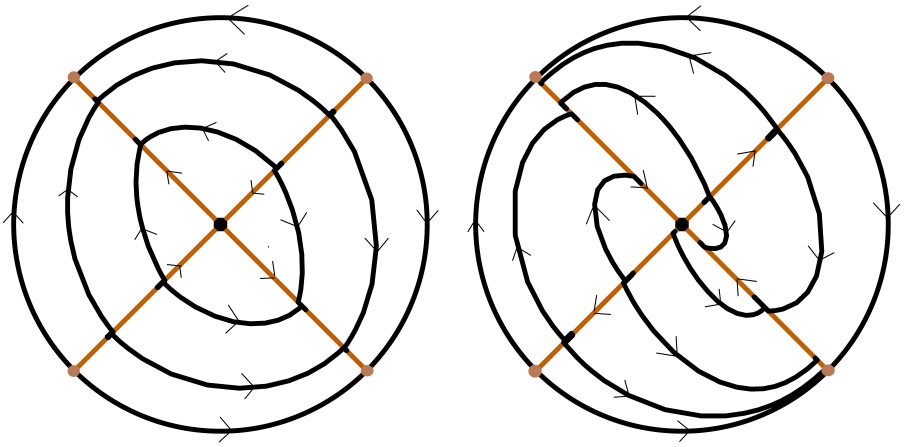

(.1) *Pseudo-node* **(.2)** *Pseudo-saddle*

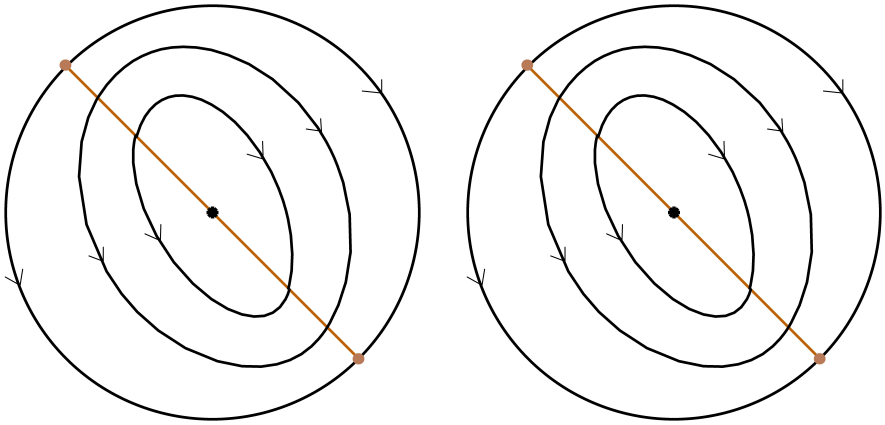

(.3) *Fake pseudo-sliding-escaping* **(.4)** *Fake pseudo-crossing*

Figure 3.2: *Pseudo equilibrium points at the infinity. In the following figures at the finite part, orange curves are the switching manifolds, orange points are tangency ones, black points are pseudo-equilibrium points. At the infinity part, brown, pink, green, red and blue points are pseudo, non-hyperbolic, saddle, repeller and attractor equilibrium ones, respectively.*

Definition 3.0.1 *Let Z be a smooth vector field, $\widetilde{Z}$ its compactification on $\mathbb{S}^2$ and p a point at the equator of $\mathbb{S}^2$. We define the following objects.*

- *p is an infinite pseudo-node for $\widetilde{Z}$ if it is an attractive (repulsive) point at the infinity, over the switching manifold, which is reached in positive (negative) finite time in the equator of $\mathbb{S}^2$ and in positive (negative) infinite time for the Filippov vector field along the switching manifold.*

- *p is an infinite pseudo-saddle for $\widetilde{Z}$ if it is an attractive (repulsive) point at the infinity, over the switching manifold, which is reached in positive (negative) finite time in the equator of $\mathbb{S}^2$ and in negative (positive) infinite time for the Filippov vector field along the switching manifold.*
- *When $\Sigma = \Sigma_1$, then p is a fake sliding-escaping pseudo-equilibrium point at the infinity for $\widetilde{Z}$ if it is an attractive or repulsive point at the infinity, over the switching manifold, and belongs to a continuum of equilibria for the Filippov vector field along the switching manifold.*
- *When $\Sigma = \Sigma_2$, then p is a fake crossing pseudo-equilibrium point at the infinity for $\widetilde{Z}$ if it is a regular point at the infinity for the exterior vector field and an attractive and/or repulsive point for the Filippov vector field along the switching manifold. Those vector fields do not match at the infinity but that will be the convention that we will study. The cases where the fake crossing points are also singularities at the infinity for some of the vector fields are omitted because that situation is not generic.*

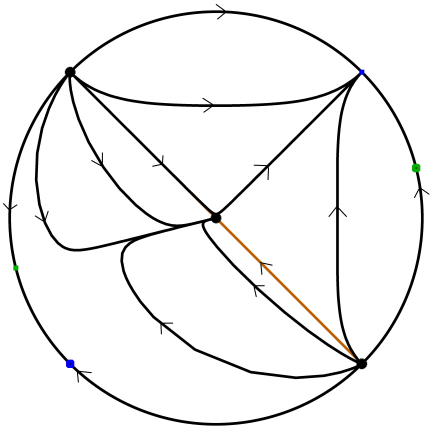

Figure 3.3: *Flat behavior.*

Remark 3.0.1 *In this chapter we do not consider configurations for which the orbits of the vector fields are coincident with the discontinuity region. For example, taking $x+y=0$, $m=1$ as switching manifold, let N be a non-smooth vector field where*

$$A = \begin{pmatrix} 0 & 1 \\ 1 & 0 \end{pmatrix},$$

$$B = \begin{pmatrix} -2 & 4 \\ 1 & -5 \end{pmatrix},$$

$$F(\boldsymbol{x}) = \frac{1}{2} \begin{pmatrix} -2 & 5 \\ 2 & -5 \end{pmatrix} \begin{pmatrix} x \\ y \end{pmatrix}.$$

One can see that the first vector field has a saddle equilibrium point with $\lambda_1 = 1$ *and* $\lambda_2 = -1$ *and the second one has an attractive node, where its eigenvalues are* $\lambda_1 = -6$ *and* $\lambda_2 = -1$. *The discontinuity line coincides with an invariant manifold of the two vector fields, so the orbits do not reach the line except at the infinity (in the past or in the future). In this case we say that the contact with the discontinuity line is flat, see Figure 3.3.*

We are going to work with generic differential systems in the sense of considering residual sets in the whole set of inelastic differential equations, adding for instance centers and other sets, that in fact have measure zero.

Thus we can define the main equivalence and the stability classes in this piecewise smooth context.

Definition 3.0.2 *Two phase portraits* Z_1 *and* Z_2 *of the vector field (2-4) are topologically equivalent if there exists a homeomorphism* $h : \mathbb{D}^2 \to \mathbb{D}^2$ *which carries orbits of* Z_1 *onto orbits of* Z_2, *preserving the orientation of all trajectories. In that way, the switching manifolds,* Σ^1 *and* Σ^2 *respectively. and other canonical regions are preserved by h.*

Considering $A, B \in C^r(\mathbb{R}^2, \mathbb{R}^2)$ and following [34], we can get a norm in $\mathfrak{L}_{inesl}(M)$:

$$||(X,Y)|| = ||(A,B)|| = \sup_{\mathbf{x} \in \mathbb{S}^1} \{||A\mathbf{x}|| + ||B\mathbf{x}||\}.$$

Thus it induces a distance and the corresponding definition of neighborhood through

$$d(Z_1,Z_2) = d((X,Y),(\bar{X},\bar{Y})) = ||(A-\bar{A},B-\bar{B})||.$$

Definition 3.0.3 *Let $Z \in \mathfrak{L}_{inesl}(M)$ a vector field over M, in this case compact. N is structurally stable over M if there exists a neighborhood $V(Z)$ such that, for every $\tilde{Z} \in V(Z)$, it is topologically equivalent to N. If N does not satisfy the above, then it is structurally unstable.*

There is another fact which is necessary to consider:

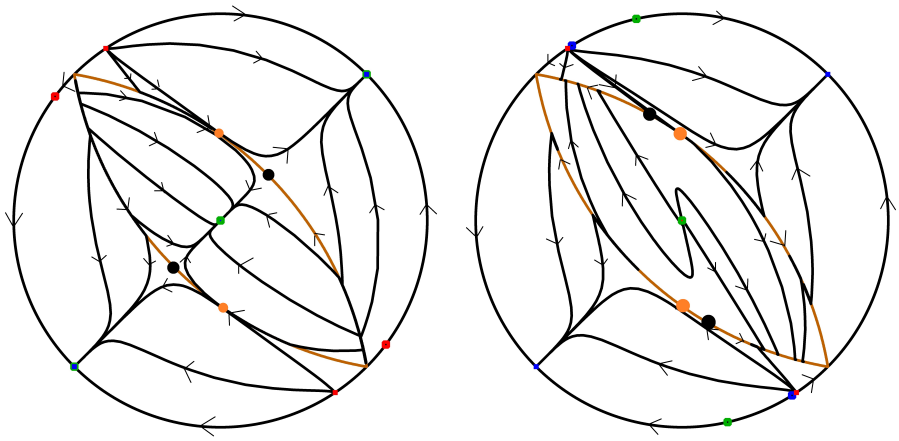

(.1) *S-N 4* **(.2)** *S-N 4-INV*

Figure 3.4: *Phase portraits of a saddle and a node with two parallel lines as switching manifold.*

Remark 3.0.2 *The notion of topological equivalence considered in this chapter does not preserve the orientation of trajectories of the Filippov vector field. Therefore, the phase portraits presented in Section 3.1 that does not present a continuum of equilibria for the Filippov vector field can present two distinct orientations, which increase the number of potential phase portraits, see Corollary 3.1.1 and Figure 3.4.*

3.1 Main results on planar piecewise linear inelastic systems

The main goal of the chapter is to classify the global phase portraits of inelastic linear PSVF. Consider the linear vector fields X and Y joint with the following system

$$\begin{cases} X(\mathbf{x}) = A\mathbf{x}, \quad A = (a_{ij}); \\ Y(\mathbf{x}) = B\mathbf{x}, \quad B = (b_{ij}); \\ \det(A)\det(B) \neq 0; \\ Z = (X,Y) \text{ is inelastic over } \Sigma, \end{cases} \tag{3-3}$$

where A and B are square matrices with real entries.

CR	TA			E			PE			∞ E			∞ PE		
QT	Σ_1	Σ_2	Σ_3	Σ_1	Σ_2	Σ_3	Σ_1	Σ_2	Σ_3	Σ_1	Σ_2	Σ_3	Σ_1	Σ_2	Σ_3
C-C	1	2	1	1^*	1	1^*	∞	0	1	0	0	0	2	2^*	4
C-F	1	2	-	1^*	1	-	1	2	-	0	0	-	2	2^*	-
C-N	1	2	-	1^*	1	-	1	2	-	1-2	0-2-4	-	2	2^*	-
C-S	1	2	1	1^*	1	1^*	1-∞	0-2	1	2	0-4	0-4	2	2^*	4
F-F	1	2	1	1^*	1	1^*	1	2	1	0	0	0	2	2^*	4
F-N	1	2	1	1^*	1	1^*	1	2	1	1-2	0-2-4	0-2-4	2	2^*	4
F-S	1	2	1	1^*	1	1^*	1	2	1	2	0-4	0-4	2	2^*	4
SN-N	-	0	-	-	1	-	-	0-2	-	-	2-4-∞	-	-	2^*	-
SN-S	-	0	-	-	1	-	-	2	-	-	4-∞	-	-	2^*	-
N-N	1	2	1	1^*	1	1^*	1	2	1	3-4	2-4	0-2-4-6-8	2	2^*	4
N-S	1	2	1	1^*	1	1^*	1	2	1	3-4	2-4	0-2-4-6-8	2	2^*	4
S-S	1	2	1	1^*	1	1^*	1-∞	0-2	1	4	4	0-4-8	2	2^*	4

Table 3.1: *Canonical regions (CR) for Tangencies (TA), Equilibrium points (E), Pseudo-Equilibrium points (PE), Equilibrium points at the infinity (∞E) and Pseudo-Equilibrium points at the infinity (∞PE) with the qualitative types (QT) centers (C), focuses (F), saddles (S), nodes (N) and star nodes (SN), coincident lines (Σ_1), parallel lines (Σ_2), transversal lines (Σ_3). For the meaning of* 1^* *and* 2^* *see Remark 3.1.1* (3).

3.1.1 Compactification and Stability Classes

The main results of the chapter are the following:

Theorem 3.1.1 *The phase portraits on the Poincaré disk of the inelastic system* (3-3) *are generically topologically equivalent, unless the orientation of trajectories on* Σ*, to:*

(i) one of the 16 phase portraits of Figure 3.5 if $\Sigma = \Sigma_1$*;*

(ii) one of the 29 phase portraits of Figure 3.6 if $\Sigma = \Sigma_2$*;*

(iii) one of the 22 phase portraits of Figure 3.7 if $\Sigma = \Sigma_3$*;*

Corollary 3.1.1 *There exist generically 123 phase portraits on the Poincaré disk of the inelastic system* (3-3)*. The global dynamics of the system is generically described by each corresponding cell of Table 3.1.*

3.1.2 Limit Sets

Theorem 3.1.2 *The* α *or* ω*-limit set of a point on the Poincaré disk of the inelastic system* (3-3) *generically is one the following objects:*

1. *a boundary equilibrium point at the origin;*
2. *a pseudo-equilibrium of the Filippov vector field;*
3. *an equilibrium point at the infinity;*
4. *a pseudo-equilibrium point at the infinity;*
5. *a fake (crossing or sliding-escaping) pseudo-equilibrium point at the infinity;*
6. *a periodic orbit in the finite part;*
7. *a periodic orbit at the infinity.*

The α or ω-limit sets of some classes of planar PSVF are studied in [22]. However, that article consider compact regions (as the Poincaré disk) within two zones and so it does not detect neither the fake pseudo-equilibrium points because in [22] the singularity must be isolated. As far as the authors know, this is the first time one identifies these two types of behavior at the infinity.

Remark 3.1.1 *We highlight some different topological behaviors among the phase portraits for those inelastic differential systems summarized in Table 3.1.*

1. *The number of equilibrium points at the infinity varies from 0 to 8.*
2. *Some configurations of inelastic systems having $\Sigma = \Sigma_1$ or $\Sigma = \Sigma_2$ may present a continuum of pseudo-equilibrium points for the Filippov vector field.*
3. *There exists one strict equilibrium point in the finite part only when $\Sigma = \Sigma_2$, in the other cases the origin is also a pseudo-equilibrium (1^*). Also in that case (2^*) is for the two fake crossing pseudo-equilibrium points at the infinity.*
4. *Some configurations combining centers and star nodes are not possible to obtain because they cannot be inelastic.*

3.2 Filippov Vector Field, Tangency Points and Infinity Dynamics

In order to prove the main results we first state and prove some auxiliary results. The first one addresses the nature of equilibrium points at the infinity, an useful result that can be found for instance in [68] and we included it here for the sake of completeness. In order to present the result, let us call J a square matrix $J = (a_{ij})$, $i, j = 1, 2$ and let $tr(J)$ and $\det(J)$ denote the trace and the determinant of J, respectively. Therefore

Proposition 3.2.1 *Let $X = A\boldsymbol{x}$, a homogeneous linear vector field in the plane, then by the Poincaré Compactification:*

1. *If $(trA)^2 - 4detA < 0$, then the vector field does not have any singularity at the infinity. (Center ($trA = 0$) and Focus ($trA \neq 0$)).*
2. *If $(trA)^2 - 4detA = 0$ and $trA \neq 0$, then there exists a line of singularities or only two non-hyperbolic equilibrium points at the infinity. (Improper nodes, star node and a node with two equilibrium points at the infinity, respectively).*
3. *If $(trA)^2 - 4detA > 0$ and $detA < 0$, then there exists four singularities (hyperbolic nodes) at the infinity. (Saddle).*

4. *If* $(trA)^2 - 4detA > 0$ *and* $detA > 0$*, then there exists four singularities at the infinity, two hyperbolic nodes and saddles. (Proper node or a node with four equilibrium points at the infinity).*
5. *If* $(trA)^2 - 4detA > 0$ *and* $detA = 0$*, then there exists four singularities at the infinity, two of them are hyperbolic. It is possible that two of those points are being connected by a singularity line in the finite part. (Parallel lines, one eigenvalue is zero).*
6. *If* $trA = 0$ *and* $detA = 0$*, then there exists two non-hyperbolic equilibrium points at the infinity. It is possible that those points are being connected by a singularity line in the finite part. (Parallel lines).*

The proof of Proposition 3.2.1 is direct and it involves some tedious algebraic manipulations, so we only present the proof of bullet (i) in what follows.

Proof. [Proof of Proposition 3.2.1] From equation (3-2), a point $(u,0) \in \mathbb{S}^1 \cap (U_1 \cup V_1)$ is a singular point of X at the infinity if u if it is a real solution of quadratic equation

$$-a_{12}u^2 + (a_{22} - a_{11})u + a_{21} = 0, \tag{3-4}$$

that is, if

$$u = \frac{(a_{22} - a_{11}) \pm \sqrt{(a_{11} - a_{22})^2 + 4a_{12}a_{21})}}{2a_{12}}.$$

On the other hand, the discriminant of the equation (3-4) is

$$(a_{11} - a_{22})^2 + 4a_{12}a_{21} = (a_{11} + a_{22})^2 - 4a_{11}a_{22} + 4a_{12}a_{21} = tr(M)^2 - 4det(M),$$

that is, X has no singularities in $\mathbb{S}^1 \cap (U_1 \cup V_1)$ if $tr(M)^2 - 4det(M) < 0$. Analogously, it can be proved that X has no singularities in $\mathbb{S}^1 \cap (U_2 \cup V_2)$ so bullet (i) is proved.

The proof of the other bullets follows similarly by adding the analysis of the Jacobian matrices $J_1 = diag(-2a_{12}u^* + a_{22} - a_{11}, -a_{12}u^* - a_{11})$ and $J_2 = diag(-2a_{21}u^* - a_{22} + a_{11}, -a_{21}u^* - a_{22})$ of systems (3-2) in $\mathbb{S}^1 \cap (U_1 \cup V_1)$ and $\mathbb{S}^1 \cap (U_2 \cup V_2)$, respectively,

where $(u,v) = (u^*,0)$ is an equilibrium point at the infinity. □

The next result consider the tangency points over the switching manifolds Σ_i, $i = 1,2,3$.

Proposition 3.2.2 *Let $X = A\boldsymbol{x}$ and $Y = B\boldsymbol{x}$ be non-degenerate linear vector fields defining an inelastic PSVF $Z = (X,Y)$. The tangency sets on Σ are generic formed by one of the following:*

(i) If $\Sigma = \Sigma_1$, then Σ^t is formed by a single point;

(ii) If $\Sigma = \Sigma_2$, then Σ^t is formed by two points, one over each connected component of Σ_2;

(iii) If $\Sigma = \Sigma_3$, then Σ^t is formed by a single point.

Proof. [Proof of Proposition 3.2.2] The tangency points over each switching manifold Σ_1, Σ_2 and Σ_3 are given by the solutions of the following equations using (2-5), respectively:

$$\begin{aligned} Xf_1(\mathbf{x}) &= (ma_{11}+a_{21})x+(ma_{12}+a_{22})y = 0;\\ Xf_2(\mathbf{x}) &= (a_{11}+a_{21})x^2+(a_{12}+a_{22})y^2+(a_{11}+a_{12}+a_{21}+a_{22})xy = 0;\\ Xf_3(\mathbf{x}) &= (a_{12}-a_{21})xy-a_{22}y^2+a_{11}x^2 = 0. \end{aligned} \tag{3-5}$$

where $(x,y) \in \Sigma$.

Each term of the equations in (3-5) are quadratic and they vanish. Thus, the conics represented by the tangency sets above but defined in the entire $\mathbb{R}^2$ must be symmetric with respect to some straight line. More precisely, generically there exists three configuration for those conics: they must be the empty set, coincident lines or two intersecting lines containing the origin. Ultimately, the tangency points are the intersection between the previous conic curves and the respective discontinuity regions.

If $\Sigma = \Sigma_1$, then from equation (3-1), either it cross the conics of tangencies at one point in a transversal contact or coincides with it. The generic situation is the transversal one so we have proved bullet (i).

If $\Sigma = \Sigma_2$, the equation for the tangencies has the form $ax^2+(a+b)xy+by^2 = (x+y)(ax+by) = 0$, so one of those straight lines is parallel to Σ_3 and the other is either transversal or does not intersect Σ_2. Thus, the intersection corresponding to tangency points is either empty or formed by two points, one over each connected component of Σ_2. In this case, the generic situation is the one having two intersections points and therefore bullet (ii) is proved.

If $\Sigma = \Sigma_3$, by the form of its unitary equation provided by the equations (3-1), it crosses the origin and the intersection with the conics of tangencies occurs at that point and so bullet (iii) is proved. □

The next result states the behaviors of Filippov vector fields over switching manifolds.

Proposition 3.2.3 *Consider $Z(\boldsymbol{x}) = (A\boldsymbol{x}, B\boldsymbol{x})$, an inelastic PSVF as in (3-3). Then the following statements generically hold:*

(i) If $\Sigma = \Sigma_1$, then A and B can be written as

$$A = \begin{pmatrix} a_{11} & a_{12} \\ -m(a_{11}+b_{11})-b_{21} & -m(a_{12}+b_{12})-b_{22} \end{pmatrix},$$

$$B = \begin{pmatrix} b_{11} & b_{12} \\ b_{21} & b_{22} \end{pmatrix},$$

and the Filippov vector field over Σ_1 is given by

$$F(\boldsymbol{x}) = \frac{1}{2}((a_{11}+b_{11})x+(a_{12}+b_{12})y, (-m(a_{11}+b_{11}))x+(-m(a_{12}+b_{12}))y).$$

Moreover, the origin is the unique pseudo-equilibrium point of F, which is attractive or repulsive whether the sign of $(a_{11}+b_{11})-m(a_{12}+b_{12})$ is negative or positive, respectively.

(ii) If $\Sigma = \Sigma_2$, then A and B can be written as

$$A = \begin{pmatrix} a_{11} & a_{12} \\ -a_{11} - b_{11} - b_{21} & -a_{12} - b_{12} - b_{22} \end{pmatrix},$$

$$B = \begin{pmatrix} b_{11} & b_{12} \\ b_{21} & b_{22} \end{pmatrix},$$

and the Filippov vector field over Σ_2 is given by

$$F(\boldsymbol{x}) = \frac{1}{2}((a_{11}+b_{11})x + (a_{12}+b_{12})y, -(a_{11}+b_{11})x - (a_{12}+b_{12})y).$$

Moreover, F has two pseudo-equilibrium points, one at each straight line of Σ_2, which is attractive or repulsive whether the sign of $(a_{11}+b_{11}) - (a_{12}+b_{12})$ is negative or positive, respectively.

(iii) If $\Sigma = \Sigma_3$, then A and B are writing as

$$A = \begin{pmatrix} -b_{11} & a_{21} + b_{21} - b_{12} \\ a_{21} & -b_{22} \end{pmatrix},$$

$$B = \begin{pmatrix} b_{11} & b_{12} \\ b_{21} & b_{22} \end{pmatrix}.$$

and the Filippov vector field over Σ_3 is given by

$$F(\boldsymbol{x}) = \frac{1}{2}((a_{21}+b_{21})y, (a_{21}+b_{21})x)$$

Moreover, F has only one equilibrium point which is a saddle at the origin.

The proof of Proposition 3.2.3 is direct, but we provide the lines of it for completeness.

Proof. [Proof of Proposition 3.2.3] From the expression of Σ_1 in (2.2.1) and from the fact that N is inelastic over Σ_1, the equality $Yf(x,y) = -Xf(x,y)$ with $y = -mx$ provides

$(ma_{11}+a_{12}) = -(mb_{11}+b_{12})$ and $(ma_{12}+a_{22}) = -(mb_{12}+b_{22})$, so we obtain the expression of the matrix A of bullet (i). Moreover, from equation (2-7) for $(x,y) \in \Sigma_1$ we obtain the expression of F of bullet (i) with $y = -mx$.

The equilibrium points of F lie on the intersection of the straight line

$$y = -\frac{a_{11}+b_{11}}{a_{12}+b_{12}}x,$$

with Σ_1, that is, the origin $(0,0)$. The eigenvalues associated with the matrix defining the linear vector field F are $\lambda_1 = 0$ and $\lambda_2 = (a_{11}+b_{11}) - m(a_{12}+b_{12})$ so the equilibrium point at $(0,0)$ is attractive if λ_2 is negative and repulsive if λ_2 is positive. That finishes the proof of bullet (i).

In (ii), since $(a_{11}+a_{21}) = -(b_{11}+b_{21})$ and $(a_{22}+a_{12}) = -(b_{22}+b_{12})$, then $\lambda_1 = 0$ and $\lambda_2 = (a_{11}+b_{11}) - (a_{12}+b_{12})$.

For (iii) the relations are $a_{11} = -b_{11}$ $a_{22} = -b_{22}$ and $(a_{21}-a_{12}) = -(b_{21}-b_{12})$, the eigenvalues are $\lambda = \pm|a_{21}+b_{21}|$.

In the two first cases, the equilibrium points are determined by a line of the form

$$y = -\frac{a_{12}+b_{12}}{a_{11}+b_{11}}x.$$

In the second one, if the line of singularities is parallel to the discontinuity lines, then there are no singularities. In the third case the unique singularity is $(x,y) = (0,0)$. □

The following result is about the last canonical region which consists of pseudo equilibrium points at the infinity.

Proposition 3.2.4 *Consider $Z(\boldsymbol{x}) = (A\boldsymbol{x}, B\boldsymbol{x})$, an inelastic PSVF satisfying system (3-3). Then the pseudo equilibrium points at the infinity generically satisfy one of the following statements.*

(i) *If $\Sigma = \Sigma_1$, then either there exist a pair of pseudo-equilibria at the infinity, one of them being an infinity pseudo-node and an infinity pseudo-saddle, or a pair of fake sliding-escaping pseudo-equilibrium points at the infinity.*

(ii) *If $\Sigma = \Sigma_2$, then there exist two fake crossing pseudo-equilibrium points at the infinity, both attractive and/or repulsive.*

(iii) *If $\Sigma = \Sigma_3$, then there exist four pseudo equilibrium points which can be either four pseudo-nodes (two attractive and two repulsive), or four pseudo-saddles at the infinity.*

Proof. [Proof of Proposition 3.2.4] To prove bullet (i), we notice that there exist two points p_1 and p_2 at the infinity corresponding to the discontinuity line Σ_1. Those two points split the Poincaré disk and because N is inelastic, one point corresponds to the sliding region, say p_1, and p_2 corresponds to the escaping region. Thus, p_1 attracts points at the infinity and p_2 repels them, both being reached in finite forward or backward time, respectively. Now, since p_1 belongs to the sliding region at the infinity, the trajectory of the Filippov vector field asymptotically tends to p_1 either in forward time (so p_1 is a pseudo-node) or a backward time (so p_1 is a pseudo-saddle).

If there exists a continuum of pseudo-equilibrium points in the finite part, by the Definition 3.0.1 we get that p_1 can be a fake sliding pseudo-equilibrium point at the infinity if it is attracting at the infinity, and then p_2 will be an escaping one, or vice-versa.

For bullet (ii), we notice that the intersection of the two parallel lines of Σ_2 meet the Poincaré disk (the infinity) at the same points, forming two opposite points at the infinity, say p_1 and p_2. Therefore, while the finite portion of the phase portrait has three connected components, separated by the two straight lines of Σ_2, the infinity has only two portions corresponding to two half circles. If we say that X is defined on the strip inside the straight lines of Σ_2 and Y is defined outside them, then the two half circles on the infinity are related to Y, that is, the trajectories in the infinity face no discontinuity. On the other hand, p_1 and p_2 are points of the infinity that attract and/or repel trajectories of the Filippov

vector field, that is, they are fake crossing equilibrium points and the proof of bullet (ii) is done.

For the proof of bullet (iii), we first notice that Σ_3 has four points at the infinity, $p_1,\ldots,p_4$. Moreover, because N is inelastic, two of them (say p_1 and p_3) are attractive and p_2, p_4 are repulsive. On the other hand, the finite part has also four components for the Filippov vector field. Since the origin is a saddle at the origin for the Filippov vector field, in the sense that two directions are attractive and two are repulsive. So, if the repelling component of Σ_3 tend to p_1 or p_3, then it is easy to see that every p_i is attractive so $p_1,\ldots,p_4$ are pseudo-nodes at the infinity. If the same repelling component tends to p_2 or p_4, then $p_1,\ldots,p_4$ are pseudo-saddles at the infinity and the proof is done. □

3.2.1 Homeomorphism

We are going to construct the homeomorphism h for using it in the next proofs and composing the stability classes. Let $Z_1 = (A,B) \in \mathfrak{L}_{inesl}(M)$. Then there exists a neighborhood $V \subset Z^r$ of (A,B) such that $Z_2 = (C,D) \in V$ is topologically equivalent to Z_1 if it satisfies some conditions, using [69] and by the Propositions 3.2.1, 3.2.2, 3.2.3 and 3.2.4:

1. (C,D) has the same number and topological type of hyperbolic (and also non-hyperbolic under the conditions of Proposition 3.2.1) singular points and periodic orbits at the infinity and the finite part as (A,B).
2. The number of points $\mathbf{q} \in \Sigma^2$ of tangency is the same as the number of $\mathbf{p} \in \Sigma^1$ of tangency.
3. The number and topological type of pseudo-equilibrium points $\mathbf{q} \in \Sigma^2$ of (C,D) at the finite and infinity parts is the same as the number of pseudo-equilibrium points $\mathbf{p} \in \Sigma^1$ of equilibrium of (A,B).

Thus, for all $(C,D) \in V$ let the homeomorphism $h : \mathbb{D}^2 \to \mathbb{D}^2$ be such that:

- Take the pseudo-equilibrium points at the finite part $\{p_1,\ldots,p_k\}$ of Σ^1 in (A,B) at the pseudo-equilibrium points $\{q_1,\ldots,q_k\}$ of Σ^2 in (C,D). Take the

pseudo-equilibrium points at the infinity $\{\gamma_1,\dots,\gamma_{2n}\}$ of Σ^1 in (A,B) at the pseudo-equilibrium points at the infinity $\{\gamma_{G1},\dots,\gamma_{G2n}\}$ of Σ^2 in (C,D). It takes the arcs of $\Sigma^1 \setminus \{p_1,\dots,p_k,\gamma_1,\dots,\gamma_{2n}\}$ of Σ^1 in (A,B) on the arcs of $\Sigma^2 \setminus \{q_1,\dots,q_k,\gamma_{G1},\dots,\gamma_{G2n}\}$ of Σ^2 in (C,D) for the arc composite. Thus, h is well defined on the switching manifold. The homeomorphism h near that curve is constructed from one canonical region to another, which are defined as pseudo-equilibrium point disks, tangency point disks and the complement of their union.

- The canonical regions near the switching manifold are also preserved using Definition 2.2.2 of global trajectories.
- Remaining regions, disks of equilibrium points at the infinity and the finite part are also preserved.

To extend h to the rest of $\mathbb{D}^2$ we use the flows of (A,B) and (C,D), so if $\mathbf{q} \in \mathbb{D}^2 \setminus \Sigma_1$ and $\gamma_t(\mathbf{q})$ is an orbit through $\mathbf{q}$ at $t=0$, then $h \circ \gamma_t(\mathbf{q})$ is an orbit of (C,D) which crosses $h(\mathbf{q})$ at $t=0$. So h makes (A,B) topologically equivalent to (B,G).

3.3 Proofs of the Main Results

Next we prove Theorem 3.1.1. We split the proof in three parts and perform a case-by-case analysis in each of those parts. We start proving bullet (i) of the referred result.

Proof. [Proof of Theorem 3.1.1 (**i**)] In this case $\Sigma = \Sigma_1$ is a straight line as switching manifold, so there is a linear system in each hemisphere and all the possibilities for the canonical regions are described in Table 3.1.

By Proposition 3.2.2, the tangency point is only the origin. By Proposition 3.2.3, generically there is an attractive or repelling Filippov vector field with a pseudo-equilibrium point in the discontinuity region. From Proposition 3.2.4, there exists a pseudo-node and a pseudo-saddle at the infinity. In the following case-by-case study the same canonical regions are determined by the last 3 propositions. Also we consider generic saddles, such that $trA \neq 0$ and $trB \neq 0$.

• **center - focus:** From Proposition 3.2.1 the vector fields do not have equilibrium points at the infinity, thus there exists a homeomorphism h, following the construction of Subsection 3.2.1, such that the phase portrait of that system is topologically equivalent to the one in Figure 3.5.2. That homeomorphism exists in the next cases for the same reason.

• **center - node:** There exist two possibilities for the configuration of the node by Proposition 3.2.1, one or two equilibrium points at the infinity, in the hemisphere where that node is located. The phase portraits are then topologically equivalent to one of those in Figures 3.5.3 or 3.5.4, respectively.

• **center - saddle:** In this case there are two equilibrium points at the infinity, in the hemisphere of the saddle. So, the phase portrait is topologically equivalent to Figure 3.5.6.

• **focus - focus:** For the case focus-focus, there are no equilibrium points at the infinity. Then the phase portrait is topologically equivalent to the one of Figure 3.5.7.

• **focus - node:** Now there exists one singularity at the infinity in the hemisphere of the node if $(trB)^2 - 4\det B = 0$, or two equilibrium points at the infinity if $(trB)^2 - 4\det B > 0$ and $\det B > 0$. Consequently, the phase portraits are topologically equivalent to one of those in Figures 3.5.8 and 3.5.9, respectively.

• **focus - saddle:** In this case there exist two equilibrium points at the infinity, in the hemisphere of the saddle, and the phase portrait is topologically equivalent to the one of Figure 3.5.10.

• **node - node:** There are three sub-cases. If there are two nodes with one singularity at the infinity in each hemisphere, then this case is trivial. If there is a node with one equilibrium point in its hemisphere and other node with two equilibria, the phase portrait corresponds to Figure 3.5.11. Finally, in the case of two nodes with two equilibrium points in each hemisphere, the phase portrait is topologically equivalent to the ones reassembling Figure 3.5.12.

• **node - saddle:** In this case, the hemisphere of the saddle has two equilibrium points at the infinity. In the hemisphere of the node, there exist one or two equilibrium points at the

infinity, then their phase portraits are topologically equivalent with the ones of Figures 3.5.13 and 3.5.14, respectively.

• **generic saddle - saddle:** In this case there exist two equilibrium points in each hemisphere and the phase portrait is equivalent to the one exhibited in Figure 3.5.15.

• **exceptions:** There are some exceptions for which Propositions 3.2.3 and 3.2.4 does not apply, so we must consider them separately. Some restricted cases where we get a line of singularities (pseudo-equilibria) in the Filippov vector field and also two fake sliding-escaping pseudo equilibrium points at the infinity. A normal form for the centers in $\mathbb{R}^2$ is

$$A = \begin{pmatrix} a_{11} & a_{12} \\ a_{21} & -a_{11} \end{pmatrix}, \tag{3-6}$$

with $a_{11}^2 + a_{12}a_{21} < 0$. Then if B defines also a center then the following is getting for $\mathbf{x}$ in the discontinuous line with $m \neq 0$

$$\begin{aligned} F(\mathbf{x}) &= \frac{1}{2}\begin{pmatrix} a_{11}+b_{11} & -(a_{22}+b_{22})\frac{1}{m} \\ -m(a_{11}+b_{11}) & a_{22}+b_{22} \end{pmatrix}\begin{pmatrix} x \\ -mx \end{pmatrix} \\ &= \frac{1}{2}\begin{pmatrix} a_{11}+b_{11} & (a_{11}+b_{11})\frac{1}{m} \\ -m(a_{11}+b_{11}) & -(a_{11}+b_{11}) \end{pmatrix}\begin{pmatrix} x \\ -mx \end{pmatrix} \\ &= \begin{pmatrix} 0 \\ 0 \end{pmatrix}. \end{aligned}$$

We can see that the last one is valid for every vector field A such that $a_{11} = -a_{22}$, so this could happen for saddles, but that situation is not generic. Here there is no a direction for the Fillipov vector field and then the canonical region is invariant in those cases. Thus, the phase portrait of system (3-3) can be center- center without singularities at the infinity, center-saddle with two singularities at the infinity or saddle-saddle with four singularities at the infinity, and are topologically equivalent to the one of the Figures 3.5.1, 3.5.5 and 3.5.16, respectively. □

Proof. [Proof of Theorem 3.1.1 (**ii**)] In this case we examine two parallel lines as switching manifold, so there is a linear system inside and another outside, and all the possibilities for the canonical regions are described in Table 3.1.

By Proposition 3.2.2 there are generically two tangency points, one in each line, but the cases with star nodes do not have tangencies. By Proposition 3.2.3, the Filippov vector field has generically an attractive or repelling pseudo-equilibrium point in each line of the discontinuity region, also because those lines do not cross the origin, and there exists a singularity in the finite part. By Proposition 3.2.4 we get two fake crossing pseudo-equilibrium points at the infinity. The following cases share the same canonical regions determined by the last 3 propositions.

• **center - focus:** If there are a center and a focus (between and out of the lines), by Proposition 3.2.1 there exists no equilibrium points at the infinity, thus the phase portraits of the two possible systems are topologically equivalent to the ones of Figures 3.6.2 and 3.6.3.

• **center - node:** For the case center-node, using the Proposition 3.2.1, if the center is the exterior vector field then there are no equilibrium points at the infinity and the phase portrait of the system is equivalent to Figure 3.6.4, and with a node in the exterior there exist two or four equilibrium points at the infinity and thus their phase portraits are topologically equivalent to the ones of Figures 3.6.5 and 3.6.6, respectively.

• **center - saddle:** If there are a center and a saddle, by Proposition 3.2.1 if the center is in the exterior region there are no equilibrium points at the infinity, if the saddle is outside then we get four equilibrium points at the infinity, and the phase portraits of the two possible systems are topologically equivalent to the ones of Figures 3.6.7 and 3.6.8, respectively.

• **focus - focus:** For the case focus-focus, using the Proposition 3.2.1, there are no equilibrium points at the infinity and the phase portrait of the system is equivalent to Figure 3.6.11.

• **focus - node:** If there are a focus and a node, using the Proposition 3.2.1, if there is a node in the exterior, there can exists two or four equilibrium points at the infinity and then their phase portraits are topologically equivalent to the ones of the Figures 3.6.13 and 3.6.14, respectively. Also if the focus is the exterior vector field then there are no equilibrium points at the infinity and the phase portrait of the system is equivalent to the Figure 3.6.12.

• **focus - saddle:** For the case focus-saddle, by Proposition 3.2.1 if the focus is in the exterior region there are no equilibrium points at the infinity, if the saddle is outside then there exists four equilibrium points at the infinity, then the phase portraits of the systems are equivalent to the Figures 3.6.15 and 3.6.16, respectively.

• **node - node:** If there are two nodes, by Proposition 3.2.1 there can exists an exterior node with two equilibrium points at the infinity or another one with four points, then the phase portraits of those systems are topologically equivalent to the Figures 3.6.17 and 3.6.18, respectively.

• **node - saddle:** For the case node-saddle, there are two types of nodes outside, by Proposition 3.2.1 with two or four equilibrium points at the infinity, or the saddle with 4 points, so the phase portraits of those systems are topologically equivalent to Figures 3.6.19, 3.6.20 and 3.6.21, respectively.

• **star node - node:** If we consider a star node, which has infinitely many equilibrium points at the infinity, and a improper one with four equilibrium points, then the phase portraits are topologically equivalent to the ones of the Figures 3.6.22 and 3.6.23, respectively depending on what vector field is in the exterior part.

• **star node - saddle:** For the case star node-saddle, the same options as before are getting using Proposition 3.2.1 and the phase portraits are topologically equivalent to the ones of the Figures 3.6.24 and 3.6.25.

• **saddle - saddle:** If there are two saddles, there exist four equilibrium points at the infinity by Proposition 3.2.1 and thus the phase portrait is topologically equivalent to the one of the Figure 3.6.28.

• **exceptions:** There are other exceptions to Proposition 3.2.3, for some restricted cases where we get a constant field along the lines. If there is a center X of the form of equation (3-6), then for each parallel line there are opposite constant vector fields. That is because

$$
\begin{aligned}
F_1(\mathbf{x}) &= \frac{1}{2}\begin{pmatrix} a_{11}+b_{11} & -(a_{22}+b_{22}) \\ -(a_{11}+b_{11}) & a_{22}+b_{22} \end{pmatrix}\begin{pmatrix} x \\ -x+1 \end{pmatrix} \\
&= \frac{1}{2}\begin{pmatrix} a_{11}+b_{11} & (a_{11}+b_{11}) \\ -(a_{11}+b_{11}) & -(a_{11}+b_{11}) \end{pmatrix}\begin{pmatrix} x \\ -x+1 \end{pmatrix} \\
&= \frac{1}{2}\begin{pmatrix} a_{11}+b_{11} \\ -(a_{11}+b_{11}) \end{pmatrix},
\end{aligned}
$$

$$
\begin{aligned}
F_2(\mathbf{x}) &= \frac{1}{2}\begin{pmatrix} a_{11}+b_{11} & -(a_{22}+b_{22}) \\ -(a_{11}+b_{11}) & a_{22}+b_{22} \end{pmatrix}\begin{pmatrix} x \\ -x-1 \end{pmatrix} \\
&= \frac{1}{2}\begin{pmatrix} a_{11}+b_{11} & (a_{11}+b_{11}) \\ -(a_{11}+b_{11}) & -(a_{11}+b_{11}) \end{pmatrix}\begin{pmatrix} x \\ -x-1 \end{pmatrix} \\
&= \frac{1}{2}\begin{pmatrix} -(a_{11}+b_{11}) \\ a_{11}+b_{11} \end{pmatrix}.
\end{aligned}
$$

In order to get the last one, again it is necessary the conditions $a_{22} = -a_{11}$ and $b_{22} = -b_{11}$, thus the cases which satisfy that are center-center, center-saddle or saddle-saddle as in the case of Σ_1.

Although, the Filippov vector field that is tangent to each line of Σ_2 does not vanish and has opposite and unique directions for each line, because fixing Y and perturbing X, the last one changes from a center to a saddle or vise-versa. Those phase portraits are topologically equivalent to the ones of the Figures 3.6.1, 3.6.9, 3.6.10 and 3.6.29.

$$
\frac{1}{2}\begin{pmatrix} a_{11}+b_{11} & (a_{11}+b_{11}) \\ -(a_{11}+b_{11}) & -(a_{11}+b_{11}) \end{pmatrix} = \frac{1}{2}\begin{pmatrix} a_{11} & (a_{11}+b_{11})-b_{12} \\ -(a_{11}+b_{11})-b_{21} & -a_{11} \end{pmatrix} +
$$

$$+\frac{1}{2}\begin{pmatrix} b_{11} & b_{12} \\ b_{21} & -b_{11} \end{pmatrix}$$

and $\det A = a_{11}b_{11} + a_{11}b_{21} + b_{11}a_{11} + b_{11}^2 + b_{11}b_{21} - a_{11}b_{12} - b_{11}b_{12} - b_{12}b_{21}$ thus one get $\det A = b_{11}^2 + b - 11(2a_{11} + b_{21} - b_{12}) + a_{11}(b_{21} - b_{12}) - b_{12}b_{21}$ such that

$$b_{11_\pm} = (-(2a_{11} + b_{21} - b_{12}) \pm \sqrt{4a_{11}^2 + (b_{21} + b_{12})^2})/2.$$

Then generically $\det A < 0$ (saddle) or $\det A > 0$ (center) in an open interval $I = (b_{11_-}, b_{11_+})$ and the other case in $\mathbb{R} \setminus I$.

Also, it is not possible the case of a star node and center or focus, the normal form for a star node is

$$B = \begin{pmatrix} -c & 0 \\ 0 & -c \end{pmatrix},$$

with $c \neq 0$, then $a_{21} = c - a_{11}$ and $a_{12} = c - a_{22}$, also for a center or focus $0 > (a_{11} + a_{22})^2 - 4(a_{11}a_{22} - a_{12}a_{21}) = ((a_{11} + a_{22}) - 2c)^2 \geq 0$, so we get a contradiction to the law of trichotomy of real numbers.

If $(a_{11} + a_{22}) - 2c = 0$, there is a node with two equilibrium points at the infinity and that implies $a_{11} - c = c - a_{22}$, therefore

$$\begin{aligned} F_1(\mathbf{x}) &= \frac{1}{2}\begin{pmatrix} a_{11} + b_{11} & a_{12} + b_{12} \\ -(a_{11} + b_{11}) & -(a_{12} + b_{12}) \end{pmatrix}\begin{pmatrix} x \\ -x + 1 \end{pmatrix} \\ &= \frac{1}{2}\begin{pmatrix} a_{11} - c & a_{11} - c \\ c - a_{11} & c - a_{11} \end{pmatrix}\begin{pmatrix} x \\ -x + 1 \end{pmatrix} \\ &= \frac{1}{2}\begin{pmatrix} a_{11} - c \\ c - a_{11} \end{pmatrix}, \end{aligned}$$

$$F_2(\mathbf{x}) = \frac{1}{2}\begin{pmatrix} a_{11}+b_{11} & a_{12}+b_{12} \\ -(a_{11}+b_{11}) & -(a_{12}+b_{12}) \end{pmatrix}\begin{pmatrix} x \\ -x-1 \end{pmatrix}$$
$$= \frac{1}{2}\begin{pmatrix} a_{11}-c & a_{11}-c \\ c-a_{11} & c-a_{11} \end{pmatrix}\begin{pmatrix} x \\ -x-1 \end{pmatrix}$$
$$= \frac{1}{2}\begin{pmatrix} c-a_{11} \\ a_{11}-c \end{pmatrix}.$$

Then the case star node-node with 2 equilibrium points at the infinity is another exception and the phase portraits of those situations are topologically equivalent to the ones of the Figures 3.6.26 and 3.6.27. □

Remark 3.3.1 *There exists a case center-center with a chaotic limit set, it will be analyzed in the next chapter.*

Proof. [Proof of Theorem 3.1.1 (**iii**)] In this case there are two transversal lines as switching manifold, so there is a linear system in each two opposite regions, and all the possibilities for the canonical regions are described in Table 3.1.

By Proposition 3.2.2 the tangency point is generically the origin. The Proposition 3.2.3 describes the behavior of the invariant manifolds of a saddle in the Filippov vector field, with a pseudo-equilibrium point at the intersection of the discontinuity region, and those lines cross the origin, so there is no a strict singularity in the finite part. Finally, by Proposition 3.2.4 there exist four pseudo-equilibrium points at the infinity, four pseudo-nodes or four pseudo-saddles. For the following cases the canonical regions are determined by the last 3 propositions.

• **center - center:** If there are centers, by Proposition 3.2.1 the vector fields do not have equilibrium points at the infinity, thus the phase portrait of that system is topologically equivalent to the one of Figure 3.7.1.

• **exceptions:** The cases C-F, C-N are not possible in this inelastic context, because if there is a center (equation (3-6)), with $tr(A) = 0$ and $\det(A) > 0$, then for B $tr(B) = tr(A) = 0$ and two possibilities $\det(B) > 0$ (center) or $\det(B) < 0$ (saddle). We are not considering the cases where $\det(B) = 0$. Also SN-N, SN-S do not appear because the orbits of the SN coincides with the switching manifold.

For the cases where a saddle is located in a side of the discontinuity, there are only 2 singularities at the infinity with other saddle because if we consider

$$B = \begin{pmatrix} a & 0 \\ 0 & -b \end{pmatrix},$$

with $a, b > 0$, a saddle with two singularities in one of the opposite regions, then $a_{11} = -a$, $a_{22} = b$ and $a_{12} = a_{21}$ and thus $(a_{11} + a_{22})^2 - 4(a_{11}a_{22} - a_{12}a_{21}) = (b+a)^2 + 4a_{12}^2 > 0$ and $\det(A) = -ab - a_{12}^2 < 0$, therefore by Proposition 3.2.1 the only option is another saddle.

• **center - saddle:** Thus, for the case center-saddle there are only two options by Proposition 3.2.1, zero or four equilibrium points at the infinity in the part where is the saddle, and the phase portraits will be topologically equivalent to Figures 3.7.2 or 3.7.3, respectively.

• **focus - focus:** If there are two focuses, by Proposition 3.2.1 there are no equilibrium points at the infinity, thus the phase portrait of that system is topologically equivalent to the one of Figure 3.7.4.

• **focus - node:** For the case focus-node there exist three possibilities by Proposition 3.2.1, zero, two or four equilibrium points at the infinity in the region where is the node, and the phase portraits will be topologically equivalent to Figures 3.7.5, 3.7.6 or 3.7.7, respectively.

• **focus - saddle:** If there are a focus and a saddle, because of the exceptions there exist only the possibilities of zero or four equilibrium points at the infinity, thus the phase

portrait of those systems are topologically equivalent to the ones of the Figures 3.7.8 and 3.7.9.

• **node - node:** For the case node-node, there are five options by Proposition 3.2.1 depending of the type of nodes that we get and the position of their equilibrium point at the infinity. Those options are zero, two, four, six or eight equilibrium points at the infinity in the region where the nodes are, and the phase portraits will be topologically equivalent to the Figures 3.7.10, 3.7.11, 3.7.12, 3.7.13 and 3.7.14, respectively.

• **node - saddle:** If there are a node and a saddle, again depending on the place of the node and the saddle, there exist nodes with zero, two or four equilibrium points at the infinity, and in the same way the saddle with zero or four singularities at the infinity in its region, them again there exist the possibilities of zero, two, four, six or eight equilibrium points at the infinity and their phase portrait of the systems are topologically equivalent to the ones of the Figures 3.7.16, 3.7.17, 3.7.18, 3.7.19, 3.7.20 and 3.7.21.

• **saddle - saddle:** For concluding, in the case saddle-saddle there are three possibilities by Proposition 3.2.1 and the previous facts, zero or four equilibrium points at the infinity for each saddle, thus we can get at the end zero, four or eight equilibrium points for the NSVF and the phase portraits are topologically equivalent to the Figures 3.7.20, 3.7.21 and 3.7.22, respectively. □

Fig/Op	(1)	(2)	(3)	(4)	(5)	(6)	(7)
3.5.1	-	x	-	-	x	-	-
3.5.2	-	x	-	x	-	-	-
3.5.3	-	x	x	x	-	-	-
3.5.4	-	x	x	x	-	-	-
3.5.5	-	x	x	-	x	-	-
3.5.6	-	x	x	x	-	-	-
3.5.7	-	x	-	x	-	-	-
3.5.8	-	x	x	x	-	-	-

Fig/Op	(1)	(2)	(3)	(4)	(5)	(6)	(7)
3.5.9	-	x	x	x	-	-	-
3.5.10	-	x	x	x	-	-	-
3.5.11	-	x	x	x	-	-	-
3.5.12	-	x	x	x	-	-	-
3.5.13	-	x	x	x	-	-	-
3.5.14	-	x	x	x	-	-	-
3.5.15	-	x	x	x	-	-	-
3.5.16	-	x	x	-	x	-	-

Table 3.2: ω-*limit options (Op) for the phase portraits of Figures 3.5 (Fig).*

Proof. [Proof of Theorem 3.1.2] For the α or ω-limit sets of a point $\mathbf{x} \in \mathbb{R}^2$ in the

differential systems (3-3), we can see due to the Poincaré-Bendixson theorem in the Poincaré disk, Proposition 3.2.1 and [22] in the phase portraits of Figures 3.5, 3.6 and 3.7, described in the Tables 3.2, 3.3 and 3.4. □

Fig/Op	(1)	(2)	(3)	(4)	(5)	(6)	(7)
3.6.1	x	-	-	-	x	x	x
3.6.2	x	x	-	-	x	-	x
3.6.3	x	x	-	-	x	x	x
3.6.4	x	x	-	-	x	-	x
3.6.5	x	x	x	-	x	x	-
3.6.6	x	x	x	-	x	x	-
3.6.7	x	x	-	-	x	-	x
3.6.8	x	x	x	-	x	-	-
3.6.9	x	-	-	-	x	-	x
3.6.10	x	-	x	-	x	-	-
3.6.11	x	x	-	-	x	-	x
3.6.12	x	x	-	-	x	-	x
3.6.13	x	x	x	-	x	-	-
3.6.14	x	x	x	-	x	-	-
3.6.15	x	x	-	-	x	-	x

Fig/Op	(1)	(2)	(3)	(4)	(5)	(6)	(7)
3.6.16	x	x	x	-	x	-	-
3.6.17	x	x	x	-	x	-	-
3.6.18	x	x	x	-	x	-	-
3.6.19	x	x	x	-	x	-	-
3.6.20	x	x	x	-	x	-	-
3.6.21	x	x	x	-	x	-	-
3.6.22	x	x	x	-	x	-	-
3.6.23	x	x	x	-	x	-	-
3.6.24	x	x	x	-	x	-	-
3.6.25	x	x	x	-	x	-	-
3.6.26	x	-	x	-	x	-	-
3.6.27	x	-	x	-	x	-	-
3.6.28	x	x	x	-	x	-	-
3.6.29	x	-	x	-	x	-	-

Table 3.3: ω-*limit options (Op) for the phase portraits of Figures 3.6 (Fig).*

Fig/Op	(1)	(2)	(3)	(4)	(5)	(6)	(7)
3.7.1	-	x	-	x	-	-	-
3.7.2	-	x	-	x	-	-	-
3.7.3	-	x	x	x	-	-	-
3.7.4	-	x	-	x	-	-	-
3.7.5	-	x	-	x	-	-	-
3.7.6	-	x	x	x	-	-	-
3.7.7	-	x	x	x	-	-	-
3.7.8	-	x	-	x	-	-	-
3.7.9	-	x	x	x	-	-	-
3.7.10	-	x	-	x	-	-	-
3.7.11	-	x	x	x	-	-	-

Fig/Op	(1)	(2)	(3)	(4)	(5)	(6)	(7)
3.7.12	-	x	x	x	-	-	-
3.7.13	-	x	x	x	-	-	-
3.7.14	-	x	x	x	-	-	-
3.7.15	-	x	-	x	-	-	-
3.7.16	-	x	x	x	-	-	-
3.7.17	-	x	x	x	-	-	-
3.7.18	-	x	x	x	-	-	-
3.7.19	-	x	x	x	-	-	-
3.7.20	-	x	-	x	-	-	-
3.7.21	-	x	x	x	-	-	-
3.7.22	-	x	x	x	-	-	-

Table 3.4: ω-*limit options (Op) for the phase portraits of Figures 3.7 (Fig).*

3.4 Conclusions

We have shown 123 phase portraits which correspond to all cases that one can get with generic linear vector fields and coincident, parallel or transversal lines as switching manifold in $\mathbb{R}^2$, forming an inelastic piecewise differential system. We made the global analysis considering tangencies and equilibrium and pseudo-equilibrium points in the finite and infinite part. Also we get a result for the limit sets in inelastic planar PSVF. Also, as future work, we will compare this theory with other results in refractive piecewise differential systems and try to find another types of canonical regions.

3.5 Phase Portraits

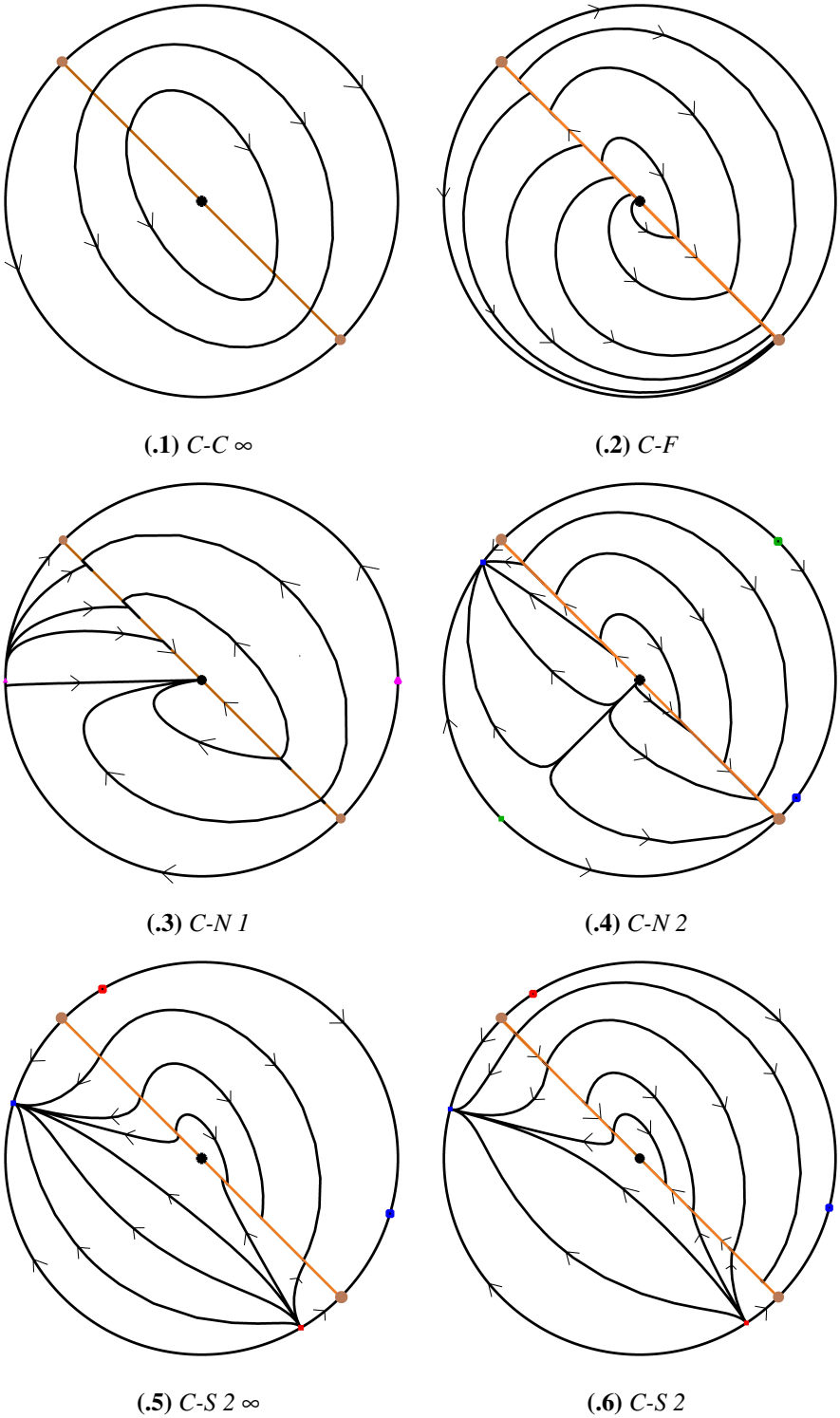

(.1) *C-C* ∞ **(.2)** *C-F*

(.3) *C-N 1* **(.4)** *C-N 2*

(.5) *C-S 2* ∞ **(.6)** *C-S 2*

Figure 3.5: *Phase portraits with a line as switching manifold.*

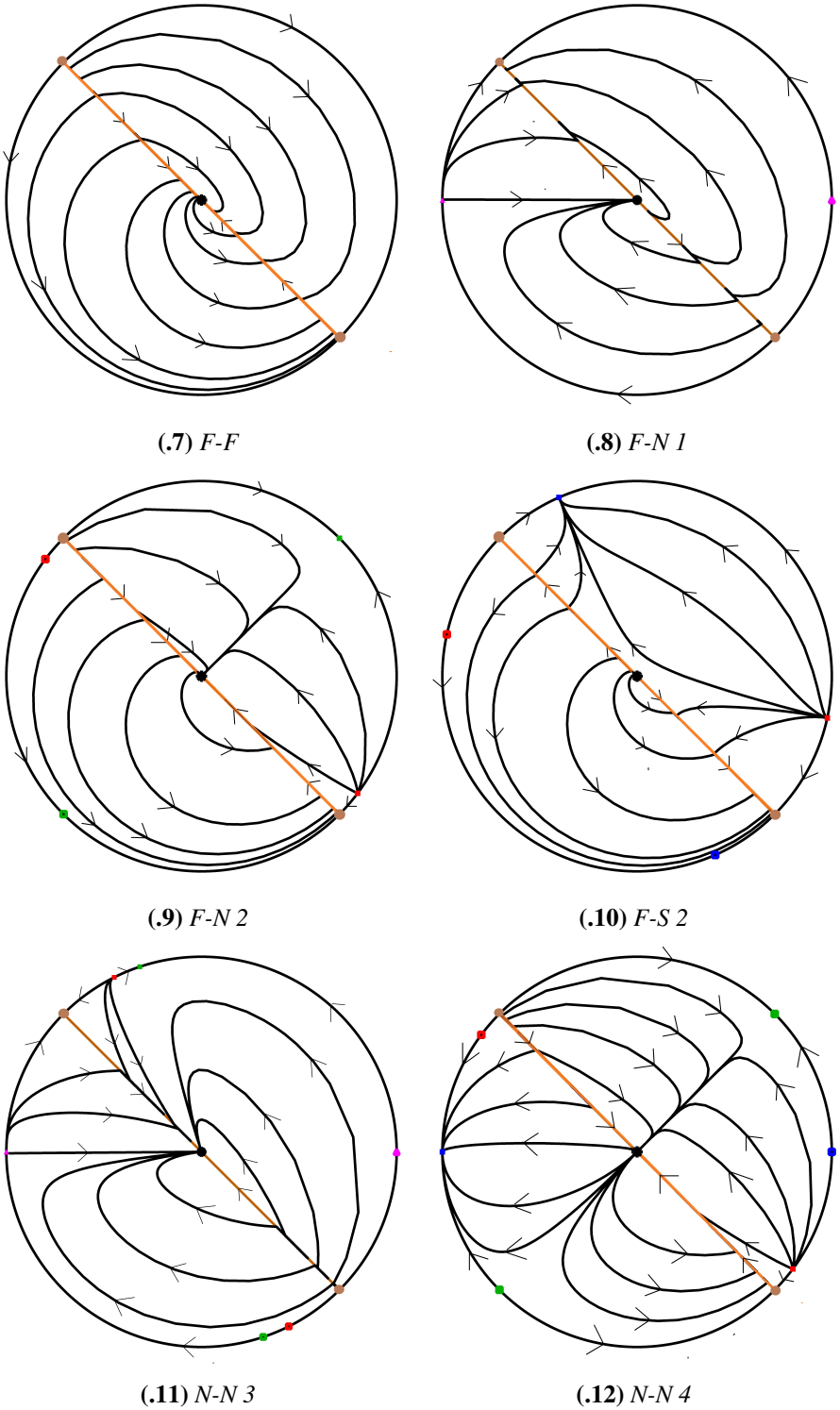

(.7) *F-F* **(.8)** *F-N 1*

(.9) *F-N 2* **(.10)** *F-S 2*

(.11) *N-N 3* **(.12)** *N-N 4*

Figure 3.5: *Phase portraits with a line as switching manifold.*

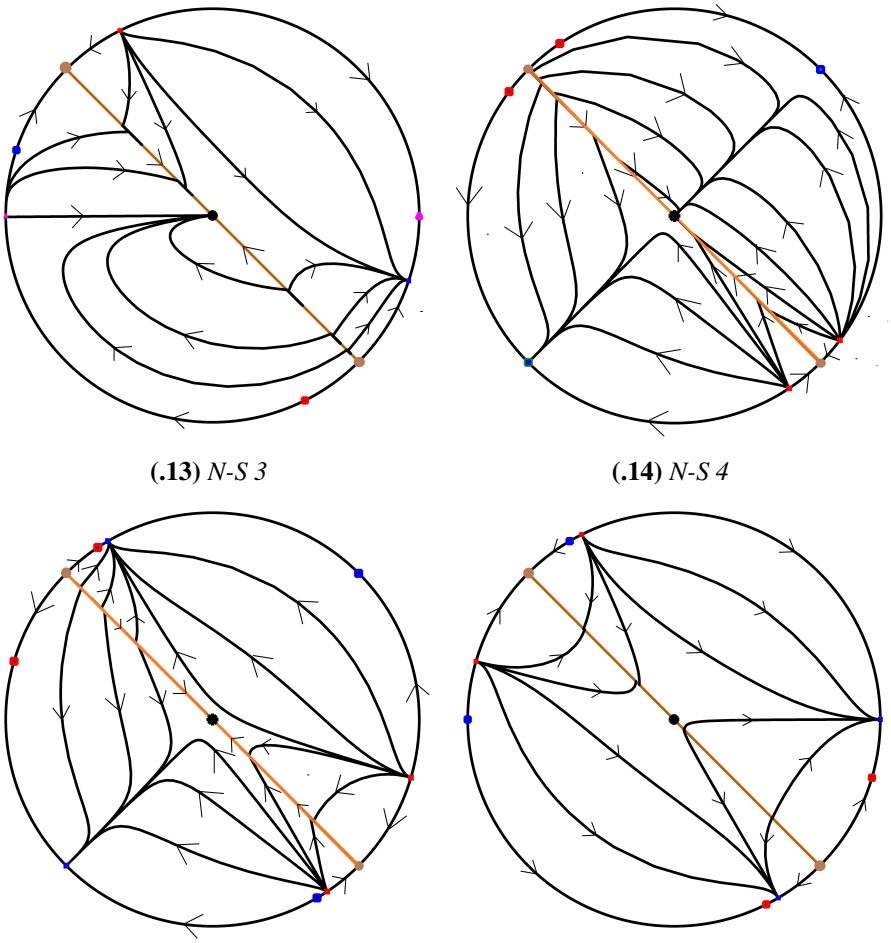

(.13) *N-S 3* **(.14)** *N-S 4*

(.15) *S-S 4* **(.16)** *S-S 4 ∞*

Figure 3.5: *Phase portraits with a line as switching manifold.*

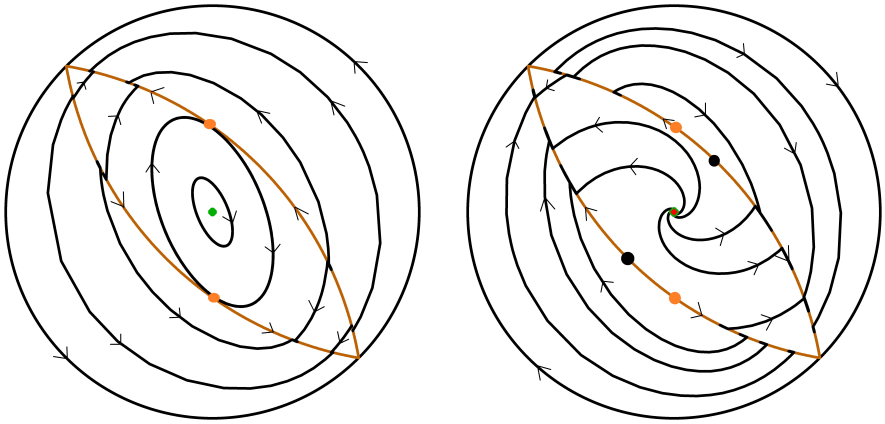

(.1) *C-C Constant* **(.2)** *C-F*

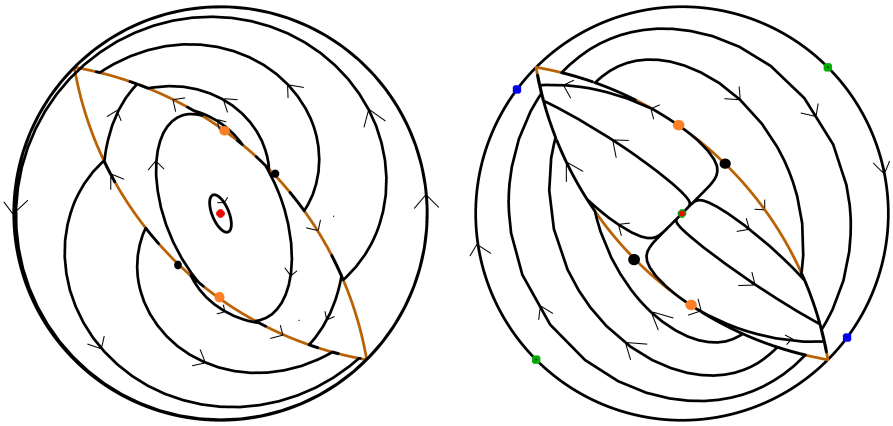

(.3) *F-C* **(.4)** *C-N 0*

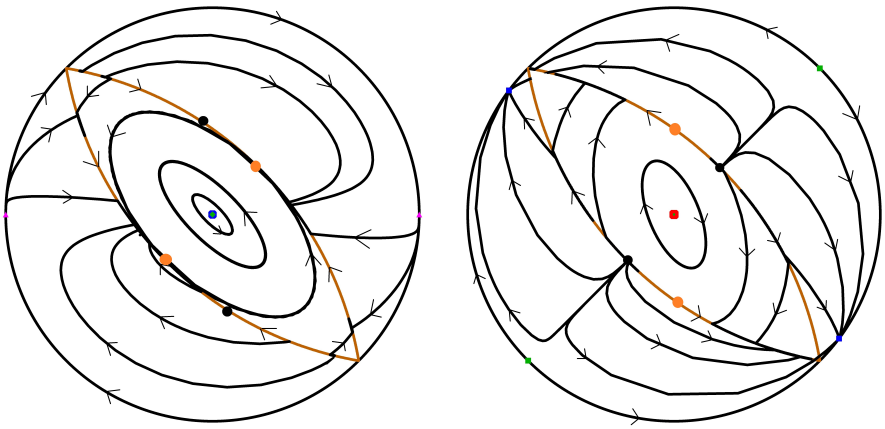

(.5) *C-N 2* **(.6)** *C-N 4*

Figure 3.6: *Phase portraits with two parallel lines as switching manifold.*

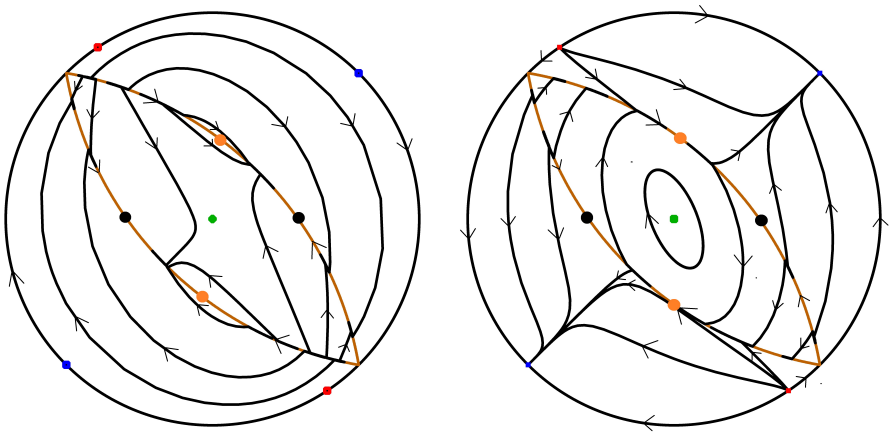

(.7) *C-S 0* **(.8)** *C-S 4*

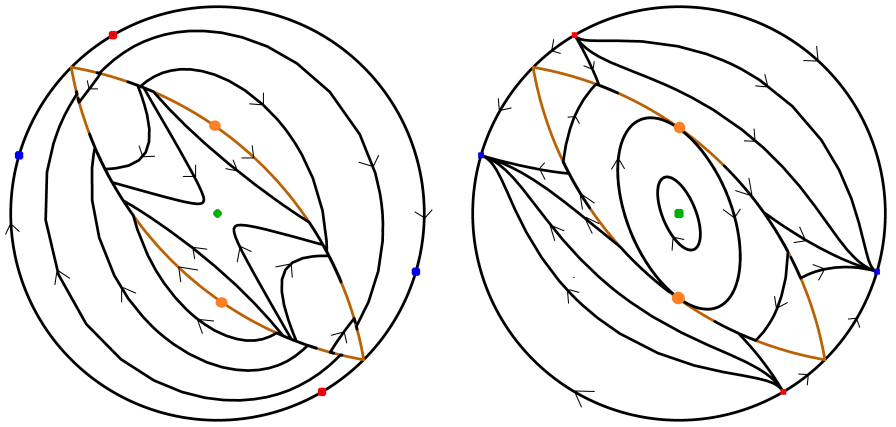

(.9) *C-S 0 Const* **(.10)** *C-S 4 Const*

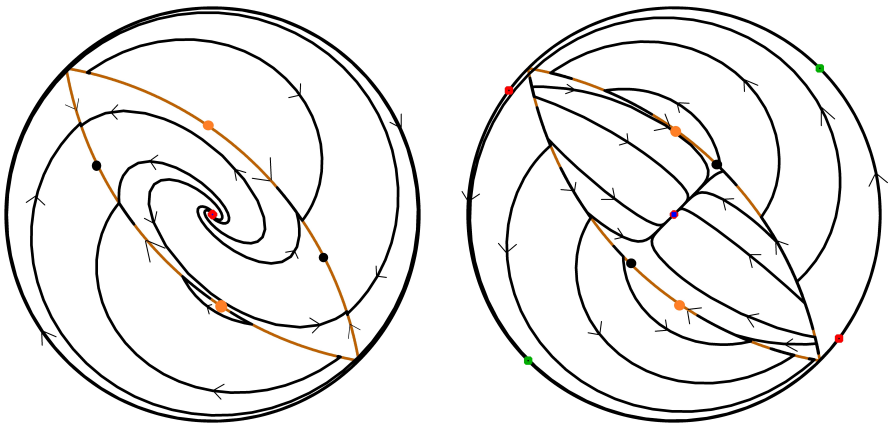

(.11) *F-F* **(.12)** *F-N 0*

Figure 3.6: *Phase portraits with two parallel lines as switching manifold.*

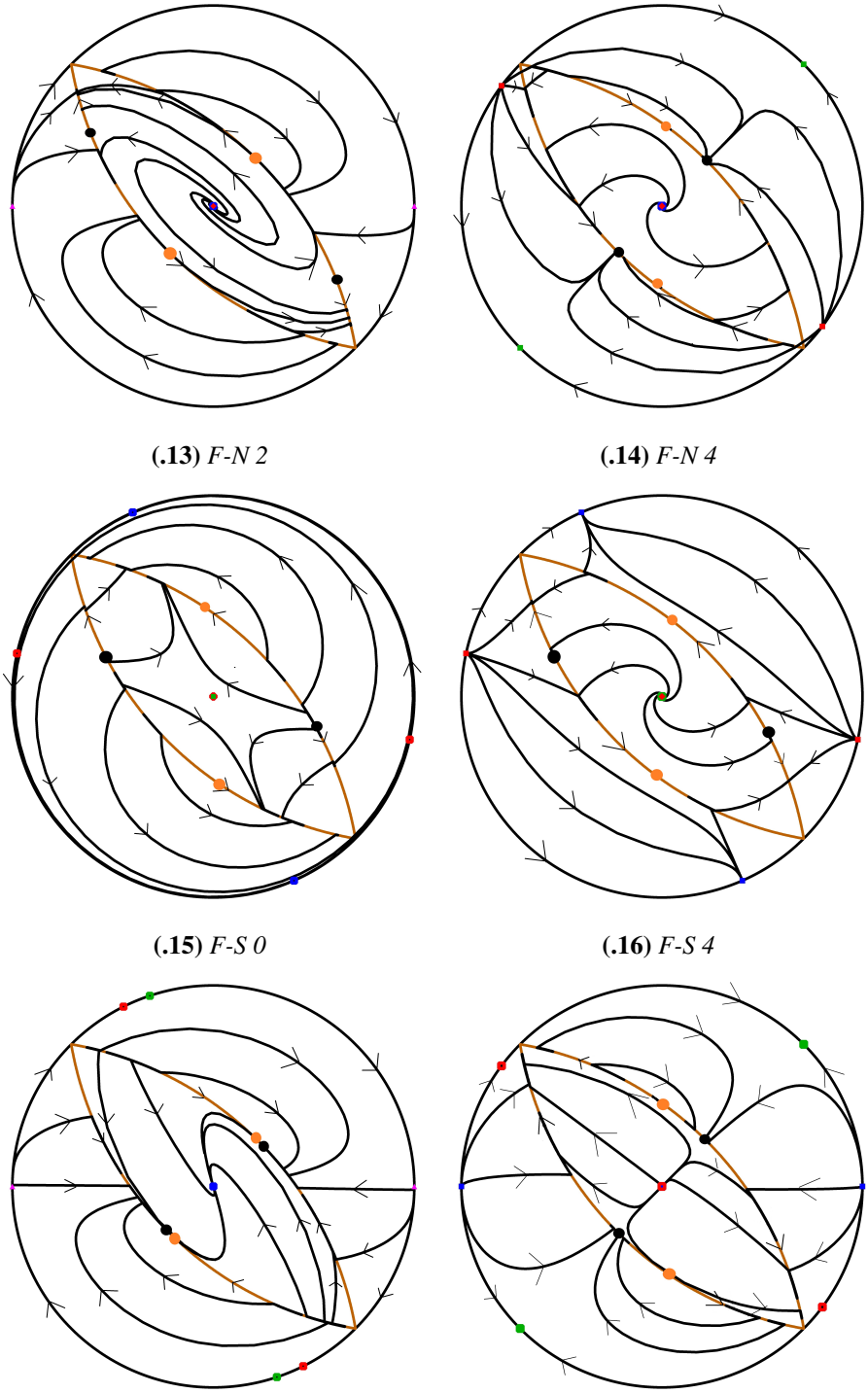

(.13) *F-N 2*

(.14) *F-N 4*

(.15) *F-S 0*

(.16) *F-S 4*

(.17) *N-N 2*

(.18) *N-N 4*

Figure 3.6: *Phase portraits with two parallel lines as switching manifold.*

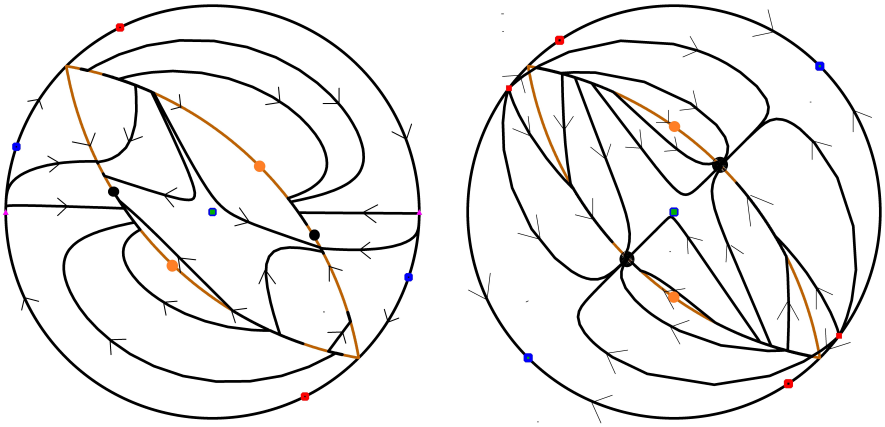

(.19) *N-S 2* **(.20)** *N-S 4*

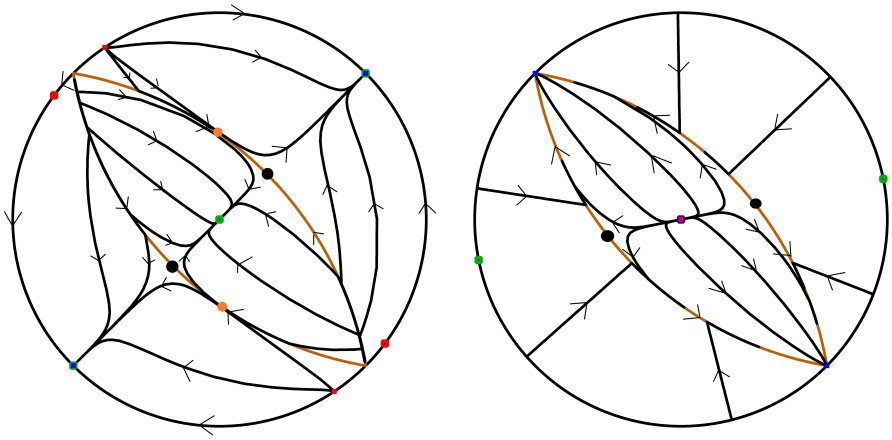

(.21) *S-N 4* **(.22)** *SN-N ∞*

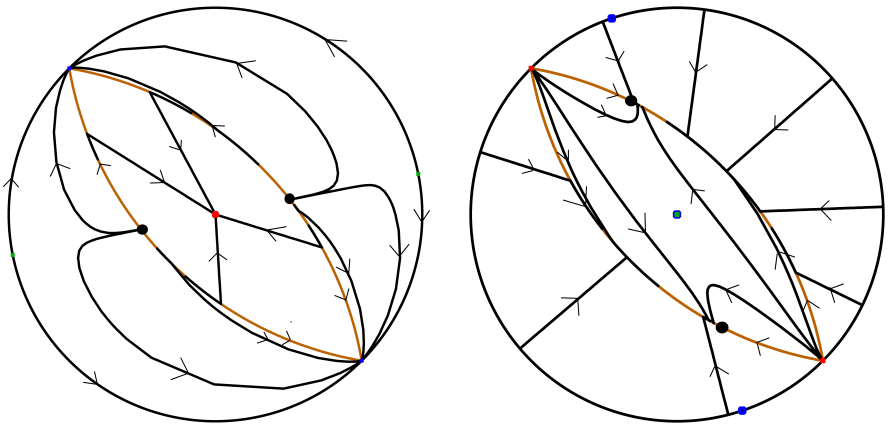

(.23) *SN-N 4* **(.24)** *SN-S ∞*

Figure 3.6: *Phase portraits with two parallel lines as switching manifold.*

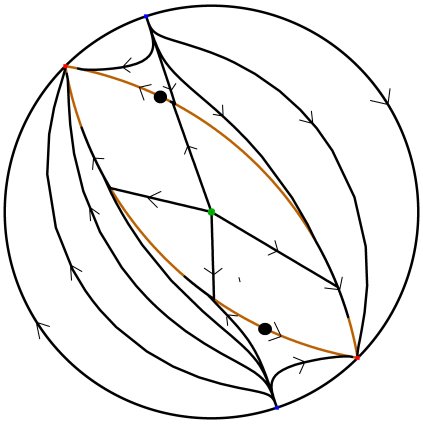

(.25) *SN-S 4*

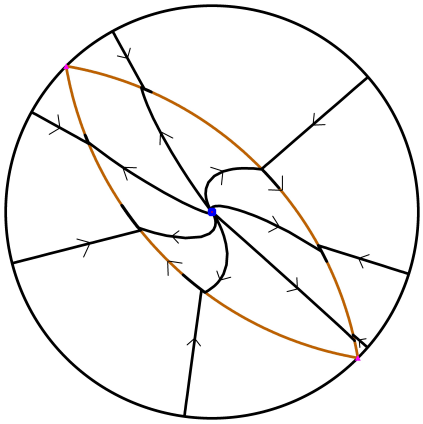

(.26) *SN-N 2 ∞ Const*

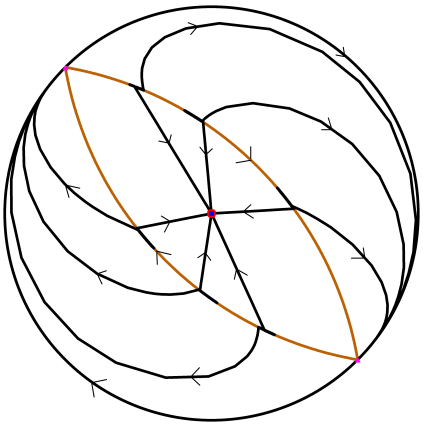

(.27) *SN-N 2 Const*

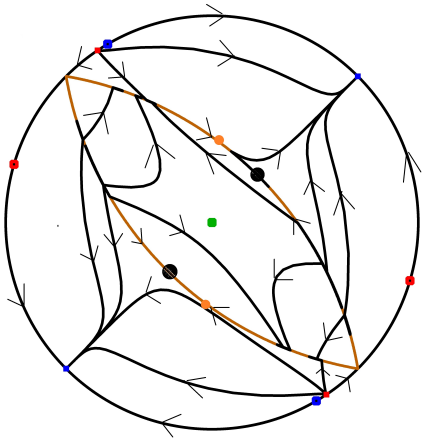

(.28) *S-S 4*

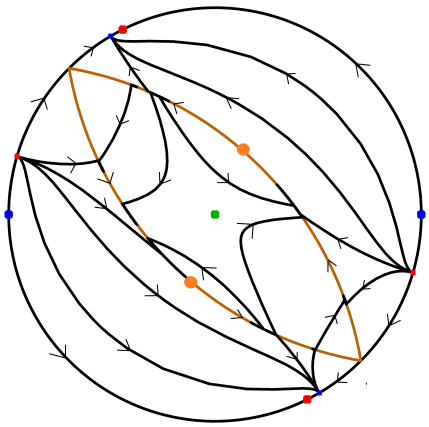

(.29) *S-S 4 Const*

Figure 3.6: *Phase portraits with two parallel lines as switching manifold.*

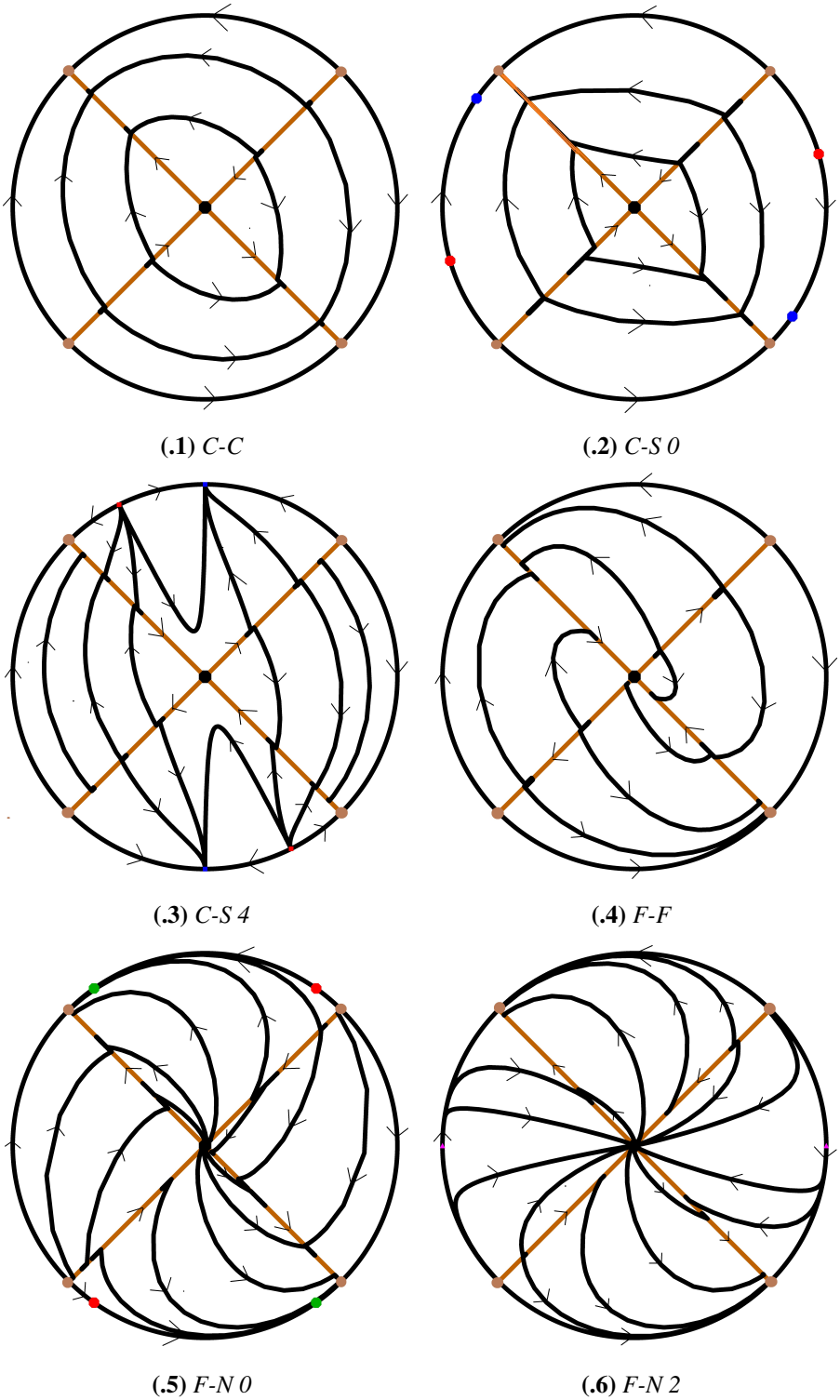

(.1) *C-C* **(.2)** *C-S 0*

(.3) *C-S 4* **(.4)** *F-F*

(.5) *F-N 0* **(.6)** *F-N 2*

Figure 3.7: *Phase portraits for the case* $\Sigma = \Sigma_3$.

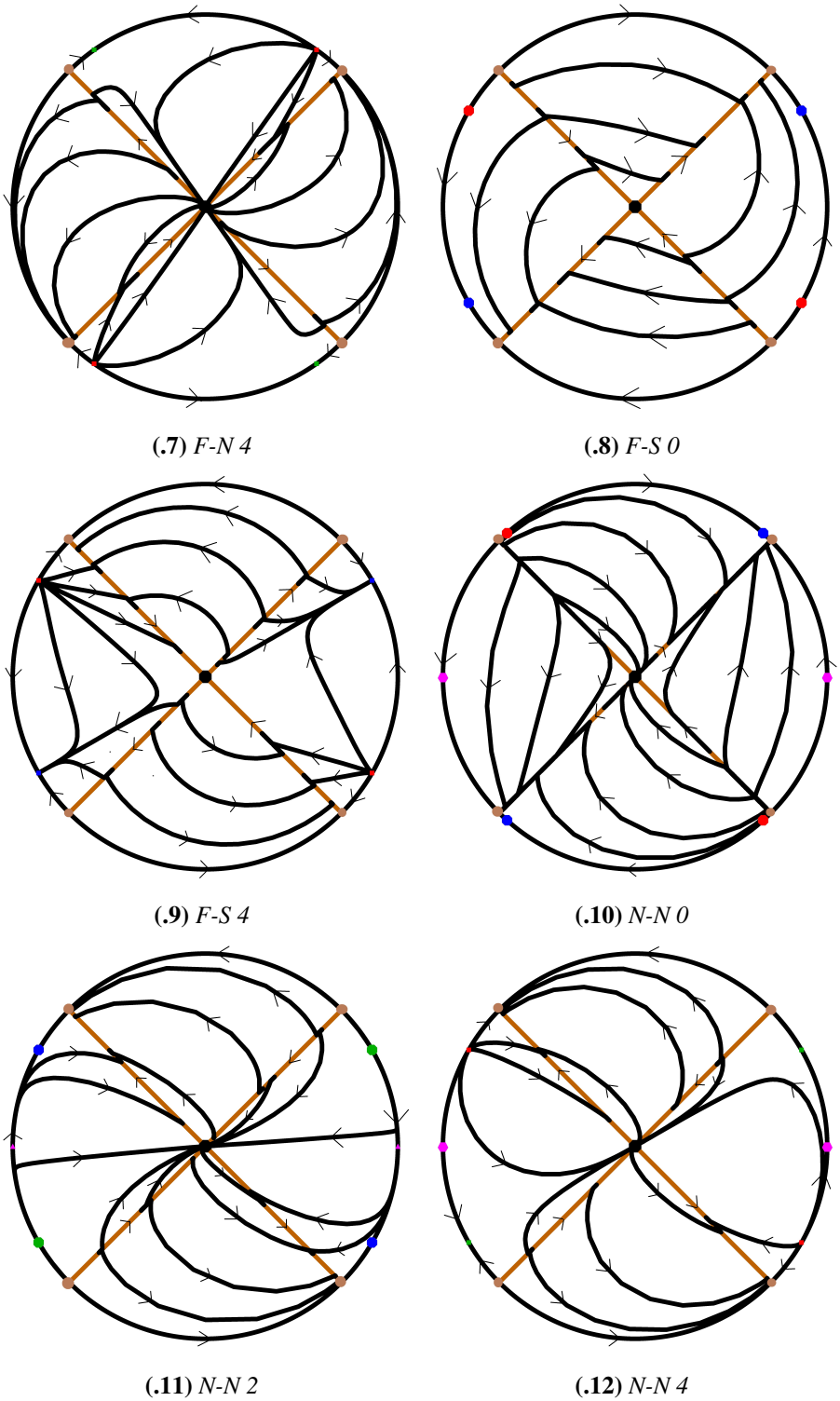

(.7) *F-N 4* **(.8)** *F-S 0*

(.9) *F-S 4* **(.10)** *N-N 0*

(.11) *N-N 2* **(.12)** *N-N 4*

Figure 3.7: *Phase portraits for the case* $\Sigma = \Sigma_3$.

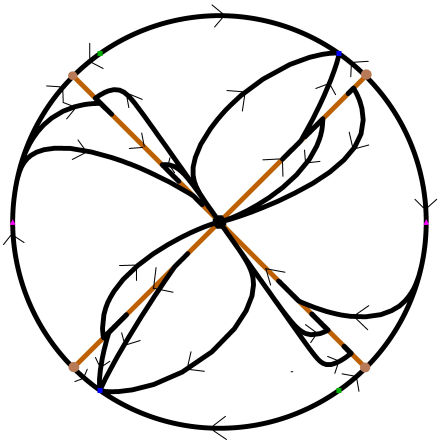

(.13) *N-N 6*

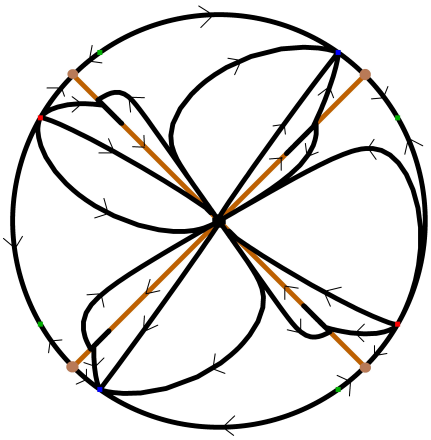

(.14) *N-N 8*

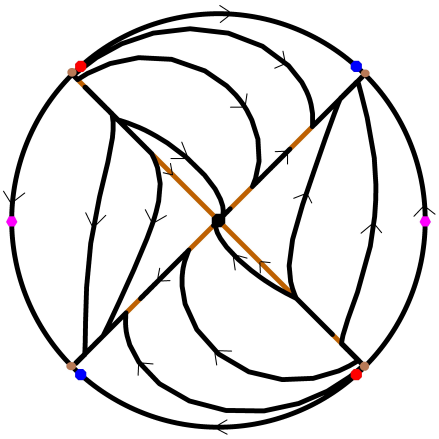

(.15) *N-S 0*

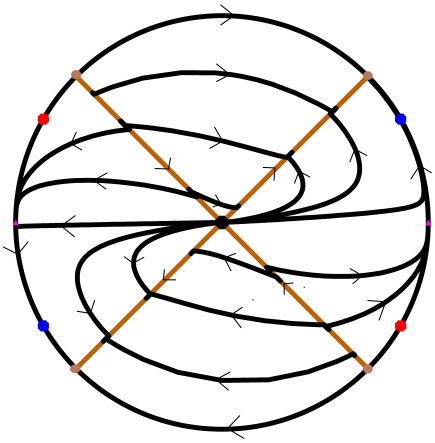

(.16) *N-S 2*

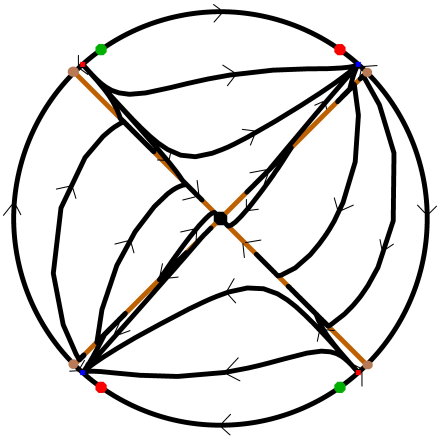

(.17) *N-S 4*

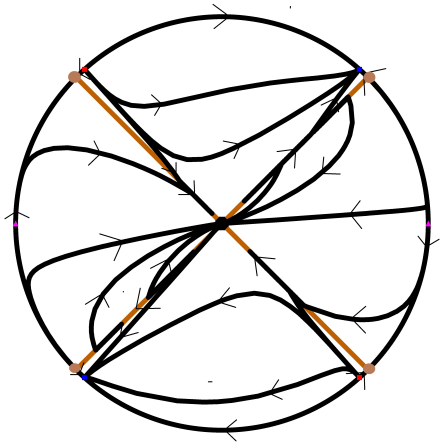

(.18) *N-S 6*

Figure 3.7: *Phase portraits for the case* $\Sigma = \Sigma_3$.

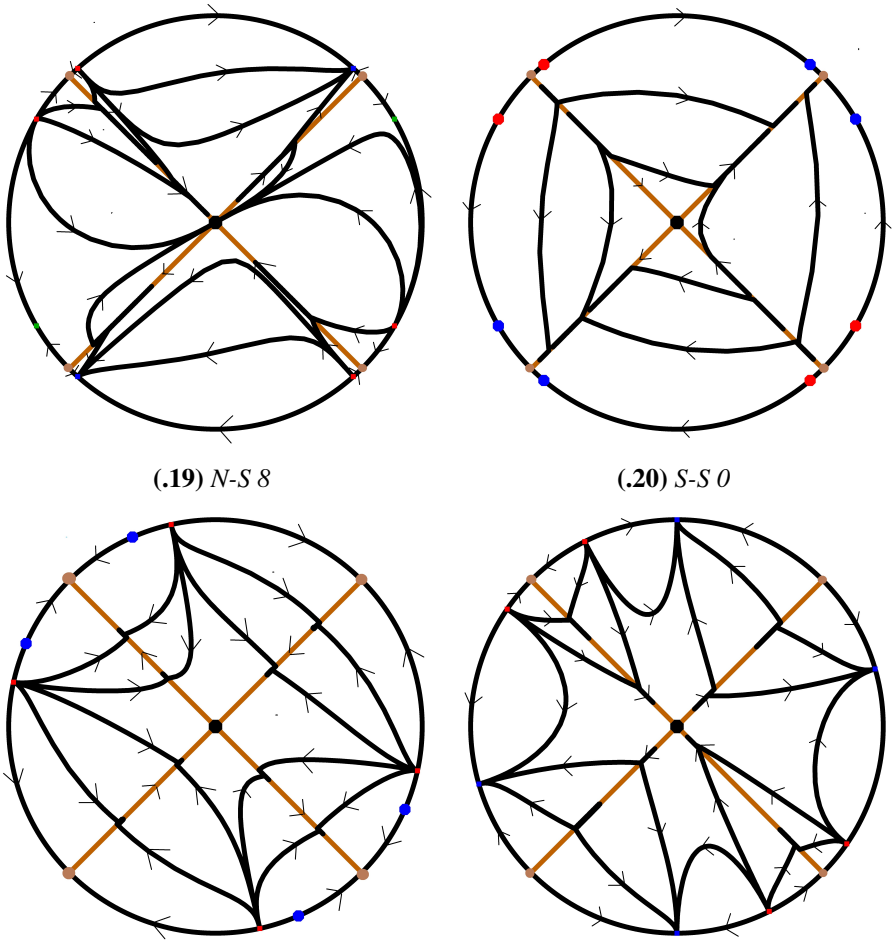

(.19) *N-S 8* **(.20)** *S-S 0*

(.21) *S-S 4* **(.22)** *S-S 8*

Figure 3.7: *Phase portraits for the case* $\Sigma = \Sigma_3$.

CHAPTER 4

Global Dynamics of Inelastic Non-Smooth Linear Vector Fields in $\mathbb{R}^2$ Considering Conics and Algebraic Curves

Let $Z = (X, Y)$ be a PSVF. In this chapter we will continue the study presented in the last one, for switching manifolds as unitary conics and algebraic curves.

Firstly, we are going to describe the discontinuity regions Σ of a PSVF (2-4). According to the normal forms shown in [6], there are 9 possibilities for the curves in $\mathbb{R}^2$, but only six are in the real space, beyond the one element set, coincident lines, ellipse, hyperbola, parabola, and intersecting or parallel lines. Hence, the switching manifolds Σ remained to be considered are non-degenerate quadrics: circle-ellipse (Σ_1), hyperbola (Σ_2) and parabola (Σ_3) where we include algebraic curves of the form $y - x^n = 0$, for $n \in \mathbb{N}$ and $n \geq 2$. Thus

(1) $\Sigma_1 = \{(x,y) \in \mathbb{R}; x^2 + y^2 = 1\} = f_1^{-1}(0)$, $f_1(x,y) = x^2 + y^2 - 1$;
(2) $\Sigma_2 = \{(x,y) \in \mathbb{R}; x^2 - y^2 = 1\} = f_2^{-1}(0)$, $f_2(x,y) = x^2 - y^2 - 1$;
(3) $\Sigma_3 = \{(x,y) \in \mathbb{R}; y - x^n = 0\} = f_3^{-1}(0)$, $f_3(x,y) = y - x^n$.

Then $\Sigma_i = f_i^{-1}(0)$, where each $f_i(x,y) = a_i x^2 + 2b_i xy + c_i y^2 + 2d_i x + 2e_i y + g_i$, and

$$\begin{vmatrix} a_i & b_i & d_i \\ b_i & c_i & e_i \\ d_i & e_i & g_i \end{vmatrix} \neq 0,$$

for some constants $a_i, \ldots, g_i \in \mathbb{R}$, $i = 1,2,3$.

The main goal of the chapter is to study the global trajectories of linear PSVF. Consider the linear vector fields $X(\mathbf{x}) = A\mathbf{x}$ and $Y(\mathbf{x}) = B\mathbf{x}$ where $A = (a_{ij})$, $B = (b_{ij})$, $i, j = 1,2$, are square matrices with real entries such that $\det(A) \neq 0$ and $\det(B) \neq 0$, $A \neq -B$. We assume that $Z = (X,Y)$ is inelastic over Σ.

4.1 Main Results

The main goal of the chapter is to classify the global phase portraits of inelastic linear PSVF. As before we consider the linear vector fields X and Y joint with the following system

$$\begin{cases} X(\mathbf{x}) = A\mathbf{x}, \quad A = (a_{ij}); \\ Y(\mathbf{x}) = B\mathbf{x}, \quad B = (b_{ij}); \\ \det(A)\det(B) \neq 0; \\ Z = (X,Y) \text{ is inelastic over } \Sigma, \end{cases} \tag{4-1}$$

where A and B are square matrices with real entries.

4.1.1 Compactification and Stability Classes

Theorem 4.1.1 *(i) If the switching manifold is Σ_1, then generically any PSVF is topologically equivalent to one of the 23 phase portraits of Figure 4.2.*

(ii) If the switching manifold is Σ_2, generically the phase portraits are topologically equivalent to one of the 34 of Figure 4.3.

(iii) If the switching manifold is Σ_3, consisting of even curves ($y - x^{2n} = 0$) or odd ones ($y - x^{2n+1} = 0$), the PSVF can be generically one of the 30 phase portraits of Figure 4.4.

CR	TA			E			PE			∞ E			∞ PE		
QT	Σ_1	Σ_2	Σ_3	Σ_1	Σ_2	Σ_3	Σ_1	Σ_2	Σ_3	Σ_1	Σ_2	Σ_3	Σ_1	Σ_2	Σ_3
C-C	4	2	-	1	1	-	0	0	-	0	0	-	0	4	-
C-F	-	-	m	-	-	1^*	-	-	1	-	-	0	-	-	0-2
C-N	-	-	m	-	-	1^*	-	-	1	-	-	0-2-4	-	-	0-2
C-S	4	2	-	1	1	-	0	0	-	0-4	0-4	-	0	4	-
F-F	2-4	2	m	1	1	1^*	0	0	1	0	0	0	0	4	0-2
F-N	2-4	2	m	1	1	1^*	0	0	1	0-2-4	0-2-4	0-2-4	0	4	0-2
F-S	4	2	m	1	1	1^*	0	0	1	0-4	0-4	0-2-4	0	4	0-2
F-SN	0	-	-	1	-	-	0	-	-	0-∞	-	-	0	-	-
SN-N	-	0	0	-	1	1^*	-	0	1	-	∞	4-∞	-	4^*	0
SN-S	-	0	0	-	1	1^*	-	0	1	-	∞	4-∞	-	4^*	0
N-N	0-2-4	0-2-4	m	1	1	1^*	0	0	1	2-4	0-2-4-6-8	2-3-4	0	4	0-2
N-S	4	0-2-4	m	1	1	1^*	0	0	1	4	0-2-4-6-8	4	0	4	0-2
S-S	4	0-2-4	m	1	1	1^*	0	0	1	4	0-4-8	4	0	4	0-2

Table 4.1: *Canonical regions (CR) for Tangencies (TA), Equilibrium points (E), Pseudo-Equilibrium points (PE), Equilibrium points at the infinity (∞E) and Pseudo-Equilibrium points at the infinity (∞PE) with the qualitative types (QT) centers (C), focuses (F), saddles (S), nodes (N) and star nodes (SN), circle (Σ_1), hyperbola (Σ_2), Algebraic curves (Σ_3).*

Corollary 4.1.1 *There exists generically 174 phase portraits on the Poincaré disk of the inelastic system* (4-1)*. The global dynamics of the system is generically described by each corresponding cell of Table 4.1.*

Remark 4.1.1 *We can see some different topological behaviors among the phase portraits for those inelastic differential systems in Table 4.1 that deserve to be distinguished.*

1. There are different number of equilibrium points at the infinity, from 0 to 8 and also infinitely many singularities (proper node).
2. There is a strict equilibrium point in the finite part with a circle and a hyperbola, in the other cases the origin is also a pseudo-equilibrium (with notation 1^*). For Σ_2 the notation 4^* is for the four fake crossing pseudo-equilibrium points at the infinity.
3. Some cases having centers and proper nodes are not realizable inside the class of inelastic vector fields.
4. When $\Sigma = \Sigma_2$, a different kind of points at the infinity take place, where the two lines converge at the infinity, the vector fields X and Y reach or leave those points in

finite time at the infinity but in the finite part the ones reach and leave those points in infinite time.

5. We are not considering the cases where the orbits of the vector fields coincide with the discontinuity region. For example, centers which coincides with the circle, or saddles with orbits over the hyperbola.
6. Fixing one vector field of $Z = (X, Y)$, we can get another direction for the Filippov vector field (when it is different from zero) by perturbing the other one. Thus, looking at the whole set of canonical regions, for each phase portrait in the Figures 4.2, 4.3 and 4.4 there exists an analogous phase portrait, but now the Filippov vector field points in the opposite direction.
7. The case focus-saddle with an algebraic curve as discontinuity region is the only one which depends on the degree of the algebraic curve $y = x^n$.

4.1.2 Strange Attractors, Periodic Orbits and Chaos

Some phase portraits of those stability classes show interesting behaviors.

Theorem 4.1.2 *Consider the unit circle as switching manifold. If the exterior vector field, related to the circle, has eigenvalues with negative real part, and the ones of the interior vector field have positive real part. Then*

1. *If either there is no tangency points or only two tangency points over the circle, then* $\mathbb{S}^1$ *is an attractive limit cycle and the* $\omega-$*limit set for all* $\boldsymbol{x} \in \mathbb{R}^2 \setminus \{0\}$.
2. *If there are four tangency points over the circle, then we get a minimal global strange attractor* Γ *such that* $\mathbb{S}^1 \subset \Gamma$. *See Figure 4.1.*

Remark 4.1.2 *The differential systems (2-4) which are topologically equivalent to the phase portraits of the Figures 4.2.13 to 4.2.23 can have a periodic orbit and 4.2.4, 4.2.5, 4.2.6 and 4.2.9 can have a strange attractor (repulsor) which are the global* (α) ω*-limit sets for all* $\boldsymbol{x} \in \mathbb{R}^2$.

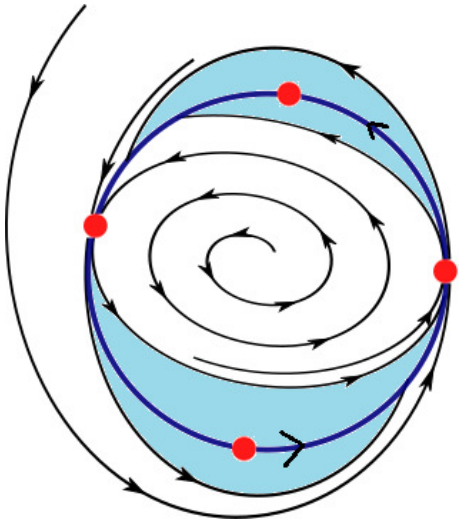

(.1) *Focus-Focus*

Figure 4.1: *Example of a strange attractor.*

4.1.3 Limit Sets

Following the same idea of the last chapter, we present a result for limits sets according to the stability classes.

Theorem 4.1.3 *The* α *or* ω*-limit set of a point on the Poincaré disk of the inelastic system* (4-1) *generically is one the following possibilities:*

1. *a boundary equilibrium point at the origin;*
2. *a pseudo-equilibrium of the Filippov vector field;*
3. *an equilibrium point at the infinity;*
4. *a pseudo-equilibrium point at the infinity;*
5. *a fake crossing pseudo-equilibrium point at the infinity;*
6. *a periodic orbit in the finite part;*
7. *a periodic orbit at the infinity;*
8. *a chaotic graphic;*
9. *a strange attractor.*

4.2 Filippov Vector Field, Tangency Points and Infinity Dynamics

In this section we will study the main properties of the Filippov vector field for system (4-1), also the configuration of tangency points and the behavior at the infinity.

Using equation (2-5), then

$$Xf(\mathbf{x}) = (a_{11}x+a_{12}y, a_{21}x+a_{22}y)\cdot(2ax+2by+2d, 2cy+2bx+2f) \tag{4-2}$$

$$= x^2(2aa_{11}+2a_{21}b)+y^2(2ba_{12}+2c_{22}b)+xy(2ba_{11}+2aa_{12}+2ca_{21}+2ba_{22})+$$

$$+x(2da_{11}+2fa_{21})+y(2da_{12}+2fa_{22})$$

$$= 0.$$

Proposition 4.2.1 *Consider an inelastic PSVF $Z(\boldsymbol{x}) = (A\boldsymbol{x}, B\boldsymbol{x})$ satisfying system (4-1). The tangency sets on Σ are generically formed by one of the following configurations:*

i) A circle Σ_1 can be four points, although it is possible to get zero or two tangency points.

ii) A hyperbola Σ_2 occurs in two points, also there are the cases of zero and four tangencies.

iii) An algebraic curve Σ_3 happens at the real roots of a specific polynomial.

Proof. [Proof of Proposition 4.2.1] Firstly, the intersection between the quadratic curves of the Lie derivatives, which come from equation (4-2), and the circle and the hyperbola determines the tangency points.

Then, in those cases, there are only three possibilities which satisfy the equations: one point, coincident lines or two intersecting lines which contain the origin. By the form of the unitary equations, those switching manifolds do not cross the origin and the intersection will occur in zero, two or four points.

Switching manifold	Unitary Equation	Tangencies
Σ_1 Circle	$x^2+y^2=1$	$a_{11}x^2+a_{22}y^2+xy(a_{12}+a_{21})=0$
Σ_2 Hyperbola	$x^2-y^2=1$	$a_{11}x^2-a_{22}y^2+xy(a_{12}-a_{21})=0$
Σ_3 Algebraic curves	$y-x^n=0$	m = Number of real roots of $P(x) = x((-na_{12}x^{n-1}+a_{22}-na_{11})x^{n-1}+a_{21})$

Table 4.2: *Tangency curves for the switching manifolds.*

The generic tangency points for the circle are four points because of the Transversality Theorem and for the hyperbola there are generically two points because for getting zero points the angle between the tangency lines should be less than $\pi/2$ without intersection with hyperbola, and for four points the angle between the tangency lines also should be less than $\pi/2$ and those points intersect the hyperbola.

Secondly, for algebraic curves

$$Xf_3(\mathbf{x}) = -na_{11}x^n - na_{12}x^{2n-1} + a_{21}x + a_{22}x^n = 0, \tag{4-3}$$

using equation (4-2) over Σ_3, thus in this case the tangencies are the real roots of equation (4-3). We can see that the origin is always a tangency point. □

In this part we present a non-generic result of the tangency set related to asymptotic stability for all dimensions.

Proposition 4.2.2 *Consider $X(\boldsymbol{x}) = A\boldsymbol{x}$ a linear differential system in $\mathbb{R}^{n+1}$. The following statements are equivalent.*

(i) There are no tangency points on $a\mathbb{S}^n$ and $\dot{V}(x,y) > 0$ (or $\dot{V}(x,y) < 0$) in a neighborhood of the singularity.

(ii) A is positive (respec. negative) definite.

Proof. To prove that $(i) \Rightarrow (ii)$ suppose that A is not positive definite, so there exists $\mathbf{x} \in a\mathbb{S}^n$ such that $Xf(\mathbf{x}) = \mathbf{x}^t(A+A^t)\mathbf{x} \leq 0$. If $\mathbf{x}^t(A+A^t)\mathbf{x} = 0$, we get a tangency point which is a contradiction. If $\mathbf{x}_1^t(A+A^t)\mathbf{x}_1 < 0$ and $\mathbf{x}_2^t(A+A^t)\mathbf{x}_2 > 0$ for different $\mathbf{x}_1, \mathbf{x}_2 \in \mathbb{S}^n$,

there exists a quadratic form that is a polynomial in several variables and so continuous, using the intermediate value theorem over the sphere [46] there exists $\mathbf{x} \in a\mathbb{S}^n$ such that $\mathbf{x}^t(A+A^t)\mathbf{x} = 0$.

Thus, we get tangency points if A is not positive or definite positive.

$(ii) \to (i)$ Using Remark (1) of [39], A is positive (negative) definite if and only if its symmetric part is also positive (negative) definite. Therefore, by equation (2-5) $Xf(\mathbf{x})/2 = \frac{1}{2}\mathbf{x}^t(A+A^t)\mathbf{x} > 0\ (<0)\ \forall \mathbf{x} \in a\mathbb{S}^n$. So there exists no $\mathbf{x}$ in the sphere such that $Xf(\mathbf{x}) = 0$, there are no tangency points for X. □

Next result provides the relation between $X = A\mathbf{x}$ and $Y = B\mathbf{x}$ forming a PSVF $Z = (X,Y)$.

Proposition 4.2.3 *Consider $Z(\boldsymbol{x}) = (A\boldsymbol{x}, B\boldsymbol{x})$ an inelastic PSVF as in equation (4-1). Then the following statements hold:*

(i) Differential system (2-4) will depend on 5 parameters, a_{21}, b_{11}, b_{12}, b_{21} and b_{22} and

$$A = \begin{pmatrix} a_{11} & a_{12} \\ a_{21} & a_{22} \end{pmatrix},$$

$$B = \begin{pmatrix} -a_{11} & -a_{21} - b_{21} - a_{12} \\ b_{21} & -a_{22} \end{pmatrix}.$$

The Filippov vector field over $\mathbb{S}^1$ is given by

$$F(\boldsymbol{x}) = \frac{1}{2}\begin{pmatrix} 0 & -a_{21} - b_{21} \\ a_{21} + b_{21} & 0 \end{pmatrix}\begin{pmatrix} x \\ y \end{pmatrix},$$

which give us a periodic orbit in the circle without equilibrium points.

(ii) System (2-4) will depend on 5 parameters, a_{11}, a_{12}, a_{21}, a_{22}, and b_{12} and

$$A = \begin{pmatrix} a_{11} & a_{12} \\ a_{21} & a_{22} \end{pmatrix},$$

$$B = \begin{pmatrix} -a_{11} & b_{12} \\ a_{12}+b_{12}-a_{21} & -a_{22} \end{pmatrix}.$$

The Filippov vector field over the hyperbola is given by

$$F(\boldsymbol{x}) = \frac{1}{2}\begin{pmatrix} 0 & a_{12}+b_{12} \\ a_{12}+b_{12} & 0 \end{pmatrix}\begin{pmatrix} x \\ y \end{pmatrix},$$

which give us a saddle, where an orbit of the saddle is on one branch and other with opposite direction in the other one.

(iii) System (2-4) will depend on 5 parameters, a_{11}, a_{12}, a_{21}, a_{22}, and b_{11} and

$$A = \begin{pmatrix} a_{11} & a_{12} \\ a_{21} & a_{22} \end{pmatrix},$$

$$B = \begin{pmatrix} b_{11} & -a_{12} \\ -a_{21} & n(a_{11}+b_{11})-a_{22} \end{pmatrix}.$$

The Filippov vector field over those kinds of algebraic curves is given by

$$F(\boldsymbol{x}|_{y=x^n}) = ((a_{11}+b_{11})x, n(a_{11}+b_{11})x^n),$$

which give us an attractive or repulsive equilibrium point at the origin.

Proof. [Proof of Proposition 4.2.3] In order to prove bullet (i) it is sufficient to use that $-a_{11} = b_{11}$, $-a_{22} = b_{22}$ and $-(a_{12}+a_{21}) = (b_{12}+b_{21})$. Then we get a skew-symmetric matrix, thus the eigenvalues are two conjugated pure complex numbers, $\lambda_1 = (a_{21}+b_{21})i$ and $\lambda_2 = -(a_{21}+b_{21})i$.

To prove bullet (ii), we consider the rules $-a_{11} = b_{11}$, $-a_{22} = b_2$ and $-(a_{12}-a_{21}) =$

$(b_{12}-b_{21})$, then we get other saddle with $\lambda = \pm|a_{12}+b_{12}|$.

Finally, for (iii) we get $b_{12} = -a_{12}$, $b_{21} = -a_{21}$ and $-(a_{22}-na_{11}) = (b_{22}-nb_{11})$ by equation (4-3). Thus, we get a polynomial vector field over the curve $f(\mathbf{x}) = y - x^n = 0$ of degree n, generated by linear vector fields such that satisfy the identities and $\langle F(\mathbf{x}|_{y=x^n}), \nabla f(\mathbf{x}|_{y=x^n})\rangle = 0$. □

Also we get a result for the discontinuous canonical regions at the infinity.

Proposition 4.2.4 *Consider $Z(\boldsymbol{x}) = (A\boldsymbol{x}, B\boldsymbol{x})$ an inelastic PSVF satisfying system (4-1). Then the pseudo-equilibrium points at the infinity satisfy generically one of the following statements:*

- *(i) if $\Sigma = \Sigma_1$, then there is no pseudo-equilibria at the infinity.*
- *(ii) if $\Sigma = \Sigma_2$, for the pseudo-equilibrium points at the infinity we get four points which can be pseudo-nodes (two attractors and two repellers), two pseudo-saddles and two pseudo-nodes or four pseudo-saddles, determined by the vector fields X, Y and F in the finite part along the discontinuity curve.*
- *(iii) if $\Sigma = \Sigma_3$ and the degree of the algebraic curve is even, then one fake crossing pseudo-equilibrium point at the infinity take place. If the degree is odd, we will get two pseudo-equilibrium points at the infinity, which can be only a pseudo-node and a pseudo-saddle.*

Proof. [Proof of Proposition 4.2.4] For (i), the discontinuity region is in a compact set in the finite part, thus there are no pseudo-equilibrium points at the infinity.

For (ii), there are the two curves of the hyperbola as discontinuity region with inelastic differential systems, then we get four pseudo-equilibrium points at the infinity, two of them will repel and the other two ones will attract with finite time. Also, in the finite part the Filippov vector field, in one line repel from the origin to those points and attract in the other line. Thus the options are four pseudo-saddles, two pseudo-saddles and two pseudo-nodes or four pseudo-nodes.

For (iii), for even curves there is a fake pseudo-equilibrium point at the infinity because the intersection of the two branches of the even curve at the infinity is a single point at each direction. The exterior vector field at the infinity will pass across them but in the finite part they will attract or repel in the Filippov vector field.

For odd curves we get always two points at the infinity by the line of discontinuity, which divide the Poincaré disk in two inelastic parts, thus one point repels and the other one attracts at the infinity (with finite time). Also, generically we get that the two points attract or repel the Filippov vector field in the finite part, then those may be a pseudo-node and the other a pseudo-saddle. □

4.3 Proofs of the Main Results

Proof. [Proof of Theorem 4.1.1 (**i**)] Consider the unitary circle as switching manifold, so there is a linear system inside and other outside, and all the possibilities for the canonical regions are described in Table 4.1. By Proposition 4.2.1 generically there are four tangency points, by Proposition 4.2.3 the Filippov vector field over the circle is a periodic orbit, without pseudo-equilibrium points, and by the Proposition 4.2.4 there is no pseudo-equilibrium points at the infinity.

• **center - center:** If there are two centers, by Proposition 3.2.1 there are no equilibrium points at the infinity, thus there exists a homeomorphism h, using Subsection 3.2.1 in last chapter, such that the phase portrait of the PSVF is topologically equivalent to the one of Figure 4.2.1. In the following proofs we are going to skip h, but it is implicit.

• **center - saddle:** For the case center-saddle, by Proposition 3.2.1 there are zero or four equilibrium points at the infinity depending on the exterior vector field, center or saddle respectively, thus the phase portraits of the PSVF are topologically equivalent to the ones of Figures 4.2.2 and 4.2.3, respectively.

• **focus - focus:** If there are two focuses, there are equilibrium points at the infinity by Proposition 3.2.1 and the phase portrait corresponds to Figure 4.2.4.

• **focus - node:** For the case focus-node with four equilibrium points at the infinity, using Proposition 3.2.1, for the PSVF there exist zero or four equilibrium points at the infinity if the node is inside or outside the circle, thus the phase portraits are topologically equivalent to Figures 4.2.5 and 4.2.6, respectively.

• **focus - saddle:** If there are a focus and a saddle, again there exist zero or four equilibrium points at the infinity depending on the position of the saddle, by Proposition 3.2.1, and the phase portraits corresponds to the ones of Figures 4.2.7 and 4.2.8, respectively.

• **node - node:** For the case of two nodes with four equilibrium points at the infinity, by Proposition 3.2.1 generically its phase portrait is topologically equivalent to the one of Figure 4.2.9.

• **node - saddle:** If there are saddle and an node with four equilibrium points at the infinity by Proposition 3.2.1, there are four tangency points over the circle because of the saddle and the possible phase portraits are topologically equivalent to one of Figures 4.2.10 and 4.2.11.

• **saddle - saddle:** For the case of two saddles, by Proposition 3.2.1 there are four equilibrium points at the infinity and the phase portrait is topologically equivalent to the one of the Figure 4.2.12.

• **exceptions:** There exist some exceptions for Proposition 4.2.1. Firstly, by Proposition 4.2.2, there are cases with positive (negative) definite matrices and zero tangency points over the circle, and $a_{11}x^2+(a_{12}+a_{21})xy+a_{22}y^2=0$ is satisfied only by the origin. There are the cases with a focus and star node, where there exists a periodic orbit or infinitely many equilibrium points at the infinity, respectively depending on the vector field outside by Proposition 3.2.1, and then the phase portraits are topologically equivalent to the ones of the Figures 4.2.13 and 4.2.14, respectively. Other possible case is with two nodes with four equilibrium points at the infinity, its phase portrait corresponds to the one of the Figure 4.2.15.

A second exception occurs with two tangency points over the circle $\mathbb{S}^1$, such that $a_{11}x^2+(a_{12}+a_{21})xy+a_{22}y^2=(ax+by)^2$. For a focus and a node with two equilibrium points at the infinity as exterior and then interior vector fields, by Proposition 3.2.1 the phase portraits corresponds to the ones of the Figures 4.2.16 and 4.2.17, respectively. If there are again a focus and a node with four equilibrium points at the infinity, depending on what vector field is outside, the phase portraits are topologically equivalent to the ones of the Figures 4.2.18 and 4.2.19, respectively. For two nodes, one of them with two and the other one with four equilibrium points at the infinity, by Proposition 3.2.1 the phase portraits are topologically equivalent to the ones of the Figures 4.2.20 and 4.2.21, respectively. If there are two nodes with four equilibrium points at the infinity, the phase portrait corresponds to the one of the Figure 4.2.22. Finally, for the case with two focuses with a periodic orbit at the infinity the phase portrait is topologically equivalent to the one of the Figure 4.2.23. It is not possible, in this inelastic context, to have centers and saddles with two tangencies over the circle.

Also the cases C-F, C-NI are not possible because if there is a center,

$$A=\begin{pmatrix} a_{11} & a_{12} \\ a_{21} & -a_{11} \end{pmatrix},$$

with $tr(A)=0$ and $\det(A)>0$, then for B $tr(B)=tr(A)=0$ and there are two possibilities $\det(B)>0$ (center) or $\det(B)<0$ (saddle). We are not considering the cases where $\det(B)=0$.

The same occurs in the cases SN-N, SN-S because if there is a star node

$$A=\begin{pmatrix} a_{11} & 0 \\ 0 & a_{11} \end{pmatrix},$$

$$B=\begin{pmatrix} -a_{11} & b_{12} \\ -b_{12} & -a_{11} \end{pmatrix},$$

which B give us a focus, with $tr(B) = -2a_{11} \neq 0$ and $(trB)^2 - 4\det B = -4b_{12} < 0$. □

Proof. [Proof of Theorem 4.1.1 (**ii**)] Consider a hyperbola as switching manifold, so there is a linear system between the curves of the hyperbola and other outside (considering the hyperbola as a circle in the projective plane), and all the possibilities for the canonical regions are described in Table 4.1. By Proposition 4.2.1 generically there are two tangency points, by Proposition 4.2.3 the Filippov vector field over the hyperbola acts like the trajectories of a saddle, without pseudo-equilibrium points and with opposite directions along the branches, also the origin is a singularity, and by Proposition 4.2.4 we get four pseudo-equilibrium points at the infinity.

• **center - center:** If there is two centers, by Proposition 3.2.1 there are no equilibrium points at the infinity, thus the phase portrait of the PSVF is topologically equivalent to the one of the Figure 4.3.1.

• **remark:** For the cases with a saddle in some side of the discontinuity, there exist 2 singularities at the infinity only with other saddle because

$$B = \begin{pmatrix} a & 0 \\ 0 & -b \end{pmatrix},$$

with $a, b > 0$, a saddle with two singularities in one of the opposite regions, then $a_{11} = -a$, $a_{22} = b$ and $a_{12} = a_{21}$ and thus $(a_{11} + a_{22})^2 - 4(a_{11}a_{22} - a_{12}a_{21}) = (b+a)^2 + 4a_{12}^2 > 0$ and $\det(A) = -ab - a_{12}^2 < 0$, therefore by Proposition 3.2.1 it is a saddle.

• **center - saddle:** Then, for the case center-saddle there are only two options, zero or four equilibrium points at the infinity (in the part where is located the saddle), and the phase portraits corresponds to the ones of Figures 4.3.2 and 4.3.3, respectively.

• **focus - focus:** If there are two focuses, using Proposition 3.2.1 there are no equilibrium points at the infinity and the phase portrait of the PSVF is topologically equivalent to Figure 4.3.4.

• **focus - node:** For the case focus-node we get three options by Proposition 3.2.1, zero, two or four equilibrium points at the infinity in the region where is located the node, and the phase portraits are topologically equivalent to the ones of Figures 4.3.5, 4.3.6 and 4.3.7, respectively.

• **focus - saddle:** If there are a focus and a saddle, again there exists zero or four equilibrium points at the infinity and the phase portraits are topologically equivalent to the ones of Figures 4.3.8 and 4.3.9, respectively.

• **node - node:** For the case node-node, there are five options by Proposition 3.2.1 depending of the type of nodes that we get and the position of their equilibrium point at the infinity. Those options are zero, two, four, six or eight equilibrium points at the infinity in the region where the nodes are, and the phase portraits will be topologically equivalent to Figures 4.3.10, 4.3.11, 4.3.12, 4.3.13 and 4.3.14, respectively.

• **node - saddle:** If there are a node and a saddle, again depending on the place of the node and the saddle, there exist nodes with zero, two or four equilibrium points at the infinity, and in the same way the saddle with zero or four singularities at the infinity in its region, then again there exist the possibilities of zero, two, four, six or eight equilibrium points at the infinity and their phase portrait of the systems are topologically equivalent to the ones of Figures 4.3.15, 4.3.16, 4.3.17, 4.3.18 and 4.3.19.

• **saddle - saddle:** For the case saddle-saddle there are only three options by Proposition 3.2.1 and the previous facts, zero or four equilibrium points at the infinity for each saddle, thus we can get at the end zero, four or eight equilibrium points for the PSVF and the phase portraits are topologically equivalent to Figures 4.3.20, 4.3.21 and 4.3.22, respectively.

• **exceptions:** The tangency is composed generically by two transversal lines, Table 4.2, and the intersection with the hyperbola are two points, except when the angle between the tangency lines is less than $\pi/2$ inside or outside the hyperbola. In that not residual case there are only a saddle and a node, as in the Figures 4.3.24, 4.3.25, 4.3.26 and 4.3.27. The asymptotes of the hyperbola are determined by the equation $x^2 - y^2 = 0$, consider the

normal form

$$A = \begin{pmatrix} a_{11} & a_{12} \\ a_{21} & a_{22} \end{pmatrix},$$

such that $0 < a_{11} < 1, 0 < a_{22} < 1$ and $a_{11} \neq a_{22}$. The parameter $a_{12} - a_{21}$ is the coefficient of the term xy which works as a rotation and this has to satisfy $|a_{12} - a_{21}| < |a_{11} - a_{22}| < 1$, this is for keeping the equation (2-5) different from $(x+y)(-a_{22}y + a_{11}x) = 0$. Then for A and B, $a_{21} - a_{12} = b_{12} - b_{21}$ and also $|b_{12} - b_{21}| < |a_{11} - a_{22}| < 1$, therefore

$$(a_{11} - a_{22})^2 - (b_{12} - b_{21})^2 > 0,$$

$$(a_{11} + a_{22})^2 - 4a_{11}a_{22} + 4b_{12}b_{21} > (b_{12} + b_{21})^2 \geq 0.$$

Then we obtain a saddle or a node with four points at the infinity, and there are four tangency points. If we make the following coordinate change $a_{11} \to a$, $a_{12} \to b$, $a_{21} \to c$, $a_{22} \to d$ and then $d \to a_{11}$, $c \to a_{12}$, $b \to a_{21}$, $a \to a_{22}$, there are no tangency points, as in Figures 4.3.27, 4.3.28, 4.3.29 and 4.3.30.

There exists other case where there are no tangency points. With a star node and a node with four equilibrium points at the infinity which coincide with the pseudo-equilibrium points at the infinity, or also a saddle with the same property as before.

Thus, using Proposition 3.2.1 in our PSVF there are infinitely many equilibrium points at the infinity, in the region where is located the star node, the phase portraits of the cases SN-NI are topologically equivalents to the ones of the Figures 4.3.31 and 4.3.32, and the cases SN-S correspond to the Figures 4.3.33 and 4.3.34.

The case SN-F does not appear because if there is a star node

$$A = \begin{pmatrix} a_{11} & 0 \\ 0 & a_{11} \end{pmatrix},$$

$$B = \begin{pmatrix} -a_{11} & b_{12} \\ b_{12} & -a_{11} \end{pmatrix},$$

which B give us a saddle or a node, with $tr(B) = -2a_{11} \neq 0$ and $(trB)^2 - 4\det B = 4b_{12} > 0$.

If there is a vector field X of the form

$$A = \begin{pmatrix} a_{11} & a_{12} \\ a_{21} & -a_{11} \end{pmatrix},$$

with $tr(A) = 0$ and $\det(A) > 0$, then for B $tr(B) = tr(A) = 0$ and again two possibilities $\det(B) > 0$ (center) or $\det(B) < 0$ (saddle). □

Proof. [Proof of Theorem 4.1.1 (**iii**)] Consider an algebraic curve as switching manifold, so there is a linear system inside the even curve and other outside, or one differential system in each hemisphere defined by an odd curve, and all the possibilities for the canonical regions are described in Table 4.1. By Proposition 4.2.1 the tangencies depend on the real roots of a polynomial, there are until $2n-1$ points over the switching manifold and the origin is always a tangency (in the Figures it is only representative), by Proposition 4.2.3 the Filippov vector field over the curve has a pseudo-equilibrium point at the origin and it repels or attracts, and by Proposition 4.2.4 we get a fake crossing pseudo-equilibrium point at the infinity for an even curve, and two pseudo-equilibrium points at the infinity for an odd curve.

• **center - focus:** If there are a center and a focus (inside and out of the even curve), by Proposition 3.2.1 there are no equilibrium points at the infinity, thus the phase portraits of the two possible systems are topologically equivalent to the ones of Figures 4.4.1 and 4.4.2.

• **center - node:** For the case center-node, using Proposition 3.2.1, if the center is the exterior vector field then there are no equilibrium points at the infinity and the phase

portrait of the system is equivalent to the Figure 4.4.3, and if there is a node in the exterior, there are four equilibrium points at the infinity and the phase portrait is topologically equivalent to the one of Figure 4.4.4.

• **focus - focus:** If there are two focuses, using Proposition 3.2.1, there are no equilibrium points at the infinity and the phase portrait of the system is equivalent to Figure 4.4.5.

• **focus - node:** For the case of a focus and a node, using Proposition 3.2.1, if there is a node in the exterior, there are four equilibrium points at the infinity and then the phase portrait is topologically equivalent to the one of Figure 4.4.7. Also if the focus is the exterior vector field then there are no equilibrium points at the infinity and the phase portrait of the system is equivalent to Figure 4.4.6.

• **node - node:** If there is a node with two equilibrium points at the infinity, using Proposition 3.2.1, and staying firstly in the exterior, the unique non trivial option is another node with four singularities at the infinity, then the phase portraits of those systems are topologically equivalent to Figures 4.4.8 and 4.4.9, respectively.

For the case of two nodes with four equilibrium points at the infinity, using Proposition 3.2.1 the phase portrait of the system is topologically equivalent to Figure 4.4.10.

• **node - saddle:** If there are a node and a saddle, there exist only a type of node outside with four equilibrium points at the infinity, or the saddle with 4 points, so the phase portraits of those systems are topologically equivalent to Figures 4.4.11 and 4.4.12, respectively.

• **saddle - saddle:** For the case of two saddles, there are four equilibrium points at the infinity by Proposition 3.2.1 and thus the phase portrait is topologically equivalent to the one of Figure 4.4.13.

• **exceptions:** Suppose that A is a star node with an even or an odd curve as switching manifold, then the unique possibilities for B are a saddle or a node

$$A = \begin{pmatrix} a_{11} & 0 \\ 0 & a_{11} \end{pmatrix},$$

$$B = \begin{pmatrix} b_{11} & 0 \\ 0 & nb_{11} + (n-1)a_{11} \end{pmatrix}.$$

Thus, using Proposition 3.2.1 there are infinitely many equilibrium points at the infinity, if the node is outside of the even curve and in any case for an odd curve. Then the phase portraits are topologically equivalent to the ones of Figures 4.4.14, 4.4.16, 4.4.28 and 4.4.29. If a node or a saddle are outside of the even curve we will get four singularities at the infinity and the phase portraits corresponds to the ones of Figures 4.4.15 and 4.4.17.

If A is a focus with $trA = a_{11} + a_{22} \neq 0$ and $\det A = a_{11}a_{22}^2 - a_{12}a_{21} > (trA)^2/4$, then

$$B = \begin{pmatrix} b_{11} & -a_{12} \\ -a_{21} & b_{22} \end{pmatrix} = \begin{pmatrix} b_{11} & -a_{12} \\ -a_{21} & n(a_{11} + b_{11}) - a_{22} \end{pmatrix}.$$

Thus $\det B = b_{11}b_{22} - a_{12}a_{21} = nb_{11}^2 + b_{11}(na_{11} - a_{22}) - a_{12}a_{21}$ describes a concave up parabola in the variable b_{11} because $(\det B)'' = 2n > 0$ and the critical point $b_{11} = -(na_{11} - a_{22})/(2n)$ is always a minimum. Then there is no a saddle if the imaginary parts of the roots of $\det B$ do not vanish. Then

$$b_{11} = (-(na_{11} - a_{22}) \pm \sqrt{(na_{11} - a_{22})^2 + 4na_{12}a_{21}})/(2n),$$

and there are no complex roots, where $\det B$ can be less than zero, if $(na_{11} + a_{22})^2 - 4n\det A \geq 0$, which can be possible for large degrees n. Then, by Proposition 3.2.1, if there is an even curve as switching manifold and the focus is outside, there are equilibrium points at the infinity and the phase portrait corresponds to Figure 4.4.18, if the saddle is outside, then there are four singularities and it is topologically equivalent to the one of Figure 4.4.19. If there is an odd curve, we will get two equilibrium points of the saddle in one hemisphere and the phase portrait corresponds to the one of Figure 4.4.30.

• **center - focus:** Continuing in the odd curves, if there are a center and a focus, by Proposition 3.2.1 there are no equilibrium points at the infinity, thus the phase portrait of that system is topologically equivalent to the one of Figure 4.4.20.

• **center - node:** For the case center-node, again there is a node with four equilibrium points at the infinity and two of them in the hemisphere where is the node, thus the phase portrait will be topologically equivalent to Figure 4.4.21.

• **focus - focus:** If there are two focuses, there are no singularities at the infinity, then the phase portrait is topologically equivalent to the one of Figure 4.4.22.

• **focus - node:** For the case of a focus and a node with four singularities at the infinity, $(trB)^2 - 4\det B > 0$ and $\det B > 0$, then there are two singularities at the infinity in the hemisphere of the node and its phase portrait will be topologically equivalent to Figure 4.4.23.

• **node - node:** If there are two nodes with one singularity at the infinity in each hemisphere, that case is trivial. So there exists a node with one equilibrium point in its hemisphere and other node with two singularities, which corresponds to Figure 4.4.24, or two nodes with 2 equilibrium points in each hemisphere and that is topologically equivalent with the system of Figure 4.4.25.

• **node - saddle:** For the case node-saddle, in the hemisphere of the saddle we will always find two equilibrium points at the infinity, and in the other there are also two singularities at the infinity, then its phase portrait is topologically equivalent with the one of Figure 4.4.26.

• **saddle - saddle:** Considering the case saddle-saddle, we get two equilibrium points in each hemisphere and the phase portrait is equivalent to Figure 4.4.27.

• **exceptions:** If A is a center with $trA = a_{11} + a_{22} = 0$ and $\det A = -a_{11}^2 - a_{12}a_{21} > 0$, then

$$B = \begin{pmatrix} b_{11} & -a_{12} \\ -a_{21} & b_{22} \end{pmatrix} = \begin{pmatrix} b_{11} & -a_{12} \\ -a_{21} & n(a_{11}+b_{11})+a_{11} \end{pmatrix}.$$

We can see that the case C-C occurs if $b_{22} = -b_{11}$, but then $b_{11} = -a_{11}$ and we get the trivial case. Suppose $a_{11} \geq 0$ (for $a_{11} \leq 0$ is similar), then $b_{22} - nb_{11} = (n+1)a_{11} \geq 0$

and for getting a saddle it must satisfy $b_{11}b_{22} < 0$. Thus if $b_{11} > 0$ and $b_{22} < 0$ we get $0 > b_{22} \geq nb_{11} > 0$ which is a contradiction.

If $b_{11} < 0$ and $b_{22} > 0$, then $(n+1)a_{11} > -nb_{11}$ and we get $\det B = (n+1)a_{11}b_{11} + nb_{11}^2 - a_{12}a_{21} > -nb_{11}^2 + nb_{11}^2 - a_{12}a_{21} > a_{11}^2 > 0$, so we get another contradiction and the case C-S is not possible. □

Proof. [Proof of Theorem 4.1.2] For (1), the exterior vector field has negative real part eigenvalues and the opposite for the interior one, if there are no tangencies or there are two tangency points, their equations are $ax^2 + by^2 = 0$ or $-(ax+by)^2 = 0$, respectively. Thus, the circle attracts the whole orbits of the PSVF in finite time for all $\mathbf{x} \in \mathbb{R}^2 \setminus \{0\}$ and they end at the Fillipov vector field over the circle.

For (2), there are sliding and escape regions, there exist orbits across the tangency points in the circle (which are tangent) and using the fact that those orbits goes to the origin, the union of those will generate a limited and closed set which contains the sphere and its interior and is positive invariant for the PSVF N.

By construction, the orbits of the interior vector field are limited by the circle and, for the exterior, we choose the visible tangent orbits with the discontinuity region. All of them are limited because these converge to the origin, and the union is closed by Tubular Flow Theorem 2.1.4. Then the escape region is compact and by the flow of X, which is a diffeomorphism, its image is also a compact contained in the sliding region over the circle. So this set is compact and positively invariant for the exterior, interior and Fillipov vector fields.

Now, we prove that the circle joined with those exterior and interior regions is a strange attractor. With a transversal section $\bar{\Sigma}$ of the form $y = kx$ which crosses the middle point between two tangency points, T_1 and T_2, in the escape region over the circle. Considering focus or nodes as interior or exterior vector fields with matrices of the form

$$A = \begin{pmatrix} a_{11} & 0 \\ 0 & a_{22} \end{pmatrix},$$

$$B = \begin{pmatrix} b_{11} & -b_{12} \\ b_{12} & b_{11} \end{pmatrix}.$$

Then their solutions are respectively

$$\mathbf{x}(t) = \begin{pmatrix} e^{a_{11}t} & 0 \\ 0 & e^{a_{22}t} \end{pmatrix} \mathbf{x}_0 = A_1(t)\mathbf{x}_0,$$

$$\mathbf{x}(t) = e^{b_{11}t} \begin{pmatrix} \cos b_{12}t & -\sin b_{12}t \\ \sin b_{12}t & \cos b_{12}t \end{pmatrix} \mathbf{x}_0 = A_2(t)\mathbf{x}_0.$$

and we define the Poincaré half map as $\Pi = \Pi_3 \circ \Pi_2 \circ \Pi_1$, where $\Pi_1 : \bar{\Sigma} \to \Sigma$ such that $\Pi_1 = \varphi$, $\mathbf{x} = (x, mx)^T \mapsto T_2$ having $i, j \in \{1,2\}$

$$T_2 = \varphi_{t(\mathbf{x})}(\mathbf{x}) = \begin{cases} \begin{cases} A_i(t_1(\mathbf{x}))\mathbf{x} \ \ if \ ||\mathbf{x}|| > 1, \\ A_2(t_2(\mathbf{x}))\mathbf{x}, \ b_{11} = 0 \ \ if \ ||\mathbf{x}|| = 1, \end{cases} \\ A_2(t)\mathbf{x}, \ b_{11} = 0 \ \ if \ ||\mathbf{x}|| = 1, \\ \begin{cases} A_j(t_1(\mathbf{x}))\mathbf{x} \ \ if \ ||\mathbf{x}|| < 1, \\ A_2(t_2(\mathbf{x}))\mathbf{x}, \ b_{11} = 0 \ \ if \ ||\mathbf{x}|| = 1, \end{cases} \end{cases}$$

where $t_1, t_2, t > 0$ and $t = t_1 + t_2$. Also $\Pi_2 : \{T_2\} \to \{T_1\}$ and $\Pi_3 : \Sigma \to \bar{\Sigma}$ such that $\Pi_3^{-1} = \psi$, $\mathbf{x} = (x, mx)^T \mapsto T_1$ having $i, j \in \{1,2\}$

$$T_1 = \psi_{\bar{t}(\mathbf{x})}(\mathbf{x}) = \begin{cases} \begin{cases} A_i(\bar{t}_1(\mathbf{x}))\mathbf{x} \ \ if \ ||\mathbf{x}|| > 1, \\ A_2(\bar{t}_2(\mathbf{x}))\mathbf{x}, \ b_{11} = 0 \ \ if \ ||\mathbf{x}|| = 1, \end{cases} \\ A_2(\bar{t})\mathbf{x}, \ b_{11} = 0 \ \ if \ ||\mathbf{x}|| = 1, \\ \begin{cases} A_j(\bar{t}_1(\mathbf{x}))\mathbf{x} \ \ if \ ||\mathbf{x}|| < 1, \\ A_2(\bar{t}_2(\mathbf{x}))\mathbf{x}, \ b_{11} = 0 \ \ if \ ||\mathbf{x}|| = 1, \end{cases} \end{cases}$$

where $\bar{t}_1, \bar{t}_2, \bar{t} < 0$ and $\bar{t} = \bar{t}_1 + \bar{t}_2$. Then we get the following properties:

1. Countable periodic orbits of any period. Suppose that the circle $\mathbb{S}^1$ has period 1, then we can find $\mathbf{x}_N \in \bar{\Sigma}$ such that $||\mathbf{x}_N|| = 1 \pm \frac{1}{2^N}$ for some $N \in \mathbb{N}$ and an orbit which starts at the intersection between $\bar{\Sigma}$ and $\mathbb{S}^1$, then crosses $\mathbf{x}_N$ at the next time in $\bar{\Sigma}$ and after returns to the intersection point has period 2. Thus, continuing inductively over $n > N$ we can find periodic orbit of any period.
2. Uncountable set of non-periodic motions. In this case, following the procedure of the last one, we can take the set I of irrational numbers such that they are norms of $\mathbf{x}_i \in \bar{\Sigma}$, thus we get non-periodic trajectories across them.
3. A dense orbit. For any point $\mathbf{x} \in \bar{\Sigma}$, there is an orbit of the PSVF by definition, the existence and uniqueness Theorem and the facts that the exterior vector field has eigenvalues with negative real part and the interior one with positive real part, then we get a trajectory which is more than a dense orbit. Thus $\forall\, \mathbf{x}_1, \mathbf{x}_2 \in \bar{\Sigma}$, $\exists t_{T_1 T_2}$ such that $\Pi_{t_{T_1 T_2}}(\mathbf{x}_1) = \mathbf{x}_2$.

□

Proof. [Proof of Theorem 4.1.3] For the α or ω-limit sets of a point $\mathbf{x} \in \mathbb{R}^2$ in this kind of differential systems, we can see due to Poincaré-Bendixson Theorem in the Poincaré disk, Proposition 3.2.1 and [22] in the phase portraits of the Figures 4.2, 4.3 and 4.4, described in Tables 4.3, 4.4 and 4.5. □

4.4 Conclusions

We presented a robust global analysis on the dynamics of inelastic non-smooth differential equations with the conic as discontinuity region. As future work we will study the global dynamics of other kind of systems where can exist other conditions for the tangency points

F/O	(1)	(2)	(3)	(4)	(5)	(6)	(7)	(8)	(9)
4.2.1	x	-	-	-	-	x	x	x	-
4.2.2	x	-	-	-	-	x	x	x	-
4.2.3	x	-	x	-	-	x	-	x	-
4.2.4	x	-	-	-	-	-	x	-	x
4.2.5	x	-	-	-	-	-	x	-	x
4.2.6	x	-	x	-	-	-	-	-	x
4.2.7	x	-	-	-	-	-	x	-	x
4.2.8	x	-	x	-	-	-	-	-	-
4.2.9	x	-	x	-	-	-	-	-	x
4.2.10	x	-	x	-	-	-	-	-	x
4.2.11	x	-	x	-	-	-	-	-	-

F/O	(1)	(2)	(3)	(4)	(5)	(6)	(7)	(8)	(9)
4.2.12	x	-	x	-	-	-	-	-	-
4.2.13	x	-	x	-	-	x	-	-	-
4.2.14	x	-	-	-	-	x	x	-	-
4.2.15	x	-	x	-	-	x	-	-	-
4.2.16	x	-	-	-	-	x	x	-	-
4.2.17	x	-	x	-	-	x	-	-	-
4.2.18	x	-	-	-	-	x	x	-	-
4.2.19	x	-	x	-	-	x	-	-	-
4.2.20	x	-	x	-	-	x	-	-	-
4.2.21	x	-	x	-	-	x	-	-	-
4.2.22	x	-	x	-	-	x	-	-	-

Table 4.3: ω-*limit options (O) for the phase portraits of Figures 4.2 (F).*

and T-singularities, structural stability and also some applications in weather predictions, epidemiology, electromagnetism and general relativity.

4.5 Phase Portraits

F/O	(1)	(2)	(3)	(4)	(5)	(6)	(7)	(8)	(9)
4.3.1	x	-	-	x	-	-	-	x	-
4.3.2	x	-	-	x	-	-	-	x	-
4.3.3	x	-	x	x	-	-	-	-	-
4.3.4	x	-	-	x	-	-	-	x	-
4.3.5	x	-	-	x	-	-	-	x	-
4.3.6	x	-	x	x	-	-	-	x	-
4.3.7	x	-	x	x	-	-	-	x	-
4.3.8	x	-	-	x	-	-	-	x	-
4.3.9	x	-	x	x	-	-	-	x	-
4.3.10	x	-	-	x	-	-	-	-	-
4.3.11	x	-	x	x	-	-	-	-	-
4.3.12	x	-	x	x	-	-	-	-	-
4.3.13	x	-	x	x	-	-	-	-	-
4.3.14	x	-	x	x	-	-	-	-	-
4.3.15	x	-	-	x	-	-	-	-	-
4.3.16	x	-	x	x	-	-	-	-	-
4.3.17	x	-	x	x	-	-	-	-	-
F/O	(1)	(2)	(3)	(4)	(5)	(6)	(7)	(8)	(9)
4.3.18	x	-	x	x	-	-	-	-	-
4.3.19	x	-	x	x	-	-	-	-	-
4.3.20	x	-	-	x	-	-	-	x	-
4.3.21	x	-	x	x	-	-	-	-	-
4.3.22	x	-	x	x	-	-	-	-	-
4.3.23	x	-	x	x	-	-	-	-	-
4.3.24	x	-	x	x	-	-	-	-	-
4.3.25	x	-	x	x	-	-	-	-	-
4.3.26	x	-	x	x	-	-	-	-	-
4.3.27	x	-	x	x	-	-	-	-	-
4.3.28	x	-	x	x	-	-	-	-	-
4.3.29	x	-	x	x	-	-	-	-	-
4.3.30	x	-	x	x	-	-	-	-	-
4.3.31	x	-	x	x	-	-	-	-	-
4.3.32	x	-	x	x	-	-	-	-	-
4.3.33	x	-	x	x	-	-	-	-	-
4.3.34	x	-	x	x	-	-	-	-	-

Table 4.4: ω-*limit options (O) for the phase portraits of Figures 4.3 (F).*

F/O	(1)	(2)	(3)	(4)	(5)	(6)	(7)	(8)	(9)
4.4.1	-	x	-	-	x	-	x	-	-
4.4.2	-	x	-	-	x	-	x	-	-
4.4.3	-	x	-	-	x	-	x	-	-
4.4.4	-	x	x	-	x	-	-	-	-
4.4.5	-	x	-	-	x	-	x	-	-
4.4.6	-	x	-	-	x	-	x	-	-
4.4.7	-	x	x	-	x	-	-	-	-
4.4.8	-	x	x	-	x	-	-	-	-
4.4.9	-	x	x	-	x	-	-	-	-
4.4.10	-	x	x	-	x	-	-	-	-
4.4.11	-	x	x	-	x	-	-	-	-
4.4.12	-	x	x	-	x	-	-	-	-
4.4.13	-	x	x	-	x	-	-	-	-
4.4.14	-	x	x	-	x	-	-	-	-
4.4.15	-	x	x	-	x	-	-	-	-
F/O	(1)	(2)	(3)	(4)	(5)	(6)	(7)	(8)	(9)
4.4.16	-	x	x	-	x	-	-	-	-
4.4.17	-	x	x	-	x	-	-	-	-
4.4.18	-	x	-	-	x	-	x	-	-
4.4.19	-	x	x	-	x	-	-	-	-
4.4.20	-	x	-	x	-	-	-	-	-
4.4.21	-	x	-	x	-	-	-	-	-
4.4.22	-	x	-	x	-	-	-	-	-
4.4.23	-	x	x	x	-	-	-	-	-
4.4.24	-	x	x	x	-	-	-	-	-
4.4.25	-	x	x	x	-	-	-	-	-
4.4.26	-	x	x	x	-	-	-	-	-
4.4.27	-	x	x	x	-	-	-	-	-
4.4.28	-	x	x	x	-	-	-	-	-
4.4.29	-	x	x	x	-	-	-	-	-
4.4.30	-	x	x	x	-	-	-	-	-

Table 4.5: ω-*limit options (O) for the phase portraits of Figures 4.4 (F).*

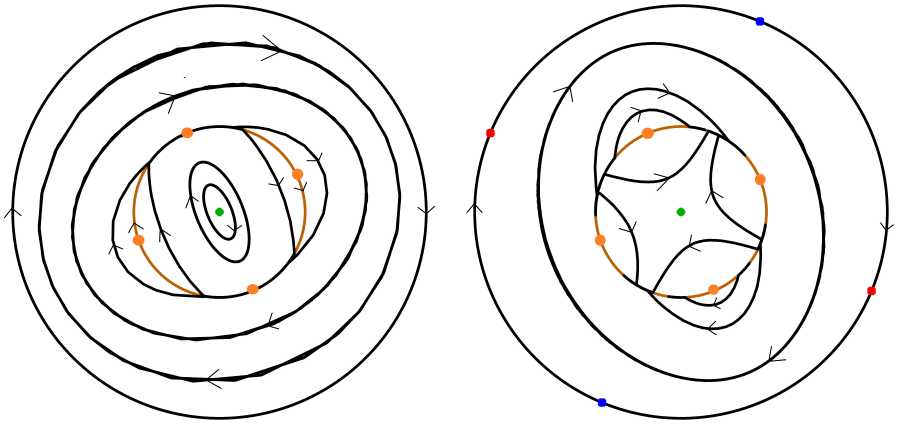

(.1) *C-C*

(.2) *C-S 0*

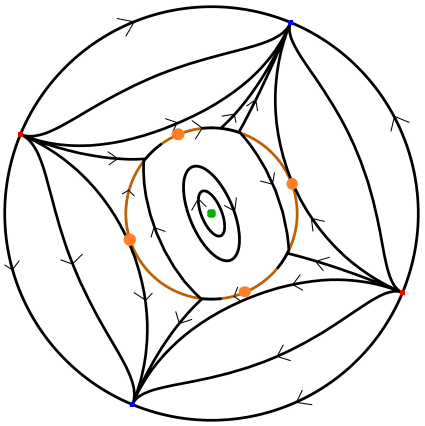

(.3) *C-S 4*

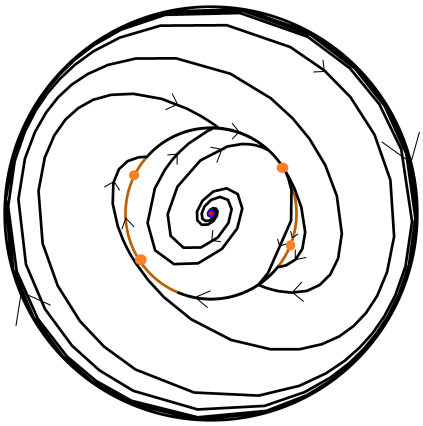

(.4) *F-F*

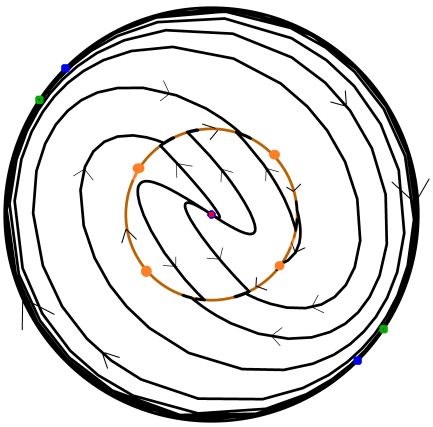

(.5) *F-N 0*

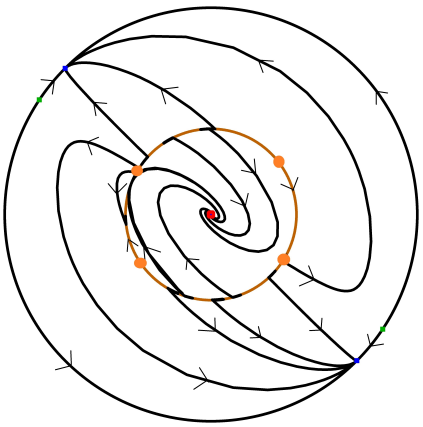

(.6) *F-N 4*

Figure 4.2: *Phase portraits with a circle as switching manifold.*

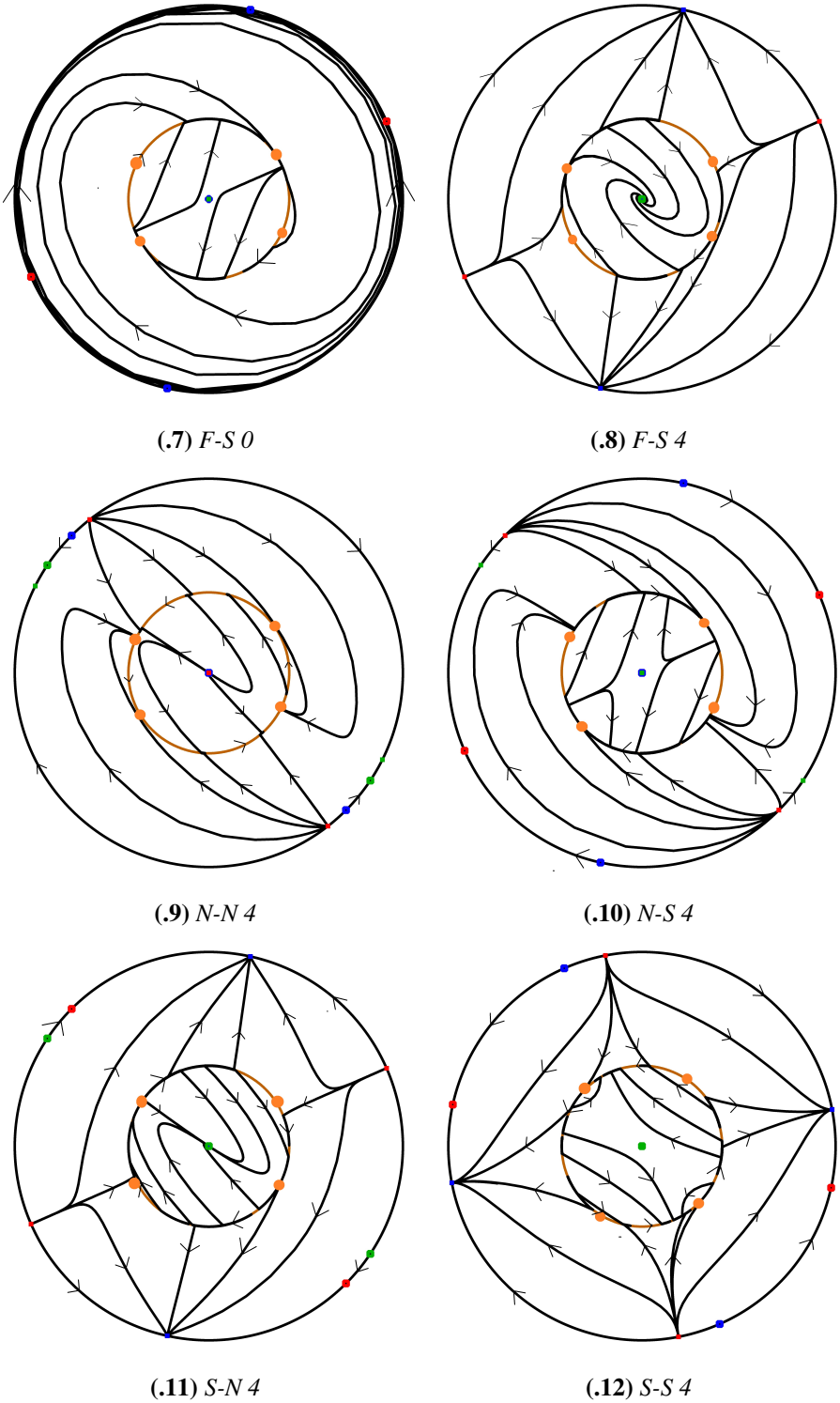

(.7) *F-S 0*

(.8) *F-S 4*

(.9) *N-N 4*

(.10) *N-S 4*

(.11) *S-N 4*

(.12) *S-S 4*

Figure 4.2: *Phase portraits with a circle as switching manifold.*

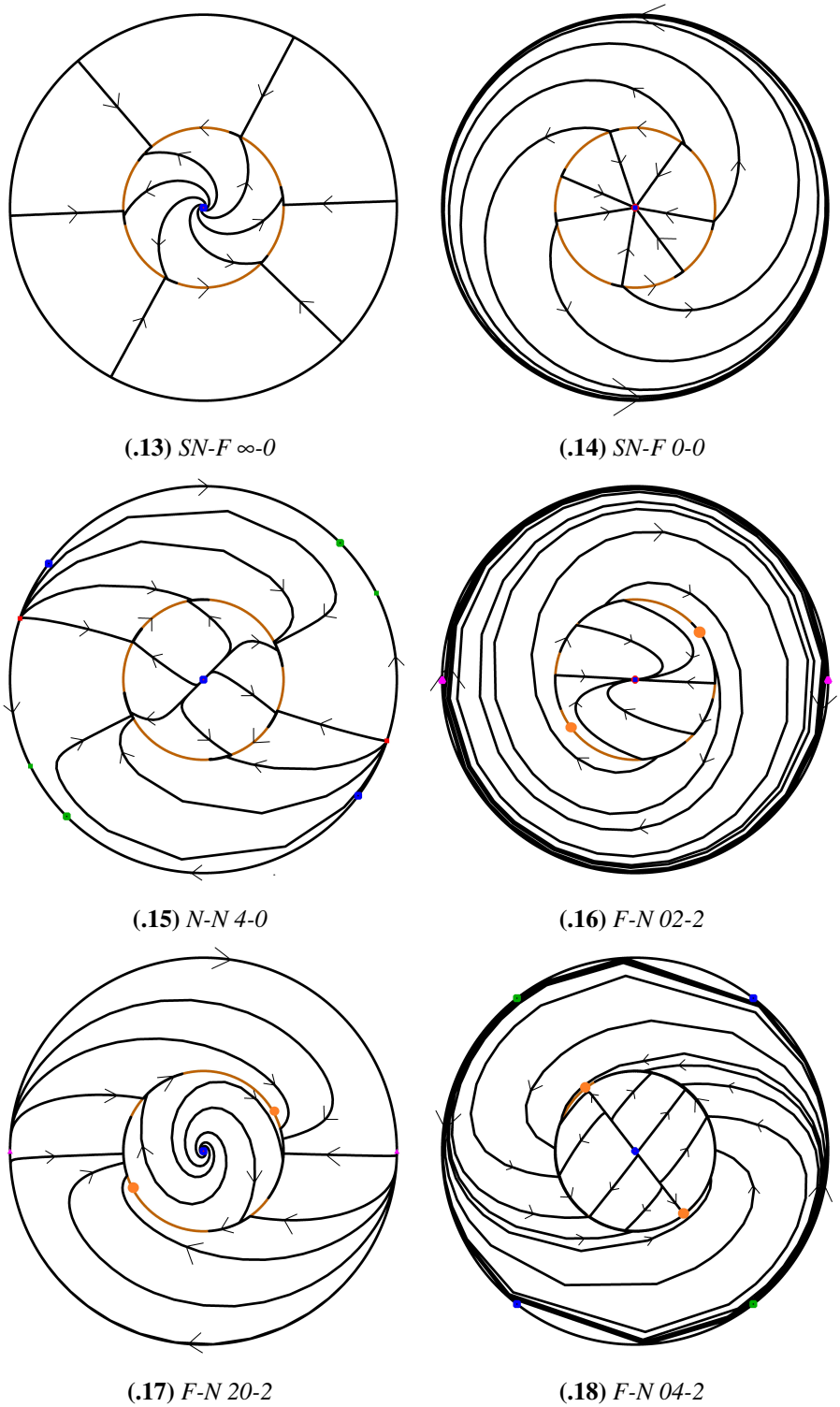

(.13) *SN-F ∞-0*

(.14) *SN-F 0-0*

(.15) *N-N 4-0*

(.16) *F-N 02-2*

(.17) *F-N 20-2*

(.18) *F-N 04-2*

Figure 4.2: *Phase portraits with a circle as switching manifold.*

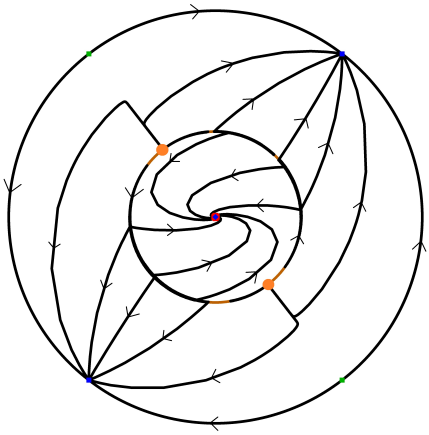

(.19) *F-N 40-2*

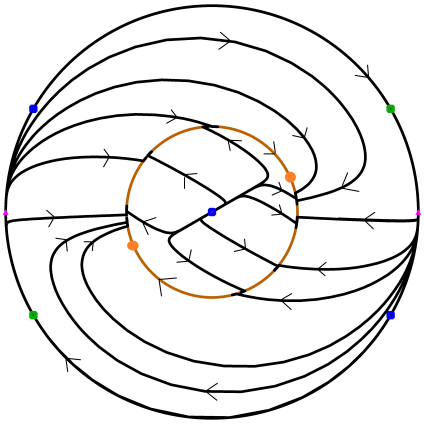

(.20) *N-N 24-2*

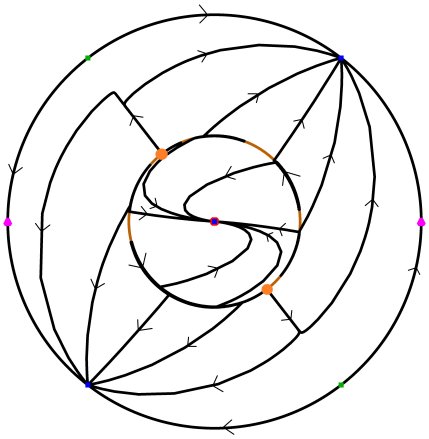

(.21) *N-N 42-2*

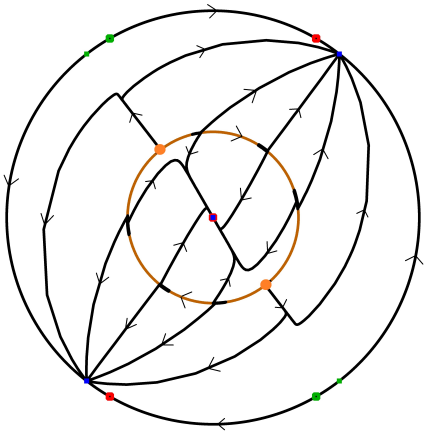

(.22) *N-N 44-2*

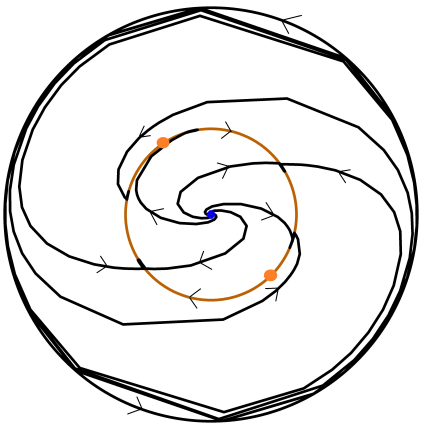

(.23) *F-F 2*

Figure 4.2: *Phase portraits with a circle as switching manifold.*

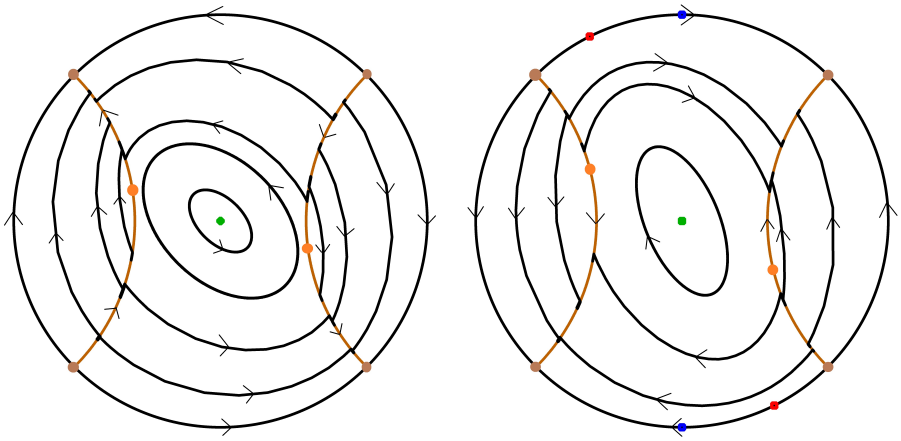

(.1) *C-C*

(.2) *C-S 0*

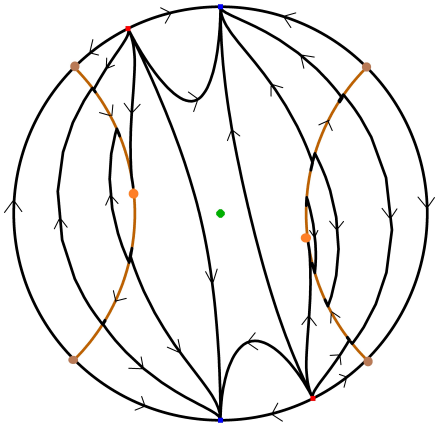

(.3) *C-S 4*

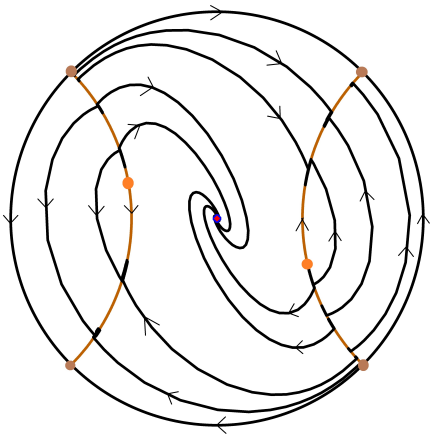

(.4) *F-F*

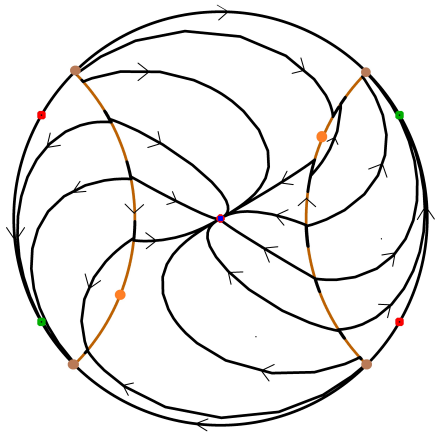

(.5) *F-N 0*

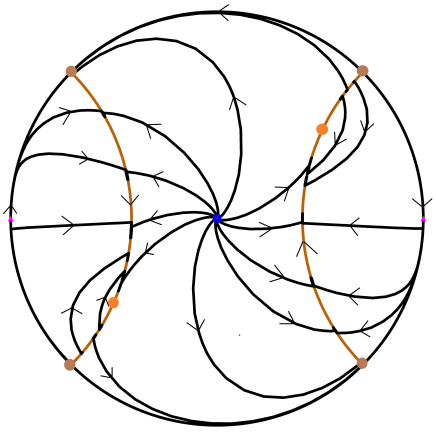

(.6) *F-N 2*

Figure 4.3: *Phase portraits with a hyperbole as switching manifold.*

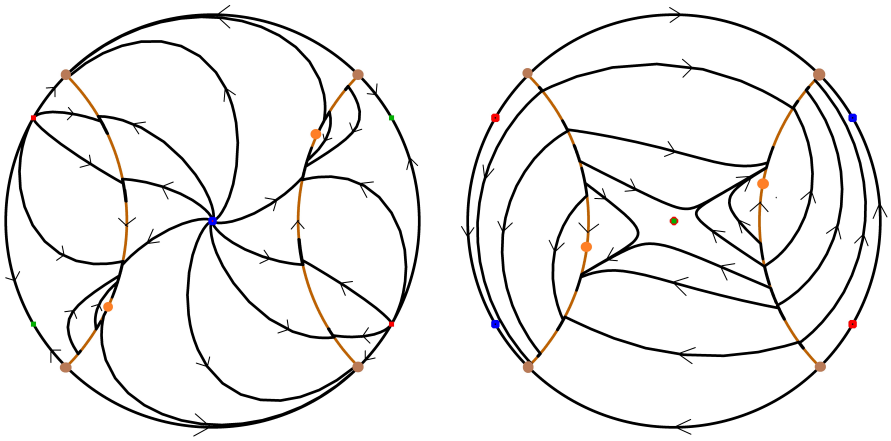

(.7) *F-N 4* **(.8)** *F-S 0*

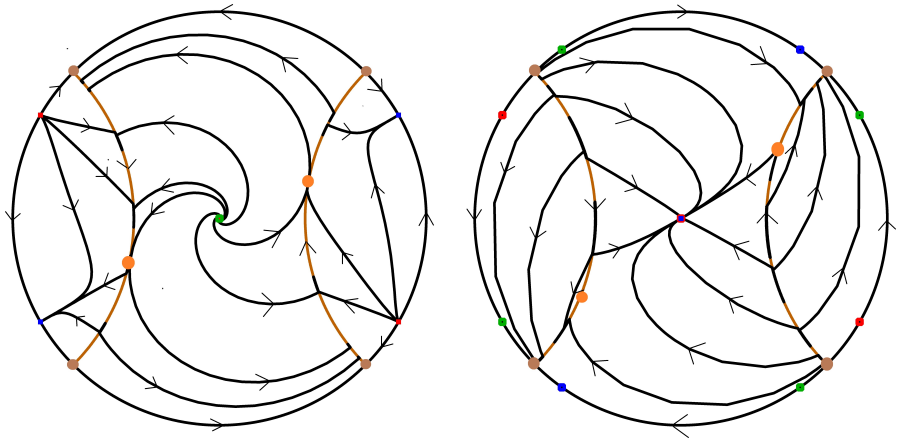

(.9) *F-S 4* **(.10)** *N-N 0*

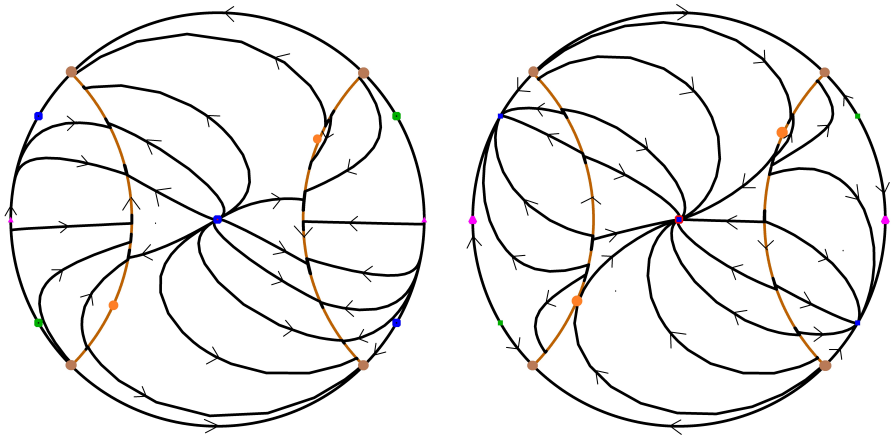

(.11) *N-N 2* **(.12)** *N-N 4*

Figure 4.3: *Phase portraits with a hyperbole as switching manifold.*

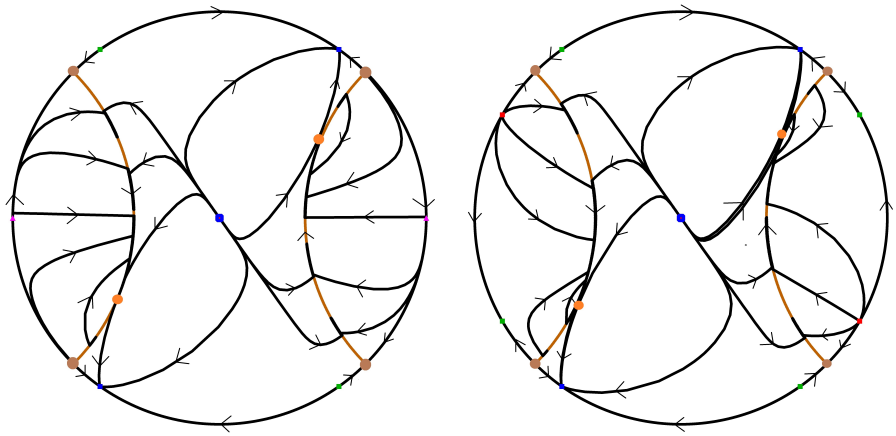

(.13) *N-N 6*

(.14) *N-N 8*

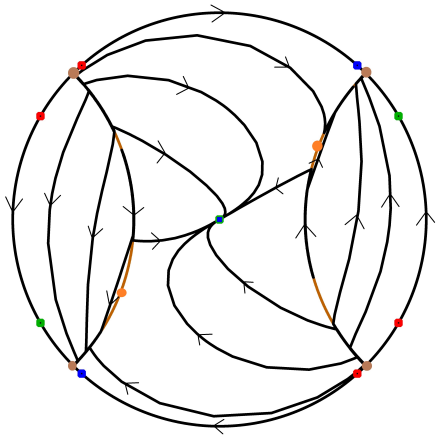

(.15) *N-S 0*

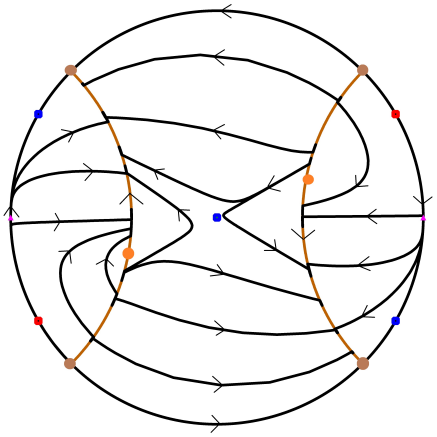

(.16) *N-S 2*

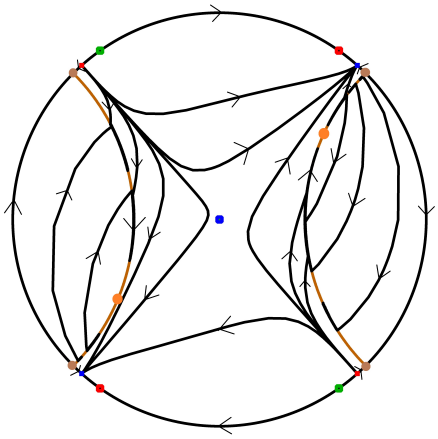

(.17) *N-S 4*

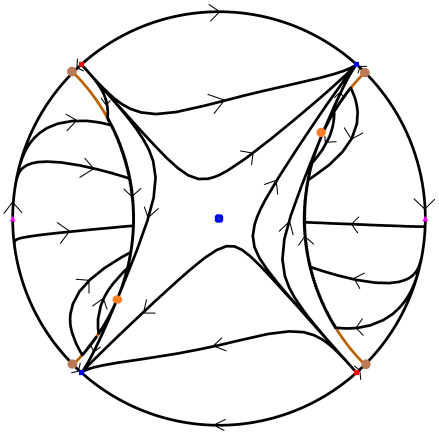

(.18) *N-S 6*

Figure 4.3: *Phase portraits with a hyperbole as switching manifold.*

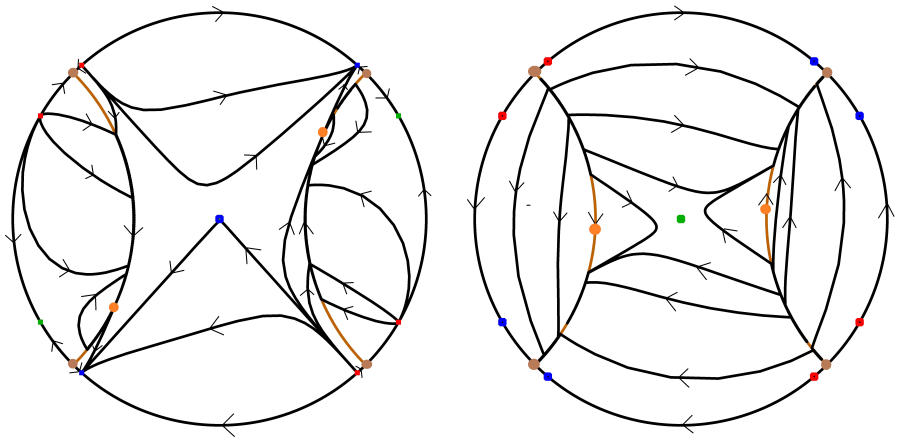

(.19) *N-S 8*

(.20) *S-S 0*

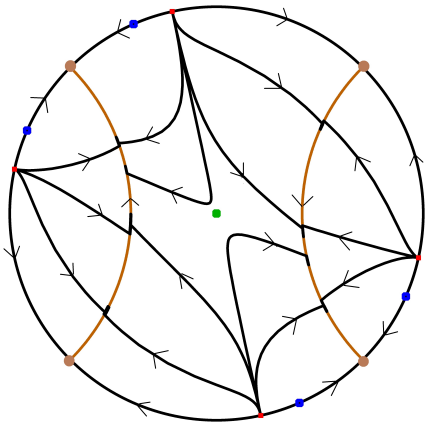

(.21) *S-S 4*

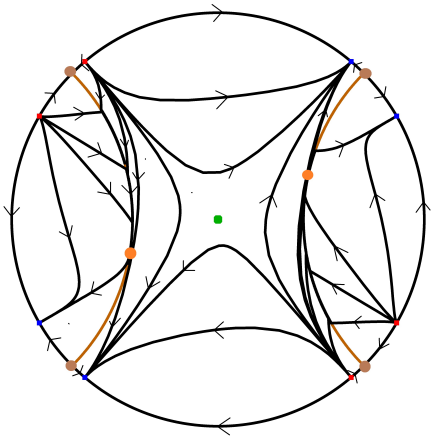

(.22) *S-S 8*

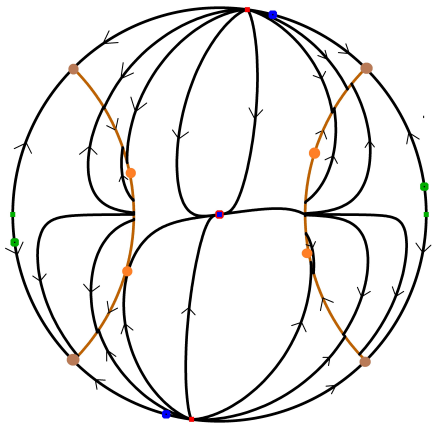

(.23) *4 N-N*

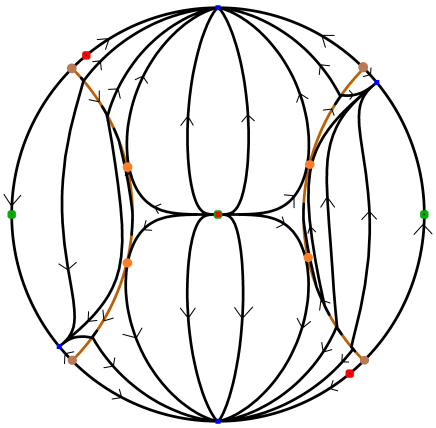

(.24) *4 N-S*

Figure 4.3: *Phase portraits with a hyperbole as switching manifold.*

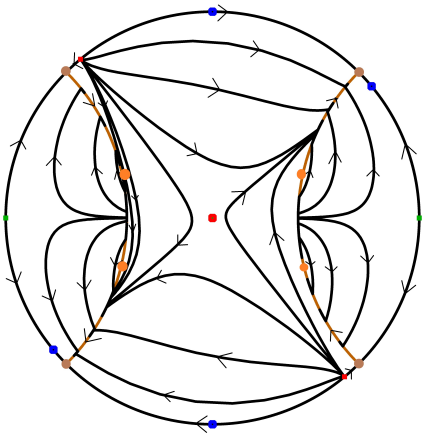

(.25) *4 S-N*

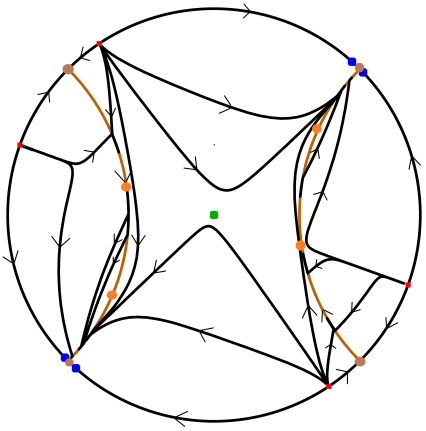

(.26) *4 S-S*

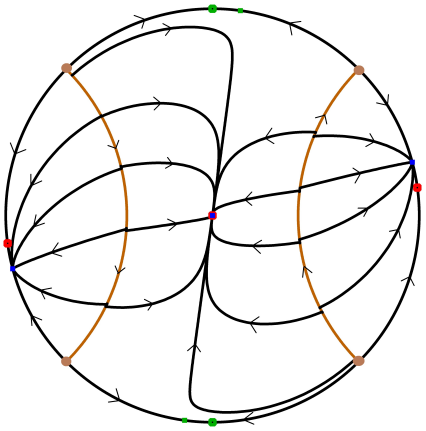

(.27) *0 N-N*

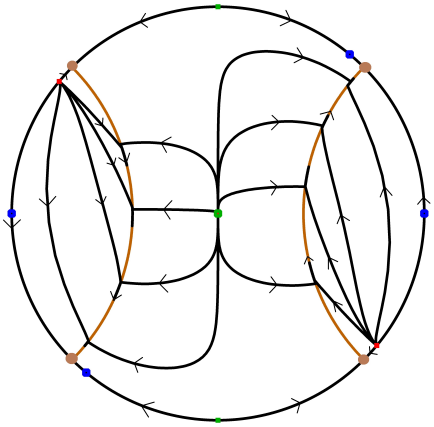

(.28) *0 N-S*

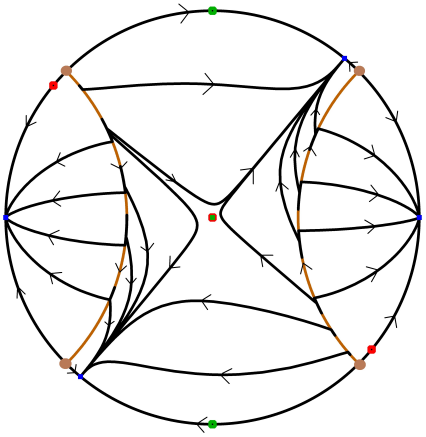

(.29) *0 S-N*

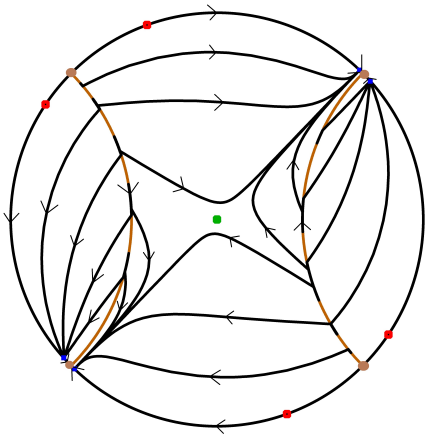

(.30) *0 S-S*

Figure 4.3: *Phase portraits with a hyperbole as switching manifold.*

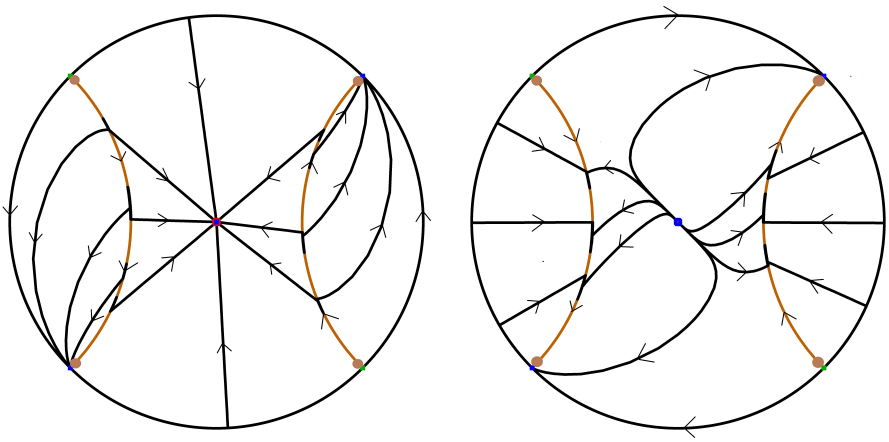

(.31) *SN-N* **(.32)** *N-SN*

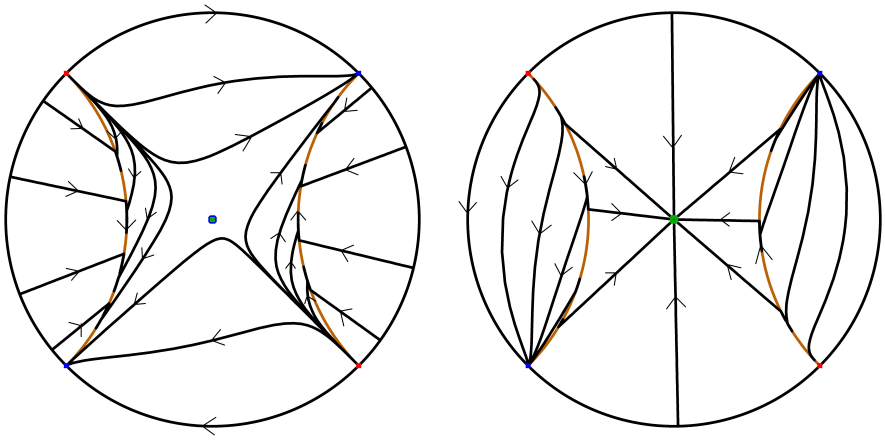

(.33) *SN-S* **(.34)** *S-SN*

Figure 4.3: *Phase portraits with a hyperbole as switching manifold.*

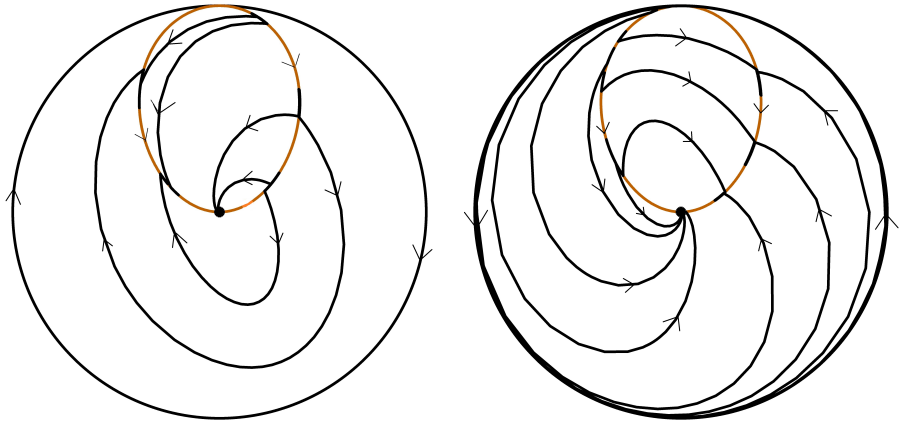

(.1) *C-F* **(.2)** *F-C*

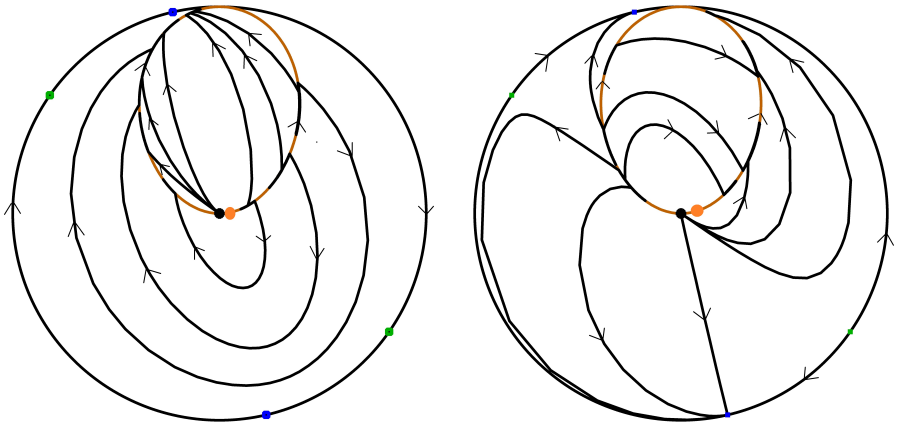

(.3) *C-NI 0* **(.4)** *C-N 4*

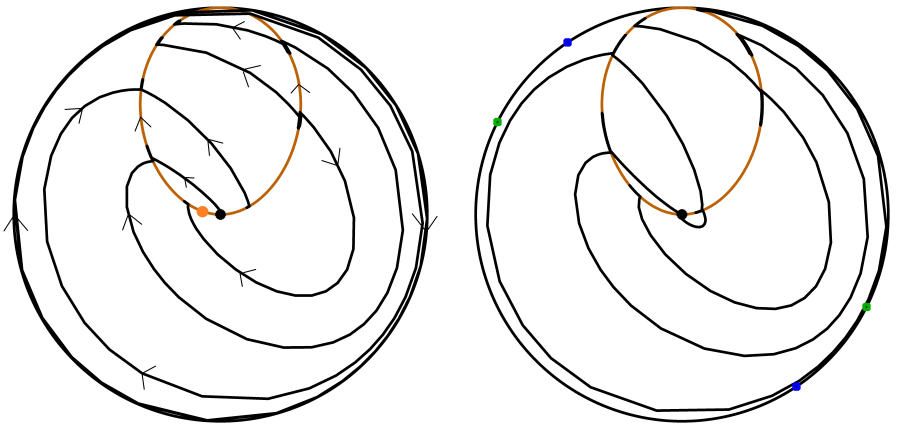

(.5) *F-F* **(.6)** *F-N 0*

Figure 4.4: *Phase portraits with algebraic curves as switching manifold.*

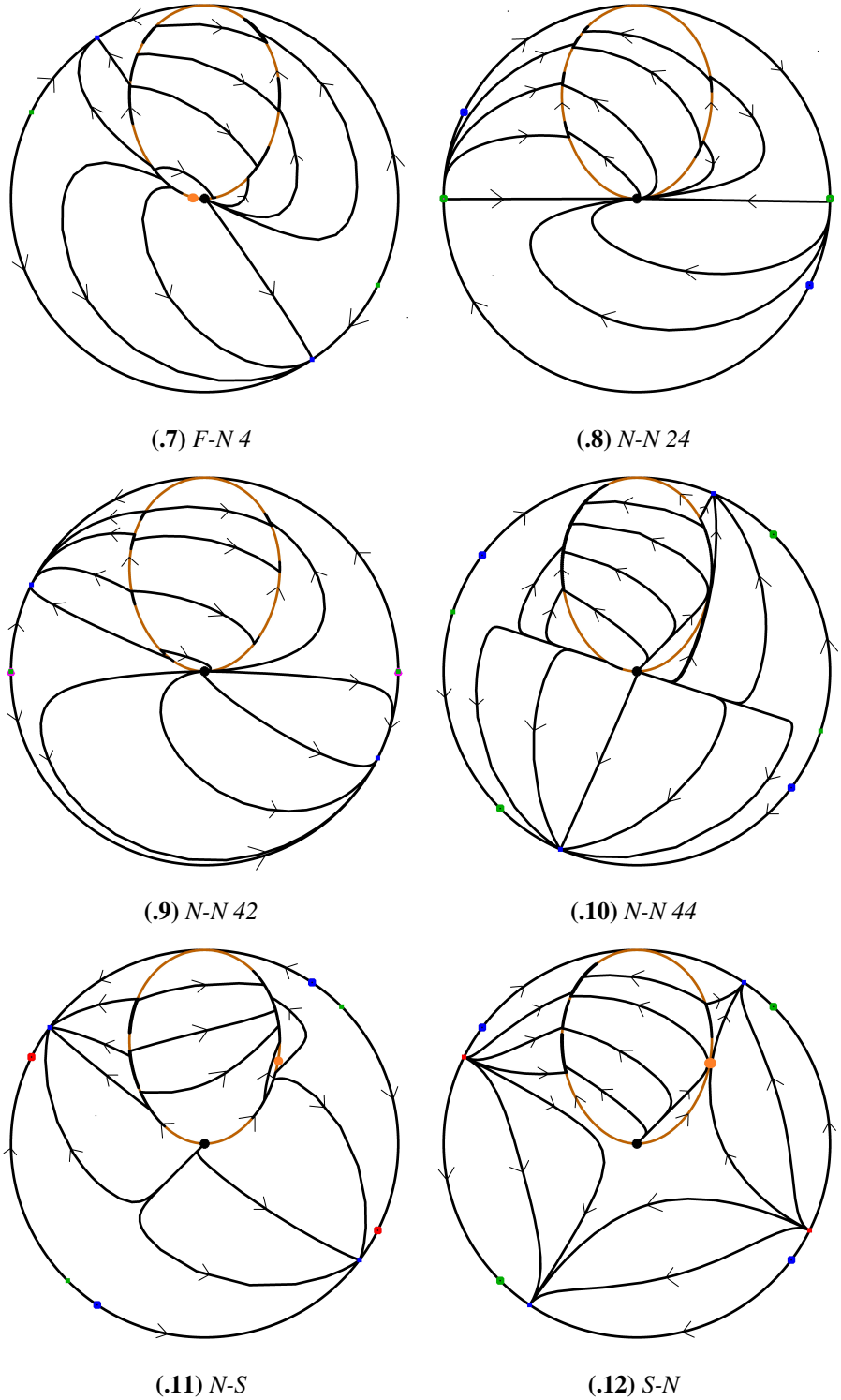

(.7) *F-N 4*

(.8) *N-N 24*

(.9) *N-N 42*

(.10) *N-N 44*

(.11) *N-S*

(.12) *S-N*

Figure 4.4: *Phase portraits with algebraic curves as switching manifold.*

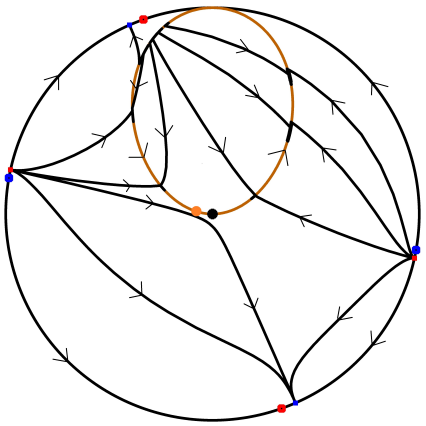

(.13) *S-S*

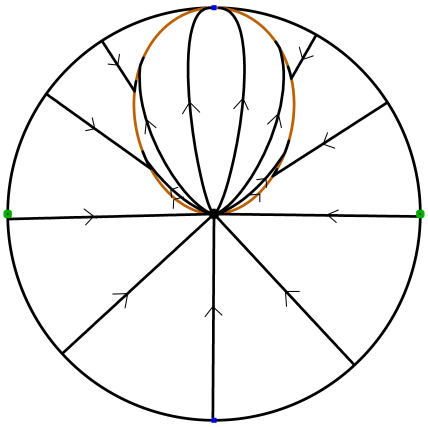

(.14) *SN-N ∞*

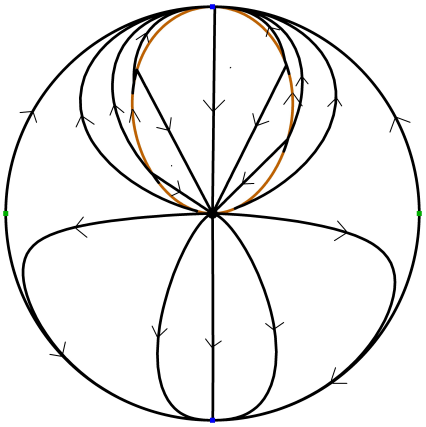

(.15) *Star Node-Node 4*

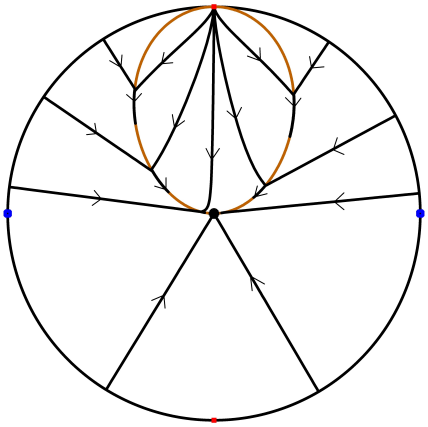

(.16) *SN-S ∞*

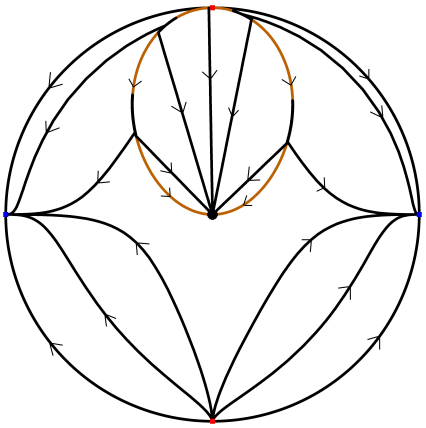

(.17) *SN-S 4*

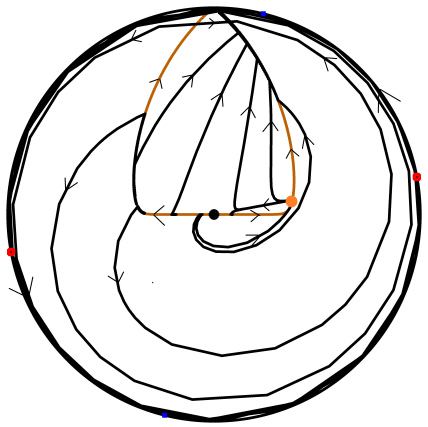

(.18) *16 F-S 0*

Figure 4.4: *Phase portraits with algebraic curves as switching manifold.*

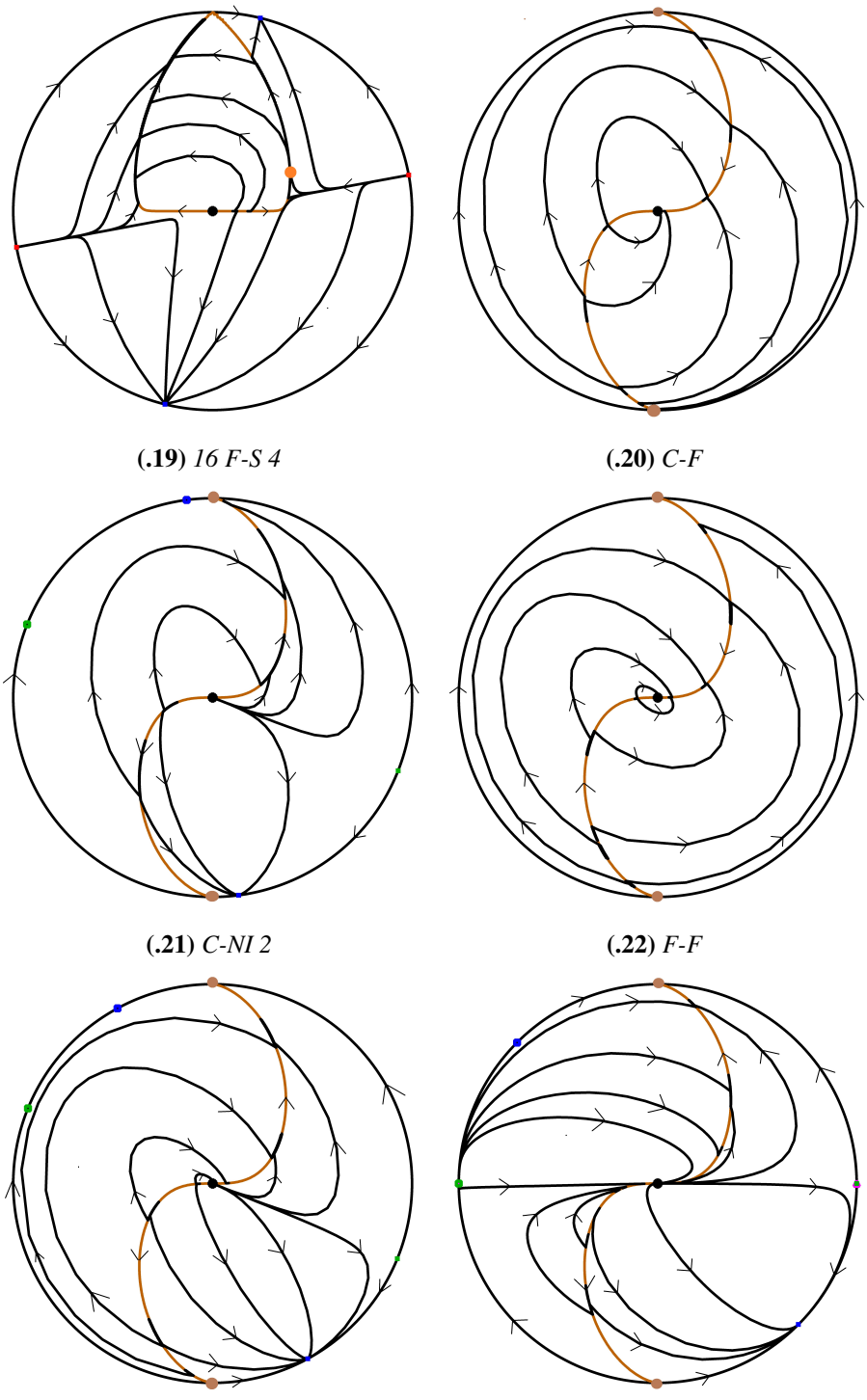

(.19) *16 F-S 4*

(.20) *C-F*

(.21) *C-NI 2*

(.22) *F-F*

(.23) *F-N 2*

(.24) *N-N 3*

Figure 4.4: *Phase portraits with algebraic curves as switching manifold.*

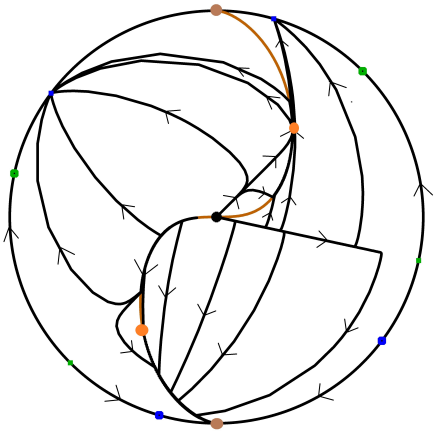

(.25) *N-N 4*

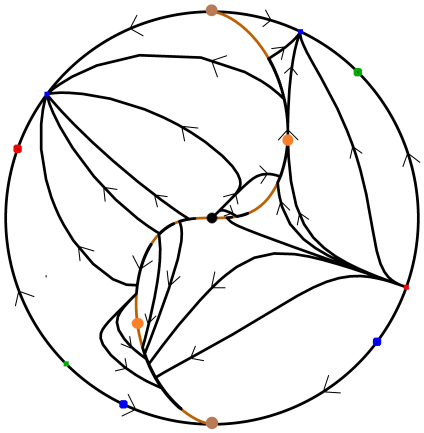

(.26) *N-S*

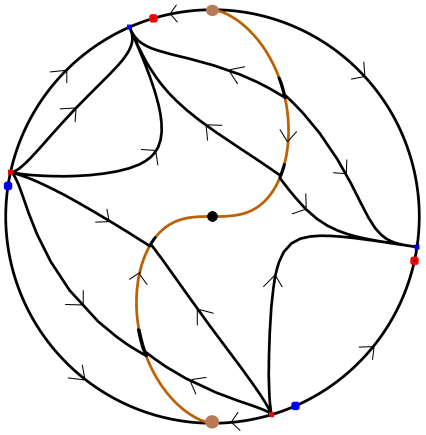

(.27) *S-S*

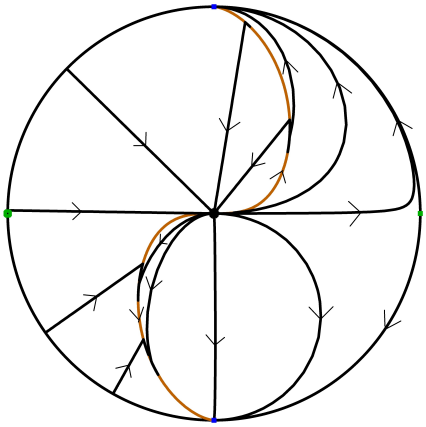

(.28) *SN-N*

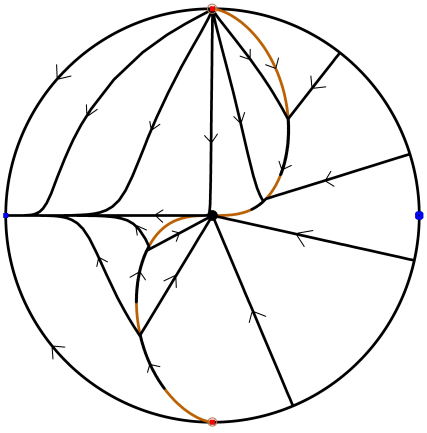

(.29) *SN-S*

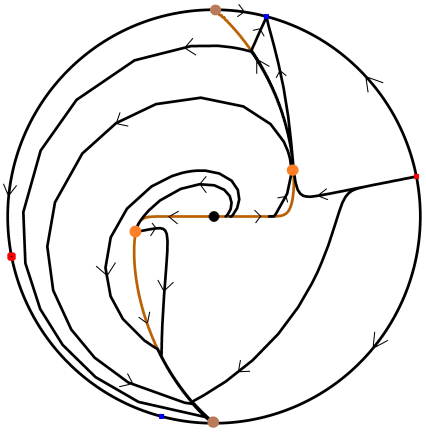

(.30) *15 F-S 2*

Figure 4.4: *Phase portraits with algebraic curves as switching manifold.*

CHAPTER 5

Inelastic non-smooth vector fields with the sphere as switching manifold

In this chapter we study, from a global point of view, homogeneous linear inelastic PSVF in $\mathbb{R}^3$ with the sphere as switching manifold. We provide a complete classification of the dynamics of those systems, together with results about asymptotic stability for a class of those PSVF.

The switching manifold we consider is the embedded sphere $R\mathbb{S}^2 \subset \mathbb{R}^3$, where $R \in \mathbb{R}^+$ is arbitrary, without loss of generality we consider the unitary sphere. Using the notation of the preliminaries, consider $\Sigma = f^{-1}(0) = \mathbb{S}^2$ where $f(x_1,x_2,x_3) = x_1^2 + x_2^2 + x_3^2 - 1$. The regions Σ^+ and Σ^- are, respectively, the exterior and the interior of the region delimited by $\mathbb{S}^2$, that is, $\Sigma^+ = \{\mathbf{x} \in \mathbb{R}^3; ||\mathbf{x}|| \geq 1\}$ and $\Sigma^- = \{\mathbf{x} \in \mathbb{R}^3; ||\mathbf{x}|| \leq 1\}$ where $||x||$ denotes the Euclidian norm of a vector $x \in \mathbb{R}^3$.

The main goal of the chapter is to study the asymptotic behavior of inelastic linear PSVF. Let $X(\mathbf{x}) = A\mathbf{x}$ and $Y(\mathbf{x}) = B\mathbf{x}$ linear vector fields, where $A = (a_{ij})$, $B = (b_{ij})$ are square matrices with real entries, $i, j = 1,2,3$. Consider $Z = (X,Y)$ such that:

$$Z(\mathbf{x}) = \begin{cases} A\mathbf{x}, \text{ if } ||\mathbf{x}|| \geq 1, \\ B\mathbf{x}, \text{ if } ||\mathbf{x}|| \leq 1, \end{cases} \tag{5-1}$$

and $Yf(\mathbf{x}) = -\lambda Xf(\mathbf{x})$ for every $\mathbf{x} \in \mathbb{S}^2$, $\lambda > 0$. It is called a generalized inelastic PSVF.

In particular, we get $\mathbb{S}^2 = \Sigma^s \cup \Sigma^e \cup \Sigma^t$. The Filippov vector field extends naturally to Σ^t and therefore it is defined on the entire sphere. Since our approach is qualitative and focused on the geometry of trajectories, we shall assume the inelastic case, satisfying $\lambda = 1$. Otherwise, the vector fields could have the same orbits, but the flow of X must be faster or slower than the other vector field, generalized inelastic, and the Filippov one over the sphere will be

$$F(\mathbf{x}) = \frac{\lambda X(\mathbf{x}) + Y(\mathbf{x})}{1+\lambda}.$$

Thus, the vector fields would be multiplied by any positive real number which does not affect trajectories and the following results at all.

In the following, we will not consider the cases $X = -Y$ because of its triviality.

5.1 The Filippov vector field and the tangency points on $\mathbb{S}^2$

In this section we study the main properties of the Filippov vector field defined on $\mathbb{S}^2$ for system (5-1) and we describe tangency points.

The next result provides the relation between $X = A\mathbf{x}$ and $Y = B\mathbf{x}$ forming the inelastic PSVF $Z = (X, Y)$.

Lemma 5.1.1 *Consider $Z(\boldsymbol{x}) = (A\boldsymbol{x}, B\boldsymbol{x})$ an inelastic PSVF as in (5-1). Then it satisfies*

$$B = \begin{pmatrix} -a_{11} & -a_{12} - b_{21} - a_{21} & -a_{13} - b_{31} - a_{31} \\ b_{21} & -a_{22} & a_{23} - b_{32} - a_{32} \\ b_{31} & b_{32} & -a_{33} \end{pmatrix}. \tag{5-2}$$

Proof. Since N is inelastic the vector fields X and Y satisfy equation (2-6), that is, the expressions

$$2x_1(a_{11}x_1 + a_{12}x_2 + a_{13}x_3) + 2x_2(a_{21}x_1 + a_{22}x_2 + a_{23}x_3) + 2x_3(a_{31}x_1 + a_{32}x_2 + a_{33}x_3)$$

and

$$-2x_1(b_{11}x_1+b_{12}x_2+b_{13}x_3)-2x_2(b_{21}x_1+b_{22}x_2+b_{23}x_3)-2x_3(b_{31}x_1+b_{32}x_2+b_{33}x_3).$$

must coincide for every $(x_1,x_2,x_2)\in\mathbb{S}^2$. Re-organizing, the coincidence of the last two expressions corresponds to the set of equations

$$\begin{cases} 2(a_{11}+b_{11})x_1+2(a_{22}+b_{22})x_2+2(a_{33}+b_{33})x_3=0,\\ 2(a_{12}+a_{21}+(-b_{12}-b_{21}))x_1x_2=0,\\ 2(a_{13}+a_{31}+(-b_{13}-b_{31}))x_1x_3=0,\\ 2(a_{23}+a_{32}+(-b_{23}-b_{32}))x_1x_3=0. \end{cases}$$

Therefore, for each $i,j\in\{1,2,3\}$ we obtain the conditions $b_{ii}=-a_{ii}$ and $b_{ij}=-(a_{ij}+a_{ji})-b_{ji}$, which replaced in matrix B yield the statement of Lemma 5-2 as we wanted. □

The next result describes the behavior of the Filippov vector field, see Figure 5.1.

Theorem 5.1.1 *Consider the inelastic PSVF $Z(\boldsymbol{x})=(A\boldsymbol{x},B\boldsymbol{x})$ as in (5-1). Then the following statements hold:*

(i) The Filippov vector field over $\mathbb{S}^2$ is given by

$$F(\boldsymbol{x})=\frac{1}{2}\begin{pmatrix} 0 & -b_{21}-a_{21} & -b_{31}-a_{31}\\ b_{21}+a_{21} & 0 & -b_{32}-a_{32}\\ b_{31}+a_{31} & b_{32}+a_{32} & 0 \end{pmatrix}\begin{pmatrix} x_1\\ x_2\\ x_3 \end{pmatrix}.$$

(ii) The equilibrium points of the Filippov vector field are of center type and determined by $p_\pm=\pm\frac{\nu}{|\nu|}$ where $\nu=(b_{32}+a_{32},-(b_{31}+a_{31}),b_{21}+a_{21})^t$.

(iii) Every orbit on $\mathbb{S}^2\setminus\{p_+,p_-\}$ is closed and surrounds the center equilibria p_+ and p_-.

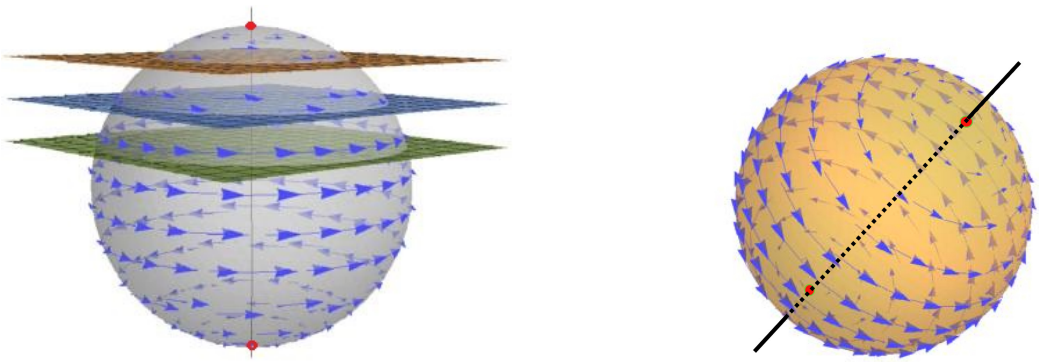

Figure 5.1: *Filippov vector field for inelastic systems and equilibrium points over the sphere* $\mathbb{S}^2$.

Proof. In order to prove (a) it is sufficient to use Lemma 5.1.1 and equation (2-7). To prove (b) and (c) we first note that, from (i), the matrix associated to the linear sliding vector field $F = (A+B)/2$ is skew-symmetric, so the eigenvalues of the matrix are 0 and a pair of conjugated pure imaginary numbers. The eigenvector associated to 0 determines a line of equilibrium points whose intersection with $\mathbb{S}^2$ are $p_{\pm}$. On the other hand, since $\langle F(\mathbf{x}), \nu \rangle = 0$ for every $\mathbf{x} \in \mathbb{S}^2$, the trajectories of the Filippov vector field are closed, planar and orthogonal to the line of singularities associated to the direction given by the zero eigenvector. □

To study the behavior of the orbits outside $\mathbb{S}^2$, we shall study the tangency points. We remark that the tangency points of X and Y with $\mathbb{S}^2$ coincide, due to equation (2-6). Therefore it is sufficient to study the tangency either of X or Y. Using equation (2-5), the tangency points over $\mathbb{S}^2$ are defined by the intersection of $\mathbb{S}^2$ with the quadratic surface

$$2[a_{11}x_1^2 + a_{22}x_2^2 + a_{33}x_3^2 + (a_{12}+a_{21})x_1x_2 + (a_{13}+a_{31})x_1x_3 + (a_{32}+a_{23})x_2x_3] = 0 \quad (5\text{-}3)$$

that is, $Xf(x_1, x_2, x_3) = 0$. We can see that this equation is independent of the radius of the sphere. In order to classify tangency points we use a preliminary classification of

quadratic surfaces provided by [6]. We obtain the following result.

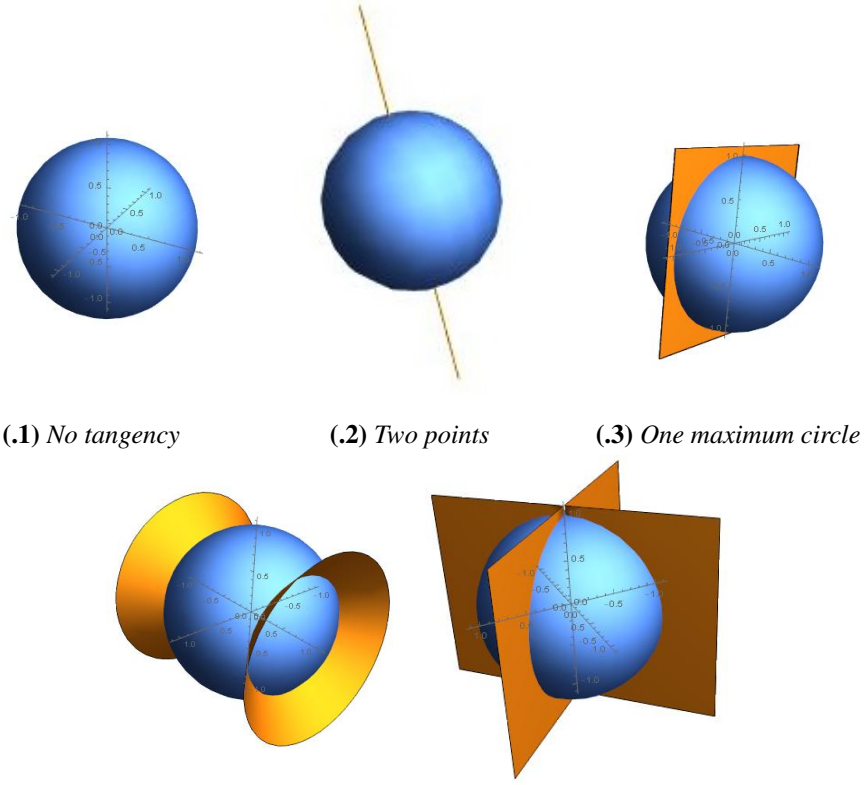

(.1) *No tangency* **(.2)** *Two points* **(.3)** *One maximum circle*

(.4) *Two disjoint circles* **(.5)** *Two maximum circles*

Figure 5.2: *The shape of the quadrics surfaces around a neighborhood of the switching manifold.*

Lemma 5.1.2 *The intersection between the quadric surfaces from equation (5-3) and the sphere is one of the following sets (see Figure 5.2):*

i) $\mathcal{S}_1 = \emptyset$*: the empty set;*

ii) $\mathcal{S}_2$*: two antipodal points;*

iii) $\mathcal{S}_3$*: one maximum circle;*

iv) $\mathcal{S}_4$*: two closed disjoint curves, each one diffeomorphic to* $\mathbb{S}^1$*;*

v) $\mathcal{S}_5$*: two transversal maximum circles.*

Proof. According to the normal forms provided in [6] there are 17 possibilities for the quadrics,

$$Q_1 : x_1^2 = 0 \qquad Q_2 : \frac{x_1^2}{a^2} + \frac{x_2^2}{b^2} + \frac{x_3^2}{c^2} = -1 \qquad Q_3 : \frac{x_1^2}{a^2} + \frac{x_2^2}{b^2} + \frac{x_3^2}{c^2} = 1$$

$$Q_4 : \frac{x_1^2}{a^2} + \frac{x_2^2}{b^2} + \frac{x_3^2}{c^2} = 0 \qquad Q_5 : \frac{x_1^2}{a^2} + \frac{x_2^2}{b^2} - \frac{x_3^2}{c^2} = 0 \qquad Q_6 : \frac{x_1^2}{a^2} + \frac{x_2^2}{b^2} = -1$$

$$Q_7 : \frac{x_1^2}{a^2} + \frac{x_2^2}{b^2} = 1 \qquad Q_8 : \frac{x_1^2}{a^2} + \frac{x_2^2}{b^2} = x_3 \qquad Q_9 : \frac{x_1^2}{a^2} - \frac{x_2^2}{b^2} = -1$$

$$Q_{10} : \frac{x_1^2}{a^2} - \frac{x_2^2}{b^2} = x_3 \qquad Q_{11} : \frac{x_1^2}{a^2} + \frac{x_2^2}{b^2} - \frac{x_3^2}{c^2} = 1 \qquad Q_{12} : \frac{x_1^2}{a^2} + \frac{x_2^2}{b^2} - \frac{x_3^2}{c^2} = -1$$

$$Q_{13} : \frac{x_1^2}{a^2} + \frac{x_2^2}{b^2} = 0 \qquad Q_{14} : \frac{x_1^2}{a^2} - \frac{x_2^2}{b^2} = 0 \qquad Q_{15} : x_1^2 + 2ax_3 = 0$$

$$Q_{16} : x_1^2 = -a^2 \qquad Q_{17} : x_1^2 = a^2$$

with $a \neq 0$. Notice that only the quadrics Q_2, Q_6 and Q_{16} are not in the real space. The others correspond (from Q_1 forward) to coincident planes, ellipsoid, the origin, elliptic cone, elliptical cylinder, elliptical paraboloid, hyperbolic cylinder, hyperbolic paraboloid, hyperboloid of one sheet or two sheets, a straight line, parabolic cylinder, and intersecting or parallel planes, respectively.

Each term in equation (5-3) is quadratic and the equation vanishes. Thus, quadrics must be symmetric with respect a plane and then we get only five options which satisfy those conditions: the origin (Q_4), a straight line (Q_{13}), coincident planes (Q_{17}), elliptic cones (Q_5) or two intersecting planes (Q_{14}). Intersecting them with the sphere we obtain (unless suitable rotations) the sets $\mathcal{S}_1, \ldots, \mathcal{S}_5$, respectively. □

From now on we say that the tangency points have a *generic configuration* if they are given by the sets $\mathcal{S}_4$ or $\mathcal{S}_5$. The sets $\mathcal{S}_2$ and $\mathcal{S}_3$ are limit situations of the previous ones (thus somehow non-generic). Now we present a relation between the Filippov vector field and the tangency points of a PSVF.

Proposition 5.1.1 *Let Γ_F be a non trivial trajectory of the Filippov vector field F over $\mathbb{S}^2$ and assume that $\mathcal{S}_i \neq \emptyset$ for some $i \in \{3,4,5\}$. If $\Gamma_F \cap \mathcal{S}_i \neq \emptyset$, then generically the intersection occurs at two points when $i = 3$ and at most 4 points when $i = 4$ or $i = 5$. On*

the other hand, if the following set of conditions hold simultaneously

$$\begin{aligned}(a_{11},a_{22},a_{33})^t &= \nu,\\ a_{12}+a_{21} &= a_{11}+a_{22},\\ a_{13}+a_{31} &= a_{11}+a_{33},\\ a_{23}+a_{32} &= a_{22}+a_{33},\end{aligned}$$

then in this case we obtain $\Gamma_F \subseteq S_i$, that is, Γ_F is entirely contained in a connected component of a tangency set.

Proof. Using the Sard's Theorem, the orbits Γ_F are generically transversal to the tangency points, and using the type of tangencies from Lemma 5.1.2 the intersection $\Gamma_F \cap \mathcal{S}_i$ is generically empty ($\mathcal{S}_1$, $\mathcal{S}_2$), two points because it is the intersection between a maximum circle ($\mathcal{S}_3$) and other circle Γ_F, or four points for two circles (maximum for $\mathcal{S}_4$, $\mathcal{S}_5$) and a circle Γ_F.

Also, we consider the following system of equations to be a tangency point also in the Filippov vector field over the sphere:

$$\begin{cases} Xf(\mathbf{x}) = 0,\\ \langle \mathbf{x}, \nu\rangle = 0,\end{cases}$$

where the first equation is $(5-3)$, a quadric, and the second one describes the plane crossing by the origin $(b_{32}+a_{32})x_1-(b_{31}+a_{31})x_2+(b_{21}+a_{21})x_3=0$, multiplying the last one step by step with x_1, x_2 and x_3 we get the identities of Proposition 5.1.1. □

Example 5.1.1 *Let $Z(\boldsymbol{x}) = (A\boldsymbol{x}, B\boldsymbol{x})$ be a non-smooth vector field defined by the matrices*

$$A = \begin{pmatrix} 0 & 2 & 1\\ -1 & 1 & 1\\ -2 & -1 & -1\end{pmatrix},\quad B = \begin{pmatrix} 0 & -1 & 0\\ 0 & -1 & -1\\ 1 & 1 & 1\end{pmatrix}.$$

Notice that A and B satisfy the conditions of Proposition 5.1.1. The tangency set in this case is given by

$$Xf(x_1,x_2,x_3) = -Yf(x_1,x_2,x_3) = x_2^2 - x_3^2 + x_1x_2 - x_1x_3 = 0$$

which corresponds to the set $\mathcal{S}_5$. In this case $\mathcal{S}_5 = \mathcal{S}_5^1 \cup \mathcal{S}_5^2$, where each one is a maximum circles from the planes $\pi_1 : \{x_2 - x_3 = 0\}$ and $\pi_2 : \{x_1 + x_2 + x_3 = 0\}$, respectively.

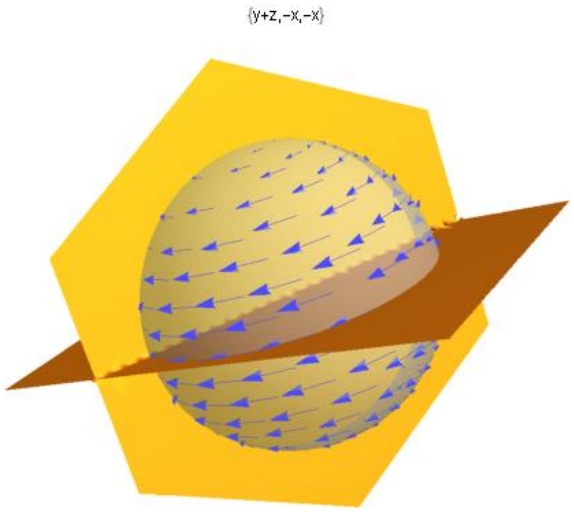

Figure 5.3: *Behaviour of the system where some trajectories of the Fillipov vector field belong to the quadric*

One of these planes, π_1, has as normal vector $(0,1,-1)$ and for the Filippov vector field

$$F(\mathbf{x}) = \frac{1}{2}\begin{pmatrix} 0 & 1 & 1 \\ -1 & 0 & 0 \\ -1 & 0 & 0 \end{pmatrix}\begin{pmatrix} x_1 \\ x_2 \\ x_3 \end{pmatrix},$$

over the sphere $\nu = (0,-1,1)$ (one of the eigenvectors), so one of the trajectories of the Filippov vector field coincides with one circle of tangency points. Also the equilibrium points lie on the other circle and this is orthogonal to the whole trajectories of the Filippov vector field.

We can see that the both systems are saddle-focus with inverse directions, where the

eigenvalues for the exterior vector field are $\lambda_1 = -0.67359$, $\lambda_2 = 0.3368 + 2.0833i$ and $\lambda_3 = 0.3368 - 2.0833i$, and for the interior one $\lambda_1 = 1$, $\lambda_2 = -\frac{1}{2} + \frac{\sqrt{3}}{2}i$ and $\lambda_3 = -\frac{1}{2} - \frac{\sqrt{3}}{2}i$. Notice that trajectories crosses the tangency lines from sliding to escape and then from escape to sliding.

5.2 Limit sets and recurrences near $\mathbb{S}^2$

In this section we are going to study a kind of asymptotic stability problem which is related to the attraction of $\mathbb{S}^2$ for positive or negative time. As we saw in the previous section, the quadric Q providing the tangency lines on $\mathbb{S}^2$ can be of five types, from $\mathcal{S}_1$ to $\mathcal{S}_5$. We study the cases without tangency points, that is, $\mathcal{S}_1$ and the other separately. In each case, we use criteria on asymptotic stability of the origin to infer on $\mathbb{S}^2$, the first case using the classical Lyapunov criteria and the others the so-called Routh-Hurwitz criteria.

5.2.1 The case $\mathbb{S}^2 \cap Q = \mathcal{S}_1$ and the degenerated cases $\mathcal{S}_2$ and $\mathcal{S}_3$.

The main result is the following.

Theorem 5.2.1 *Assume that $Z(\boldsymbol{x}) = (A\boldsymbol{x}, B\boldsymbol{x})$ an inelastic non-smooth system as in Equation (5-1). The following statements are equivalent.*

(i) *There are no tangency points on $\mathbb{S}^2$.*

(ii) *A is positive (respec. negative) and B is negative (respec. positive) definite.*

(iii) *The whole sphere is an escape (respec. sliding) region if it exists.*

(iv) *$\mathbb{S}^2$ is a compact global repulsive (respec. attractive) surface of N.*

(v) *$Xf(\boldsymbol{x}) > 0$ and $Yf(\boldsymbol{x}) < 0$ (vise versa) for all $\boldsymbol{x} \in \mathbb{S}^2$.*

Proof. [Proof of Theorem 5.2.1] To prove $(i) \Rightarrow (ii)$ suppose that A is not positive definite, so there exists $\mathbf{x} \in \mathbb{S}^2$ such that $Xf(\mathbf{x}) = \mathbf{x}^t(A + A^t)\mathbf{x} \leq 0$. If $\mathbf{x}^t(A + A^t)\mathbf{x} = 0$, we get a tangency point which is a contradiction. If $\mathbf{x}_1^t(A + A^t)\mathbf{x}_1 < 0$ and $\mathbf{x}_2^t(A + A^t)\mathbf{x}_2 > 0$ for different $\mathbf{x}_1, \mathbf{x}_2 \in \mathbb{S}^2$, there is a quadratic form that is a polynomial in several variables

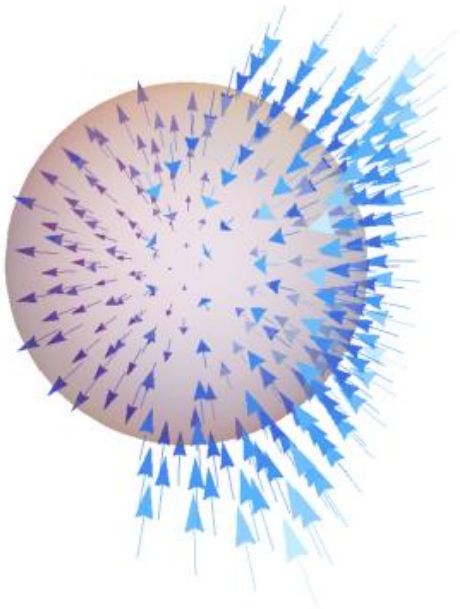

Figure 5.4: *Behavior without tangency points.*

and so continuous, using the intermediate value theorem over the sphere [46] there exists $\mathbf{x} \in \mathbb{S}^2$ such that $\mathbf{x}^t(A+A^t)\mathbf{x} = 0$.

Thus, we get tangency points if A (or B) is not positive or definite positive.

$(ii). \rightarrow (iii)$. As above, $Xf(\mathbf{x}) > 0$ without changes for all $\mathbf{x} \in \mathbb{S}^2$.

$(iii). \rightarrow (iv)$. The eigenvalues of the exterior vector field have the same real part, because trajectories are always arriving (leaving) to the whole sphere, the same occurs to the interior one. Thus the sphere is a compact repulsor (attractor).

$(iv). \rightarrow (v)$. The real part of the eigenvalues λ_i of A (at least one of them must be pure real) have the same sign, the same occurs for B although with opposite sign.

1. $\lambda_1,\ \lambda_2,\ \lambda_3 < 0$ (> 0) and moreover $\mathbb{S}^2 = \Sigma^s$ $(\mathbb{S}^2 = \Sigma^e)$. There is an attracting (repelling) node.
2. $\lambda_1 < 0$, $\lambda_2 = m + ni$, $\lambda_3 = m - ni$ with $m < 0$, $(\lambda_1, m > 0)$. There is an attracting (repelling) focus, also attracting (repelling) in third dimension.

If zero is isolated and there exists no tangency points, then centers or saddles cannot occur because the real part of the eigenvalues must have the same sign to attract or repel in every

direction, so the eigenvalues should be complex with non-zero real part. Using that this happens to the whole sphere, $Xf(\mathbf{x}) > 0$ and $Yf(\mathbf{x}) < 0$ (vise versa) for all $\mathbf{x} \in \mathbb{S}^2$.

$(v). \to (i)$. Using Remark (1) of [39], the matrix A is positive (negative) definite if and only if its symmetric part is also positive (negative) definite. Therefore, by equation (2-5) $Xf(\mathbf{x})/2 = \frac{1}{2}\mathbf{x}^t(A+A^t)\mathbf{x} > 0$ (< 0) $\forall \mathbf{x} \in \mathbb{S}^2$. So there exists no $\mathbf{x}$ in the sphere such that $Xf(\mathbf{x}) = 0$, there are no tangency points for X and the same occurs for Y and B. □

The next two results provide some partial answers for the particular case where the sphere attracts trajectories nearby. First we consider the non-generic configurations.

Theorem 5.2.2 *Assume that $Z(\boldsymbol{x}) = (A\boldsymbol{x}, B\boldsymbol{x})$ is an inelastic non-smooth system as in Equation (5-1). If the tangency set is $\mathcal{S}_2$ or $\mathcal{S}_3$, the real part of the eigenvalues of A are negative (positive) and the ones of B are positive (negative), then $Xf(x) \leq 0$ (or $Xf(x) \geq 0$) for all $x \in \Sigma^s$. Moreover, the $\omega-$limit set of every point $p \in \mathbb{R}^3$ is a sliding ($\alpha-$limit set and escaping) periodic orbit $\Gamma_p \subset \mathbb{S}^2$. For the case $\mathcal{S}_3$, the periodic orbit in $\mathbb{S}^2$ either, crosses it transversally, there exists a tangency point or coincides with $\mathcal{S}_3$, and these are all the possibilities that may occur.*

Proof. [Proof of Theorem 5.2.2] For two tangency points over the sphere consider

$$Xf(x_1, x_2, x_3) = \pm((ax_i - bx_j)^2 + cx_k^2) = 0$$

where we get the line $x_j = (a/b)x_i$ and $x_k = 0$. The last equality is a sum of squares which is always non-negative, then depending on the sign $\pm$ the possibilities are $Xf(x) \leq 0$ or $Xf(x) \geq 0$ for all $x \in \Sigma^s$, thus the Filippov vector field over the sphere is composed by a continuum of periodic orbits. Only in two of those orbits there are the tangency points and the hemispheres between them are sliding or escape regions, respectively.

Suppose that the tangency now is a maximum circle $\mathcal{S}_3$, it can be one complete orbit of the Filippov vector field following Proposition 5.1.1, or this circle can be transversal to some set or the complete set of those periodic orbits, then there exists at most two tangency

points in each of them and sliding (escaping) regions between these points because if we see the equation (5-3),

$$Xf(x_1,x_2,x_3) = \pm(ax_1 + bx_2 + cx_3)^2 = 0,$$

which describes the plane of tangencies, thus $Xf(x) \leq 0$ or $Xf(x) \geq 0$ for all $x \in \Sigma^s$. Then, as in the non-tangency case, for the interior vector field there is a repeller which sent the whole orbits to the sphere and then to some periodic orbit of the Filippov vector field.

The tangency points form a maximum circle in the sphere and generically its intersection with other circles will be transversal, in that sense it can happen in two points or zero points. Other non-generic cases are a tangencial contact between them in one point and a complete contact resulting in the coincidence of the circles. □

Corollary 5.2.1 *For the cases of Theorems 5.2.1 and 5.2.2, the sphere is a global attractor for our PSVF, for $\mathcal{S}_1$ it is is asymptotically stable (or asymptotically unstable) and for $\mathcal{S}_2$ and $\mathcal{S}_3$ it is stable (or unstable).*

Proof. Since $\dot{V}(\mathbf{x}) = Xf(\mathbf{x}) < 0$ for all $\mathbf{x} \in \mathbb{R}^3 \setminus \{0\}$, by the Liapunov criteria 2.1.4 the whole orbits of X converges asymptotically to the origin and in our PSVF do the same to the sphere. For Y it is valid $Yf(\mathbf{x}) > 0$ and in negative time also the orbits converges asymptotically, since $\dot{V} > 0$ in $\mathbb{R}^3 \setminus \{0\}$ then there exists an increasing sequence $\{t_n\}$ of positive real numbers such that $\varphi(t_n, \mathbf{x}) \to \infty$. Thus, choosing N such that $||\varphi(t_N, \mathbf{x})|| > 1$ then the trajectory arrives to the sphere which is a complete sliding region, so the sphere is an asymptotic stable set.

By Theorems 5.2.1 and 5.2.2 all trajectories have the whole set of periodic orbits in $\mathbb{S}^2$ as $\omega-$limit set, so the sphere is a global attractor. □

5.2.2 The case $\mathbb{S}^2 \cap \mathcal{Q} = \mathcal{S}_i$, $i = 4, 5$

The cases having those tangency points are more complicated than the previous studied cases. Effectively, in the presence of more tangency points, those trajectories that are tangent to $\mathbb{S}^2$ may eventually go to infinity and never return close to the sphere. This, of course, is a possible situation but the dynamics in this case is easy to see because the external vector field is linear and homogeneous, so trajectories are described by the Poincaré's Compactification. Instead, we are interested in the study of non-trivial dynamics and recurrences near (or over) $\mathbb{S}^2$.

In the following cases we will consider three or four separation regions defined by the tangencies and if there exists a sliding region, then next there is an escape one.

Lemma 5.2.1 *Assume that $Z(\boldsymbol{x}) = (A\boldsymbol{x}, B\boldsymbol{x})$ an inelastic non-smooth system as in Equation (5-1). Assume also that $(0,0,0)$ is an attractor equilibrium point for $A\boldsymbol{x}$ and a repeller one for $B\boldsymbol{x}$. If the tangency set is $\mathcal{S}_4$ or $\mathcal{S}_5$ and there is a set of periodic orbits of the Filippov vector field which are completely contained in a sliding connected component, then there exists $\boldsymbol{x} \in \mathbb{R}^3 \setminus (0,0,0)$ such that the $\omega-$limit set is one of those sliding periodic orbits $\Gamma_{\boldsymbol{x}} \subset \mathbb{S}^2$.*

Proof. Suppose that there is a set of periodic orbits of the Filippov vector field which are completely contained in a sliding connected component, let $\mathbf{x}_0 \in \mathbb{S}^2$ be a point in one of those trajectories, thus using the existence and uniqueness theorem and the Tubular Flow Theorem we know that there exist unique orbits of X and Y crossing $\mathbf{x}_0$ and these have opposite directions because they are in a sliding region. Then for the points $\mathbf{x} \in \mathbb{R}^3$ such that $||\mathbf{x}|| > 1$ and $\varphi_{\mathbf{x}}(t) = \mathbf{x}_0$ for some $t > 0$, considering the flow of X, we get that their $\omega-$limit set is $\Gamma_{\mathbf{x}_0}$. The same occurs for $||\mathbf{x}|| < 0$ using the flow of Y. □

The previous result allows us to state the following theorem.

Theorem 5.2.3 *Assume that $Z(\boldsymbol{x}) = (A\boldsymbol{x}, B\boldsymbol{x})$ an inelastic non-smooth system as in Equation (5-1). Assume also that $(0,0,0)$ is an attractor equilibrium point for $A\boldsymbol{x}$ and a repeller one for $B\boldsymbol{x}$. If the tangency set is $\mathcal{S}_4$ or $\mathcal{S}_5$, then the $\omega-$limit set of every point*

$p \in \mathbb{R}^3 \setminus (0,0,0)$ is contained in interior of a compact set with boundary $R\mathbb{S}^2$ for some $R \in \mathbb{R}^+$. Moreover, the $\omega-$limit set can be one sliding periodic orbit over the sphere and/or a compact invariant set which includes the escape regions over the sphere.

Proof. For three regions, the two exterior of them satisfy $Xf < 0$, $Yf > 0$, and the region between them with $Xf > 0$, $Yf < 0$. If there are four regions, two opposite of them fulfill $Xf < 0$, $Yf > 0$ and the others satisfy $Xf > 0$, $Yf < 0$. By Lemma 5.2.1 we can get a sliding periodic orbit.

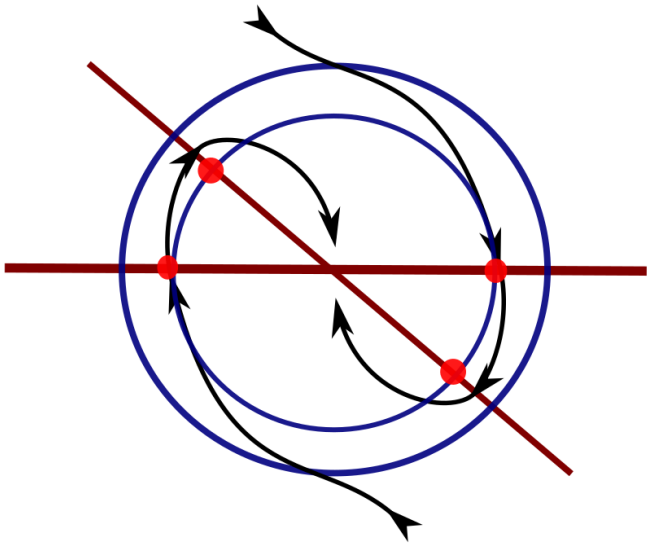

Figure 5.5: *Behavior of the trajectories for the vector field X.*

If there are periodic orbits of the Filippov vector field which have escape and sliding regions, in the escape one the trajectory can continue across the sphere or go away over an orbit of X or Y. But the origin is an attractor for the vector field X so that orbit which escapes outside the sphere has to come back in a sliding region converging to the origin, and inside the sphere can exists an orbit escaping. But for Y the origin is a repeller and this orbit has to go away from the origin to the sphere again.

Let $\mathbf{x}_0$ be a tangency point from a sliding to the corresponding escape region, this will be a visible one and the set of the whole tangencies of this type will be T_v, then there exists an orbit of X which come from the exterior of the sphere and is tangent to $\mathbb{S}^2$ in that point.

Let $R\mathbb{S}^2$ be a sphere with $R = ||\varphi_{\mathbf{x}}(t_1)|| >> 1$ for $t_1 > 0$. There exits $t_2 > t_1$ such that $\varphi_{\mathbf{x}}(t_2) = \mathbf{x}_0$, and $t_3 > t_2$ such that we reach the other tangency $\varphi_{\mathbf{x}}(t_3) = \mathbf{x}_1$ where begins the other sliding region, an invisible one and this set will be T_i, and the orbit of X has to come back to $\mathbb{S}^2$, generically to another periodic orbit of the Filippov vector field (in fact to the origin). Thus, the orbits which are escaping by the exterior vector field on the periodic orbit are limited by the last one, by the Tubular Flow Theorem, see Figure 5.5.

Thus, let $R_1 = max_{\mathbf{x}_1 \in T_i} ||\varphi_{\mathbf{x}}(t_2)||$ on the two disjoint or two transversal circles of tangencies over the sphere, which is compact, then the set of tangencies is also compact and we get that maximum. Thus, getting $R > R_1$, the $\omega-$limit set of every point $p \in \mathbb{R}^3 \setminus (0,0,0)$ is contained in interior of the compact set with boundary $R\mathbb{S}^2$.

Considering the set of tangencies such that we get a visible one, T_v, we get one or two compact escape regions respectively and using that the flow of X is a diffeomorphism (in particular continuous) then the image of the escape regions over the sliding ones is also compact, and with the trajectories of the flow we get also a compact set. Proceeding analogously for Y and joining the two compact sets we can see that this is invariant over the flow of X, Y and by the Filippov vector field, then we get a compact invariant set which is also a $\omega-$limit set for some points at the interior and exterior of $\mathbb{S}^2$. □

Remark 5.2.1 *If the tangency set is $\mathcal{S}_5$, then given $p \in \mathbb{R}^3 \setminus (0,0,0)$, either the positive orbit of p is a sliding periodic orbit $\Gamma_p \subset \mathbb{S}^2$ or p is contained in some periodic orbit not contained on $\mathbb{S}^2$.*

5.3 Examples and numerical simulations

Since the cases presenting tangency points are more complicated, we are not able to provide general conditions on the parameters to guarantee stability conditions so we only assume general hypotheses as those within Theorems 5.2.2 and 5.2.3. Instead, in this

section we provide some examples and simulations using the Routh-Hurwitz criteria, see [1, 12].

Next result is a direct consequence of that criteria.

Theorem 5.3.1 *Considering the following conditions for the exterior vector field X:*

1. $tr(A) = -tr(B) = a_{11} + a_{22} + a_{33} < 0$,
2. $\det(A) < 0$ *and* $\det(B) > 0$,
3. $tr(A)\left(\frac{2}{3}tr(A)^2 - tr(A^2)\right) + \frac{1}{3}tr(A^3) > 0$ *and* $tr(B)\left(\frac{2}{3}tr(B)^2 - tr(B^2)\right) + \frac{1}{3}tr(B^3) < 0$

then the equilibrium point at the origin is an attractor for X and a repeller for Y.

Proof. Using the Routh-Hurwitz criteria [1, 12], there are three conditions for getting three eigenvalues with negative real part for the exterior vector field and positive for the interior vector field. □

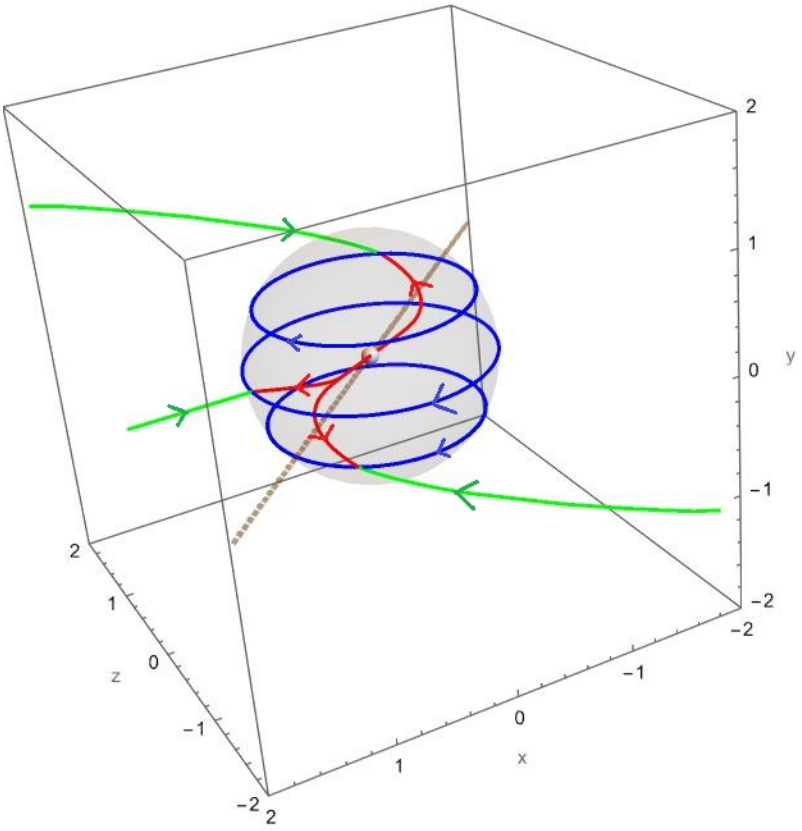

Figure 5.6: *Two improper nodes with two points as tangency in the sphere.*

The following examples come from the classification theorems in Appendix **??**.

Example 5.3.1 *The case $\mathbb{S}^2 \cap Q = \mathcal{S}_2$ (two points as tangency points).*

Consider the following systems with two tangency points:

$$A = \begin{pmatrix} -1 & 0 & -2 \\ 0 & -1 & 0 \\ 0 & 0 & -1 \end{pmatrix} \quad B = \begin{pmatrix} 1 & 0 & 1.5 \\ 0 & 1 & 0 \\ 0.5 & 0 & 1 \end{pmatrix},$$

A describes a hyperbolic attracting node with $\lambda_i = -1$ (with negative real part), and B is a repelling one with eigenvalues $\lambda_1 = 1$, $\lambda_2 = 1 + \frac{\sqrt{3}}{2}$ and $\lambda_3 = 1 - \frac{\sqrt{3}}{2}$. For this case there exists a sliding region over almost the whole sphere.

We can see the effectiveness of Routh-Hurwitz criteria in A for its characteristic polynomial $a_3\lambda^3 + a_2\lambda^2 + a_1\lambda + a_0 = \lambda^3 + 3\lambda^2 + 3\lambda + 1 = 0$, consider the following matrix:

$$M = \begin{pmatrix} 3 & 1 & 0 \\ 1 & 3 & 3 \\ 0 & 0 & 1 \end{pmatrix},$$

with $a_3 = 1 > 0$, $\Delta_1 = 3 > 0$, $\Delta_2 = 8 > 0$ and $\Delta_3 = |M| = 8 > 0$. Then the eigenvalues of A have negative real part.

For $-B$ the characteristic polynomial is $a_3\lambda^3 + a_2\lambda^2 + a_1\lambda + a_0 = \lambda^3 + 3\lambda^2 + 2\lambda + \frac{1}{4} = 0$ and then:

$$M = \begin{pmatrix} 2 & 1/4 & 0 \\ 1 & 3 & 2 \\ 0 & 0 & 1 \end{pmatrix},$$

with $a_3 = 1 > 0$, $\Delta_1 = 2 > 0$, $\Delta_2 = 23/4 > 0$ and $\Delta_3 = |M| = 23/4 > 0$. Then the eigenvalues of $-B$ have negative real part and the ones of B have positive real part.

Example 5.3.2 *The case $\mathbb{S}^2 \cap Q = \mathcal{S}_3$ (one circle as tangency points).*

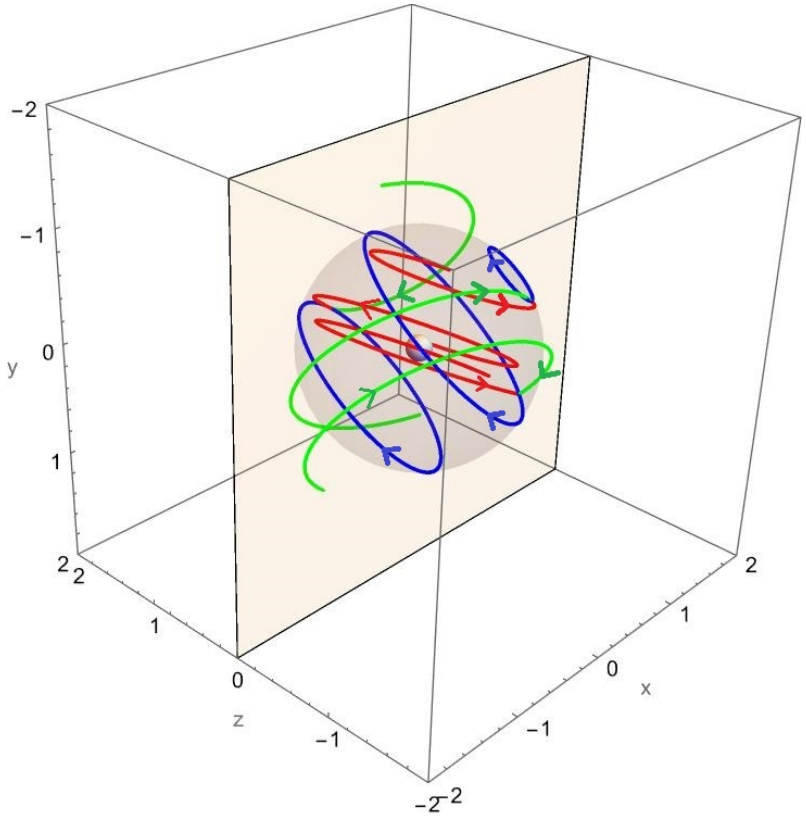

Figure 5.7: *Two nodes with maximum circle as tangency in the sphere.*

In the cases where there are diagonal matrices, Filippov vector field is equal to zero. In addition, taking the following system with two tangency points:

$$A = \begin{pmatrix} 0 & -4 & -3 \\ 4 & 0 & -2 \\ 3 & 2 & -1 \end{pmatrix}, \; B = \begin{pmatrix} 0 & 1 & 7 \\ -1 & 0 & 5 \\ -7 & -5 & 1 \end{pmatrix},$$

Using the Routh-Hurwitz criteria in A for its characteristic polynomial $\lambda^3 + \lambda^2 + 29\lambda + 16 = 0$, consider the following matrix:

$$M = \begin{pmatrix} 29 & 16 & 0 \\ 1 & 1 & 29 \\ 0 & 0 & 1 \end{pmatrix},$$

with $a_3 = 1 > 0$, $\Delta_1 = 29 > 0$, $\Delta_2 = 13 > 0$ and $\Delta_3 = |M| = 13 > 0$. Then the eigenvalues of A have negative real part.

For $-B$, its characteristic polynomial is $\lambda^3+\lambda^2+75\lambda+1=0$ we have the following matrix:

$$M=\begin{pmatrix} 75 & 1 & 0 \\ 1 & 1 & 75 \\ 0 & 0 & 1 \end{pmatrix},$$

with $a_3=1>0$, $\Delta_1=75>0$, $\Delta_2=74>0$ and $\Delta_3=|M|=74>0$. Then the eigenvalues of B have positive real part.

A describes a hyperbolic attracting focus-node with $\lambda_1=-0.556$, $\lambda_2=-0.222+5.36i$ and $\lambda_3=-0.222-5.36i$. For B the eigenvalues are $\lambda_1=0.013$, $\lambda_2=0.493+8.65i$ and $\lambda_3=0.493-8.65i$ and we get a repelling focus-node. For this case there exists a sliding region over almost the whole sphere.

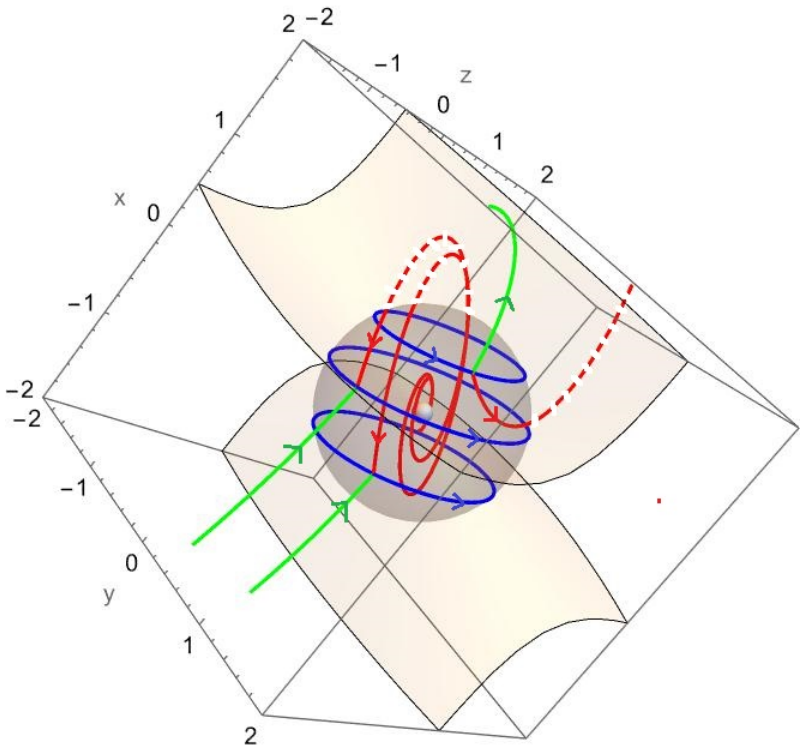

Figure 5.8: *Two focus-nodes with two parallel circles as tangency in the sphere.*

Example 5.3.3 *The case $\mathbb{R}\cap Q=\mathcal{S}_4$ (two disjoint circles as tangency points).*

Consider the following inelastic system:

$$A = \begin{pmatrix} -1 & 1 & -9 \\ -1 & -1 & 0 \\ 0 & 0 & -1 \end{pmatrix}, \; B = \begin{pmatrix} 1 & 0 & 8 \\ 0 & 1 & -5 \\ 1 & 5 & 1 \end{pmatrix}.$$

For A we get $\lambda^3 + 3\lambda^2 + 4\lambda + 2 = 0$, consider the following matrix:

$$M = \begin{pmatrix} 4 & 2 & 0 \\ 1 & 3 & 4 \\ 0 & 0 & 1 \end{pmatrix},$$

with $a_3 = 1 > 0$, $\Delta_1 = 4 > 0$, $\Delta_2 = 10 > 0$ and $\Delta_3 = |M| = 10 > 0$. Then the eigenvalues of A have negative real part.

The characteristic polynomial for $-B$ is $\lambda^3 + 3\lambda^2 + 20\lambda + 18 = 0$ and we have the following matrix:

$$M = \begin{pmatrix} 20 & 18 & 0 \\ 1 & 3 & 20 \\ 0 & 0 & 1 \end{pmatrix},$$

with $a_3 = 1 > 0$, $\Delta_1 = 20 > 0$, $\Delta_2 = 42 > 0$ and $\Delta_3 = |M| = 42 > 0$. Then the eigenvalues of B have positive real part.

For A the eigenvalues are $\lambda_1 = -1$, $\lambda_2 = -1 + i$ and $\lambda_3 = -1 - i$ forming an attracting focus-node, and for B $\lambda_1 = 1$, $\lambda_2 = 1 + \sqrt{17}i$ and $\lambda_3 = 1 - \sqrt{17}i$, which describe a repelling focus-node. For this case there is an escape region between two sliding ones.

Example 5.3.4 *The case $\mathbb{R} \cap Q = S_5$ (two maximum circles as tangency points).*

Consider the following inelastic system:

$$A = \begin{pmatrix} 0 & -4 & -3 \\ 4 & -2 & -2 \\ 3 & 2 & 1 \end{pmatrix}, \; B = \begin{pmatrix} 0 & 1 & 2 \\ -1 & 2 & 5 \\ -2 & -5 & -1 \end{pmatrix}.$$

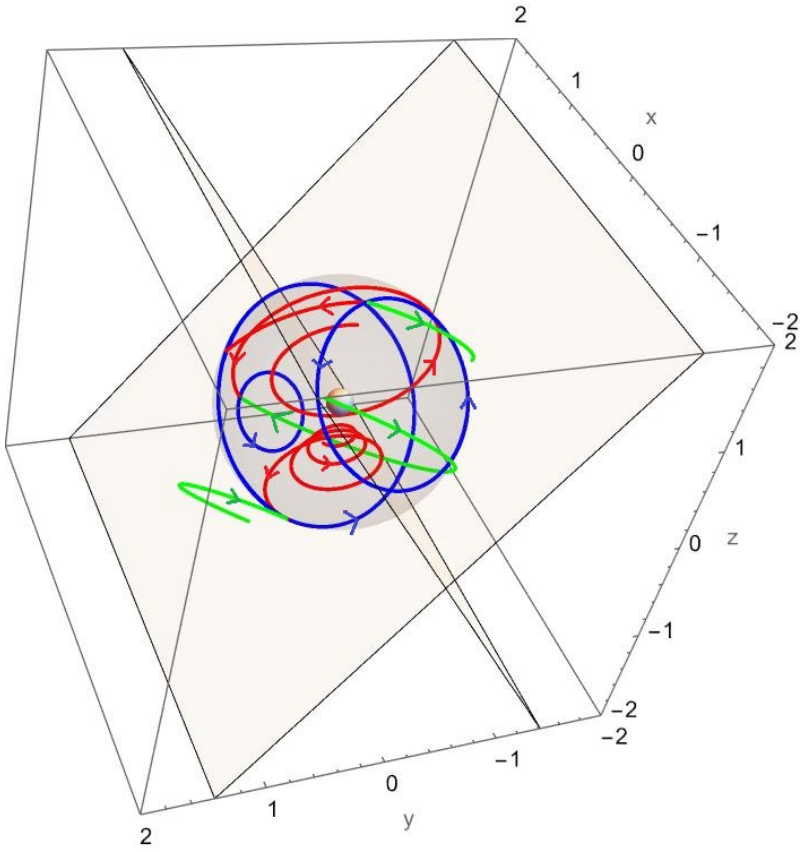

Figure 5.9: *Two focus-nodes with two points as tangency points in the sphere.*

Using the Routh-Hurwitz criteria in A for its characteristic polynomial $\lambda^3+\lambda^2+27\lambda+2=0$, consider the following matrix:

$$M=\begin{pmatrix} 27 & 2 & 0 \\ 1 & 1 & 27 \\ 0 & 0 & 1 \end{pmatrix},$$

with $a_3=1>0$, $\Delta_1=27>0$, $\Delta_2=25>0$ and $\Delta_3=|M|=25>0$. Then the eigenvalues of A have negative real part.

For $-B$ we have $\lambda^3+\lambda^2+28\lambda+7=0$ we have the following matrix:

$$M=\begin{pmatrix} 28 & 7 & 0 \\ 1 & 1 & 28 \\ 0 & 0 & 1 \end{pmatrix},$$

with $a_3 = 1 > 0$, $\Delta_1 = 28 > 0$, $\Delta_2 = 21 > 0$ and $\Delta_3 = |M| = 21 > 0$. Then the eigenvalues of B have positive real part.

Exterior vector field has an isolated hyperbolic point but the opposite case occurs for the other one. For A, the eigenvalues are $\lambda_1 = -0.0743$, $\lambda_2 = -0.463 + 5.17i$ and $\lambda_3 = -0.463 - 5.17i$ forming an attracting focus-node, and for B $\lambda_1 = 0.252$, $\lambda_2 = 0.37 + 5.26i$ and $\lambda_3 = 0.37 - 5.26i$ which define a repelling focus-node. For this case there are two escape regions between two sliding ones.

5.4 Closing remarks

5.4.1 Linear Non-Homogeneous Systems

If $X(\mathbf{x}) = A\mathbf{x} + \mathbf{c}$ and $Y(\mathbf{x}) = B\mathbf{x} + \mathbf{d}$ as an inelastic non-smooth system, where $\mathbf{c}, \mathbf{d} \in \mathbb{R}^3$, then we keep the conditions $a_{ii} = -b_{ii}$, $(a_{ij} + a_{ji}) = -(b_{ij} + b_{ji})$ and now $c_i = -d_i$, for $i \neq j \in \{1,2,3\}$. Therefore, the quadratic surface for the tangencies is:

$$\begin{aligned} Xf(x_1,x_2,x_3) = \; & 2[a_{11}x_1^2 + a_{22}x_2^2 + a_{33}x_3^2 + (a_{12}+a_{21})x_1x_2 \\ & +(a_{13}+a_{31})x_1x_3 + (a_{32}+a_{23})x_2x_3 + c_1x + c_2y + c_3z] \\ = \; & 0. \end{aligned} \tag{5-4}$$

The Filippov vector field continues in the same way as in theorem 5.1.1 with the same two center equilibrium points of the homogeneous case. Although we lost the other results in the way that we showed, now we present a description of the tangencies for this non-homogeneous inelastic PSVF.

Proposition 5.4.1 *The intersection between the quadric surfaces from equation (5-4), without homeomorphisms, and the sphere are the same of 5.1.2 with the other following options:*

1. *one closed curve homeomorphic to $\mathbb{S}^1$ and one disjoint point.*

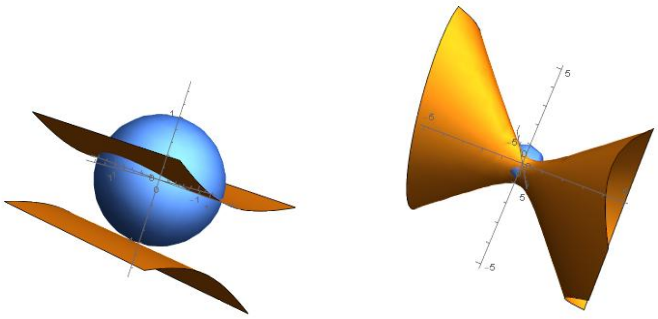

(.1) *Hyperbolic cylinder* **(.2)** *Hyperboloid of one sheet*

Figure 5.10: *Generic quadric surfaces and the sphere.*

2. *two closed curve homeomorphic to* $\mathbb{S}^1$ *connected by one point.*

Proof. The origin $(0,0,0)$ always belongs to the quadric surface, seeing the equation (5-4), which now have linear terms, and by the other normal forms of these quadrics in [6], there are also elliptic, parabolic and hyperbolic cylinders, elliptic and hyperbolic paraboloids, hyperboloids of one and two sheets, ellipsoids and parallel planes. □

5.4.2 The refractive case

In this chapter we assume an inelastic PSVF $Z = (X,Y)$ and we obtain that tangency points coincide. Conversely, if the tangency points coincide for both vector fields, the equations of the quadrics must have the same terms unless constants. Thus there exists only two cases, the inelastic and the so-called *refractive*. The refractive case corresponds to those vector fields satisfying $\lambda X f(\mathbf{x}) = Y f(\mathbf{x})$ for $\lambda \in \mathbb{R}^+$.

If $X(\mathbf{x}) = A\mathbf{x}$ and $Y(\mathbf{x}) = B\mathbf{x}$, then we get that $B = \lambda A + (M_2 - M_2^T)$ where M_2 is a lower matrix with diagonal entries equal to zero

$$M_2 = \begin{pmatrix} 0 & 0 & 0 \\ \lambda a_{12} - b_{12} & 0 & 0 \\ \lambda a_{13} - b_{13} & \lambda a_{23} - b_{23} & 0 \end{pmatrix}.$$

In this case we do not obtain a Filippov vector field on the sphere but only crossing and tangency points, being the tangency lines as the inelastic case. Indeed, we get the same quadric of equation (5-3) but now $\lambda a_{ii} = b_{ii}$ and $\lambda(a_{1j} + a_{ji}) = (b_{1j} + b_{ji})$.

5.4.3 Conclusions

We have shown a global analysis on the dynamics of inelastic non-smooth differential equations with the sphere as discontinuity region. As future work we will study the global dynamics using compactification in $\mathbb{S}^3$ and classify the canonical regions.

CHAPTER 6

Limit cycles of generic piecewise center-type vector fields in $\mathbb{R}^3$ separated by either one plane or by two parallel planes

In this chapter we will not consider inelastic vector fields, the main topic will be center-type piecewise vector fields. While the limit cycles of the piecewise differential systems in the plane $\mathbb{R}^2$ have been studied intensively during these last twenty years, this is not the case for the limit cycles of the piecewise differential systems in the space $\mathbb{R}^3$.

The goal of this chapter is to study the continuous and discontinuous piecewise differential systems in $\mathbb{R}^3$, formed by linear vector fields similar to planar centers separated by one or two parallel planes. We call those "center-type" differential systems, which have two pure imaginary numbers and zero as eigenvalues. When these kinds of piecewise differential systems are continuous or discontinuous separated by one plane, then there are no limit cycles, see section 6.1. Also, if they are continuous separated by two planes, then generically there are no limit cycles. But when the piecewise differential systems are discontinuous separated two parallel planes, we show that generically there are at most four limit cycles, and that there exist such systems with four limit cycles. The genericity here means that the statements hold in a residual set of the space of parameters associated to the differential system.

We recall that the same problem but for discontinuous piecewise differential systems in

$\mathbb{R}^2$ formed by linear differential centers separated by two parallel straight lines have at most one limit cycle [54].

6.1 Introduction and statement of the main results

We shall work with piecewise vector fields in $\mathbb{R}^2$ and $\mathbb{R}^3$, and the definition of these vector fields on the separation line of their pieces in $\mathbb{R}^2$, or on the discontinuity region of their pieces in $\mathbb{R}^3$ follow the rules of Filippov [26].

These last two decades the limit cycles of the piecewise differential systems in the plane $\mathbb{R}^2$ have been studied intensively, see for instance [4, 5, 13, 8, 11, 21, 23, 28, 29, 30, 31, 33, 35, 36, 37, 42, 48, 49, 50, 51, 52, 53, 54, 47, 55]. This is not the case for the limit cycles of the piecewise differential systems in the space $\mathbb{R}^3$.

A *center* of a differential system in the plane $\mathbb{R}^2$ is an equilibrium point $\mathbf{x}$ having a neighbourhood U such that $U \setminus \{\mathbf{x}\}$ is filled of periodic orbits. A *global* center is a center $\mathbf{x}$ such that $\mathbb{R}^2 \setminus \{\mathbf{x}\}$ is filled of periodic orbits. The notion of a center appeared already in the works of Poincaré [63] in 1881 and Dulac [18] in 1908.

One of the main objects in the study of the vector fields is the limit cycles. A *limit cycle* of a vector field is a periodic orbit isolated in the set of all periodic orbits of the vector field.

In the paper [54] it is proved that continuous and discontinuous piecewise vector fields in $\mathbb{R}^2$ formed by two pieces separated by one straight line and formed by two arbitrary linear centers cannot have limit cycles, and that also the continuous piecewise vector fields in $\mathbb{R}^2$ formed by three pieces separated by two parallel straight lines and formed by three arbitrary linear centers have no limit cycles. But the discontinuous piecewise differential systems separated by two parallel straight lines and formed by three arbitrary linear centers can have at most one limit cycle, and there are such systems which one limit cycle. The aim of this chapter is to study a similar problem for continuous and discontinuous piecewise vector fields in $\mathbb{R}^3$.

In $\mathbb{R}^3$ there are no centers in the sense that there are no equilibrium points $\mathbf{x}$ having a neighborhood U such that $U \setminus \{\mathbf{x}\}$ is filled with periodic orbits, see for instance [7].

Now we are going to study the limit cycles of the continuous and discontinuous piecewise vector fields in $\mathbb{R}^3$ separated by one plane or by two parallel planes and formed by linear "center-type" vector fields of $\mathbb{R}^3$.

More precisely, we consider the linear vector field

$$X(\mathbf{x}) = \begin{pmatrix} A_{11} & A_{12} & A_{13} \\ A_{21} & A_{22} & A_{23} \\ A_{31} & A_{32} & A_{33} \end{pmatrix} \begin{pmatrix} x \\ y \\ z \end{pmatrix} + \begin{pmatrix} B_1 \\ B_2 \\ B_3 \end{pmatrix} = A\mathbf{x} + B, \tag{6-1}$$

where

$$\begin{aligned}
A_{11} &= a_1a_3c_2 + b_1b_3c_2 - a_1a_2c_3 - b_1b_2c_3,\\
A_{12} &= a_2a_3c_2 + b_2b_3c_2 - a_2^2c_3 - b_2^2c_3,\\
A_{13} &= a_3^2c_2 + b_3^2c_2 - a_2a_3c_3 - b_2b_3c_3,\\
A_{21} &= -a_1a_3c_1 - b_1b_3c_1 + a_1^2c_3 + b_1^2c_3,\\
A_{22} &= -a_2a_3c_1 - b_2b_3c_1 + a_1a_2c_3 + b_1b_2c_3,\\
A_{23} &= -a_3^2c_1 - b_3^2c_1 + a_1a_3c_3 + b_1b_3c_3,\\
A_{31} &= a_1a_2c_1 + b_1b_2c_1 - a_1^2c_2 - b_1^2c_2,\\
A_{32} &= a_2^2c_1 + b_2^2c_1 - a_1a_2c_2 - b_1b_2c_2,\\
A_{33} &= a_2a_3c_1 + b_2b_3c_1 - a_1a_3c_2 - b_1b_3c_2,
\end{aligned}$$

$$\begin{aligned}
B_1 &= a_3a_4c_2 + b_3b_4c_2 - a_2a_4c_3 - b_2b_4c_3,\\
B_2 &= -a_3a_4c_1 - b_3b_4c_1 + a_1a_4c_3 + b_1b_4c_3,\\
B_3 &= a_2a_4c_1 + b_2b_4c_1 - a_1a_4c_2 - b_1b_4c_2.
\end{aligned}$$

The vector field (6-1) is obtained after applying the affine transformation

$$(x,y,z) \mapsto (a_1x + a_2y + a_3z + a_4, b_1x + b_2y + b_3z + b_4, c_1x + c_2y + c_3z + c_4)$$

with inverse

$$\begin{aligned}(x,y,z) \mapsto & \tfrac{-1}{\det(A)}(a_4b_3c_2-a_3b_4c_2-a_4b_2c_3+a_2b_4c_3+a_3b_2c_4-a_2b_3c_4\\ & -b_3c_2x+b_2c_3x+a_3c_2y-a_2c_3y-a_3b_2z+a_2b_3z,-a_4b_3c_1\\ & +a_3b_4c_1+a_4b_1c_3-a_1b_4c_3-a_3b_1c_4+a_1b_3c_4+b_3c_1x-b_1c_3x\\ & -a_3c_1y+a_1c_3y+a_3b_1z-a_1b_3z,a_4b_2c_1-a_2b_4c_1-a_4b_1c_2\\ & +a_1b_4c_2+a_2b_1c_4-a_1b_2c_4-b_2c_1x+b_1c_2x+a_2c_1y-a_1c_2y\\ & -a_2b_1z+a_1b_2z).\end{aligned}$$

to the linear differential system

$$\dot{x}=-y,\quad \dot{y}=x,\quad \dot{z}=0, \tag{6-2}$$

which has the two independent first integrals $f_1(\mathbf{x})=x^2+y^2$ and $f_2(\mathbf{x})=z$. Here we assume that $\det(A)=-a_3b_2c_1+a_2b_3c_1+a_3b_1c_2-a_1b_3c_2-a_2b_1c_3+a_1b_2c_3\neq 0$. We emphasize the genericity in this chapter means that some result holds in a residual set.

Note that the linear differential system (6-2) in $\mathbb{R}^3$ has the full z-axis filled with singular points, and on the invariant planes $z=z_0$ =constant there exists a global center at $(0,0,z_0)$, i.e. all the periodic orbits surrounding the center $(0,0,z_0)$ in the plane $z=z_0$ fill this plane with the exception of the singular point $(0,0,z_0)$.

In this chapter the linear differential system in $\mathbb{R}^3$ defined by a vector fields X will be called a *linear center* or simply a *center* in $\mathbb{R}^3$.

Changing the parameters (a_i,b_i,c_i) of the vector field $X(\mathbf{x})$ to $(\alpha_i,\beta_i,\gamma_i)$ for $i=1,2,3$ we get another linear vector field $Y(\mathbf{x})=C\mathbf{x}+D$.

For any piecewise vector field in $\mathbb{R}^3$ formed by two pieces and separated by one plane we can assume without loss of generality, after an affine change in $\mathbb{R}^2$ if necessary, that such a plane is $x=0$.

We define the *piecewise vector field* $N=(X,Y)$ *in* $\mathbb{R}^3$ *of two pieces separated by the plane*

$x = 0$ *and formed by the two centers* X *and* Y *of* $\mathbb{R}^3$ as

$$N(\mathbf{x}) = \begin{cases} X(\mathbf{x}) = A\mathbf{x} + B, \text{ if } x \geq 0, \\ Y(\mathbf{x}) = C\mathbf{x} + D, \text{ if } x \leq 0. \end{cases} \tag{6-3}$$

If $X = Y$ on the plane $x = 0$ we say that the piecewise vector field N is *continuous*, and if $X \neq Y$ on the plane $x = 0$ we say that the piecewise vector field N is *discontinuous*. For these two kinds of piecewise vector fields N consider the following two results.

Theorem 6.1.1 *A piecewise vector field in* $\mathbb{R}^3$ *separated by one plane and formed by two linear centers* X *and* Y *has no limit cycles.*

The limit cycles of Theorem 6.1.1 are crossing limit cycles, see for details the last part of Section 2.2.

If we assume that the discontinuity region of a piecewise vector field in $\mathbb{R}^3$ is formed by two parallel planes, then without loss of generality we can assume, after an affine change in $\mathbb{R}^3$ if necessary, that these parallel planes are $x = 1$ and $x = -1$.

We consider piecewise vector fields separated by the planes $x = \pm 1$ and formed by three centers X, Y and Z, where $Z(\mathbf{x}) = E\mathbf{x} + F$ is obtained from X changing the coefficients (a_i, b_i, c_i) by (A_i, B_i, C_i) for $i = 1, 2, 3$.

More precisely, we define the *piecewise vector field* $M = (X, Y, Z)$ *in* $\mathbb{R}^3$ *of three pieces separated by the two planes* $x = \pm 1$ *and formed by the three centers* X, Y *and* Z *of* $\mathbb{R}^3$ as

$$M(\mathbf{x}) = \begin{cases} X(\mathbf{x}) = A\mathbf{x} + B, \text{ if } x \geq 1, \\ Y(\mathbf{x}) = C\mathbf{x} + D, \text{ if } -1 \leq x \leq 1, \\ Z(\mathbf{x}) = E\mathbf{x} + F, \text{ if } x \leq -1. \end{cases}$$

As in the case when the discontinuity set was formed by a unique plane, now we can consider continuous and discontinuous piecewise vector fields. Our main results for the piecewise vector fields M are the following two theorems.

Theorem 6.1.2 *A continuous piecewise vector field separated by two parallel planes and formed by three linear centers X, Y and Z generically has no limit cycles.*

We notice that our parameter space is $\mathbb{R}^{36}$. Thus, when we claim that the continuous piecewise vector field has generically no limit cycle we mean that it has no limit cycles in a residual set of $\mathbb{R}^{36}$. It other others, the possible scenario where the result could not be verified has measure zero (here we can assume Lebesgue measure).

Theorem 6.1.3 *A discontinuous piecewise vector field separated by two parallel planes and formed by three linear centers X, Y and Z generically has at most four limit cycles, and we provide one of these piecewise vector fields with exactly four limit cycles.*

The meaning of genericity in the statement of Theorem 6.1.3 is the same as in Theorem 6.1.2. Again the limit cycles of Theorems 6.1.2 and 6.1.3 are crossing limit cycles, see for details the last part of Chapter 2. The proofs of Theorems 6.1.1, 6.1.2 and 6.1.3 are given in the Section 6.2.

6.2 Proofs of the results

Proof. [Proof of Theorem 6.1.1] **The continuous case.** Consider a continuous piecewise linear differential system in $\mathbb{R}^3$ separated by one plane and formed by two centers X and Y. Without loss of generality, we can suppose that the plane is $x = 0$.

The continuous hypothesis, $X(\mathbf{x}) = Y(\mathbf{x})$ at $(x,y,z) = (0,y_0,z_0)$, provides 3 polynomial equations of degree 1 in the variables y_0 and z_0, each equation corresponding to the coordinates of the involved vector fields. They write

$$(B_1 - D_1) + (A_{12} - C_{12})y_0 + (A_{13} - C_{13})z_0 = 0,$$

$$(B_2 - D_2) + (A_{22} - C_{22})y_0 + (A_{23} - C_{23})z_0 = 0,$$

$$(B_3 - D_3) + (A_{32} - C_{32})y_0 + (A_{33} - C_{33})z_0 = 0.$$

Thus we get 9 cubic equations for the parameters, looking at each coefficient, $B_i - D_i = 0$, $A_{i2} - C_{i2} = 0$ and $A_{i3} - C_{i3} = 0$ for $i = 1,2,3$. From those equations we get 7 parameters b_4, b_1, a_1, b_2, a_2, α_1, β_1 in terms of the other ones, as solution of the system.

If the continuous piecewise differential system has a limit cycle, this must intersect the plane $x = 0$ in two points $(0, y_0, z_0)$ and $(0, y_1, z_1)$ with $(y_0, z_0) \neq (y_1, z_1)$. The vector field X has the first integrals

$$F_1(\mathbf{x}) = (a_4 + a_1 x + a_2 y + a_3 z)^2 + (b_4 + b_1 x + b_2 y + b_3 z)^2,$$
$$F_2(\mathbf{x}) = c_4 + c_1 x + c_2 y + c_3 z,$$

and for the vector field Y the first integrals

$$G_1(\mathbf{x}) = (\alpha_1 x + \alpha_2 y + \alpha_3 z + \alpha_4)^2 + (\beta_1 x + \beta_2 y + \beta_3 z + \beta_4)^2,$$
$$G_2(\mathbf{x}) = \gamma_1 x + \gamma_2 y + \gamma_3 z + \gamma_4.$$

Clearly that the two points $(0, y_0, z_0)$ and $(0, y_1, z_1)$ with $(y_0, z_0) \neq (y_1, z_1)$ where the limit cycles intersects the plane $x = 0$ must satisfy the system of four equations

$$e_1 = F_1(0, y_0, z_0) - F_1(0, y_1, z_1) = 0,$$
$$e_2 = F_2(0, y_0, z_0) - F_2(0, y_1, z_1) = 0,$$
$$e_3 = G_1(0, y_0, z_0) - G_1(0, y_1, z_1) = 0,$$
$$e_4 = G_2(0, y_0, z_0) - G_2(0, y_1, z_1) = 0.$$

Since the unique solution of this system is $y_0 = y_1$ and $z_0 = z_1$, it follows that the continuous piecewise differential system formed by the centers X and Y has no limit cycles. See the Appendix B.

The discontinuous case. Assume that there is a discontinuous piecewise linear differential system in $\mathbb{R}^3$ separated by one plane and formed by two centers X and Y. Without loss of generality we can suppose that the plane is $x = 0$.

Then a limit cycle intersects the plane $x = 0$ in the two points $(0, y_0, z_0)$ and $(0, y_1, z_1)$ with $(y_0, z_0) \neq (y_1, z_1)$. The vector fields X and Y have the first integrals $F_1(\mathbf{x}), F_2(\mathbf{x})$ and $G_1(\mathbf{x}), G_2(\mathbf{x})$ respectively, given in the proof of Theorem 6.1.1. As in that proof the two points $(0, y_0, z_0)$ and $(0, y_1, z_1)$ must satisfy

$$e_1 = F_1(0,y_0,z_0) - F_1(0,y_1,z_1) = 0,$$
$$e_2 = F_2(0,y_0,z_0) - F_2(0,y_1,z_1) = 0,$$
$$e_3 = G_1(0,y_0,z_0) - G_1(0,y_1,z_1) = 0,$$
$$e_4 = G_2(0,y_0,z_0) - G_2(0,y_1,z_1) = 0.$$

Computing the Gröebner basis of the polynomials e_1, e_2, e_3 and e_4 respect to the variables y_0, z_0, y_1 and z_1, we obtain an equivalent polynomial system to $e_1 = e_2 = e_3 = e_4 = 0$ formed by 59 equations. One of those ones is $(z_1 - z_0)(c_3\gamma_2 - c_2\gamma_3) = 0$.

Assume that $c_3\gamma_2 - c_2\gamma_3$ is not zero. Then $z_1 = z_0$. Therefore $e_4 = (y_0 - y_1)\gamma_2$. Since y_1 cannot be equal to y_0, otherwise the point $(0,y_0,z_0)$ would be equal to $(0,y_1,z_1)$, then $\gamma_2 = 0$. Then $e_2 = (y_0 - y_1)c_2 = 0$, so $c_2 = 0$, in contradiction with the assumption that $c_3\gamma_2 - c_2\gamma_3$ is not zero. Therefore in what follows we can assume that $c_3\gamma_2 - c_2\gamma_3 = 0$ and that $z_0 \neq z_1$. Now we consider two cases.

Case 1: c_2 is not zero. Then $\gamma_3 = c_3\gamma_2/c_2$. Doing again the Gröebner basis of the polynomials e_1, e_2, e_3 and e_4 respect to the variables y_0, z_0, y_1 and z_1, we obtain an equivalent polynomial system with eight equations. After removing the non-zero factor $z_0 - z_1$ from the equations having such a factor, all these are linear in the variables y_0, z_0, y_1 and z_1 except one equation. These equations can be solved and we obtain a continuum of solutions. Consequently, again there are no limit cycles in this case.

Case 2: $c_2 = 0$. Then $e_2 = c_3(z_0 - z_1) = 0$. Hence $c_3 = 0$. It remains three equations $e_1 = e_3 = e_4 = 0$ and four unknowns. We obtain a continuum of solutions. Consequently again there are no limit cycles in this case. □

Proof. [Proof of Theorem 6.1.2] The continuous hypotheses that $X(\mathbf{x}) = Y(\mathbf{x})$ at $(x,y,z) = (1,y_0,z_0)$ and $Y(\mathbf{x}) = Z(\mathbf{x})$ at $(x,y,z) = (-1,y_1,z_1)$, provide 6 polynomial equations of degree 1 in the variables y_0, z_0, y_1 and z_1, each equation corresponding to the coordinates of the involved vector fields. Thus, similarly to the proof of Theorem 6.1.1, we get 18 equations for the parameters, looking at each coefficient. From that system we get 13

parameters, which satisfy the whole equations, b_4, b_1, a_1, b_2, a_2, α_1, β_1, B_4, B_1, A_1, B_2, A_2 and γ_1 in terms of the other ones.

The vector fields X and Y have the first integrals $F_1(\mathbf{x})$, $F_2(\mathbf{x})$ and $G_1(\mathbf{x})$, $G_2(\mathbf{x})$, respectively. The vector field Z has the firsts integrals

$$H_1(\mathbf{x}) = (A_1x+A_2y+A_3z+A_4)^2+(B_1x+B_2y+B_3z+B_4)^2,$$
$$H_2(\mathbf{x}) = C_1x+C_2y+C_3z+C_4.$$

A possible limit cycle intersects at the points $(1,y_0,z_0)$ and $(1,y_3,z_3)$ the plane $x=1$, and at the points $(-1,y_1,z_1)$ and $(-1,y_2,z_2)$ in the plane $x=-1$, with $(y_0,z_0)\neq(y_3,z_3)$ and $(y_1,z_1)\neq(y_2,z_2)$. These four points have to satisfy the following system of equations for $(y_0, y_1, y_2, y_3, z_0, z_1, z_2, z_3)$:

$$\begin{aligned}
e_1 &= F_1(1,y_3,z_3)-F_1(1,y_0,z_0)=0,\\
e_2 &= F_2(1,y_3,z_3)-F_2(1,y_0,z_0)=0,\\
e_3 &= G_1(1,y_0,z_0)-G_1(-1,y_1,z_1)=0,\\
e_4 &= G_2(1,y_0,z_0)-G_2(-1,y_1,z_1)=0,\\
e_5 &= H_1(-1,y_1,z_1)-H_1(-1,y_2,z_2)=0,\\
e_6 &= H_2(-1,y_1,z_1)-H_2(-1,y_2,z_2)=0,\\
e_7 &= G_1(-1,y_2,z_2)-G_1(1,y_3,z_3)=0,\\
e_8 &= G_2(-1,y_2,z_2)-G_2(1,y_3,z_3)=0.
\end{aligned}$$

Using the even equations we get that

$$\begin{aligned}
z_1 = {} & \frac{2(c_1C_2\gamma_3-c_1\gamma_2C_3-C_1c_2\gamma_3+C_1\gamma_2c_3)}{\gamma_3(C_2c_3-c_2C_3)}+\frac{\gamma_2y_0}{\gamma_3}-\frac{\gamma_2y_1}{\gamma_3}+z_0,\\
z_2 = {} & \frac{2(c_1C_2\gamma_3-c_1\gamma_2C_3-C_1c_2\gamma_3+C_1\gamma_2c_3)}{\gamma_3(C_2c_3-c_2C_3)}-\frac{y_1(\gamma_2C_3-C_2\gamma_3)}{\gamma_3C_3}\\
& -\frac{C_2y_2}{C_3}+\frac{\gamma_2y_0}{\gamma_3}+z_0,
\end{aligned}$$

$$\begin{aligned}
y_3 = {} & -\frac{c_3y_1(\gamma_2C_3-C_2\gamma_3)}{C_3(\gamma_2c_3-c_2\gamma_3)}+\frac{c_3y_2(\gamma_2C_3-C_2\gamma_3)}{C_3(\gamma_2c_3-c_2\gamma_3)}+y_0,\\
z_3 = {} & \frac{c_2y_1(\gamma_2C_3-C_2\gamma_3)}{C_3(\gamma_2c_3-c_2\gamma_3)}-\frac{c_2y_2(\gamma_2C_3-C_2\gamma_3)}{C_3(\gamma_2c_3-c_2\gamma_3)}+z_0.
\end{aligned}$$

Note that we are assuming that all the denominators which appear in the previous expressions of z_1, z_2, y_3 and z_3 are non-zero. That is, we are solving the system $e_1 = 0, \ldots, e_8 = 0$, in the more generic case, i.e. when the mentioned denominators do not vanish, and the denominators which will appear solving the remaining equations $e_1 = e_3 = e_5 = e_7 = 0$ do not vanish.

Then consider $e_1 = e_3 = e_5 = e_7 = 0$ for solving y_0, y_1, y_2, z_0. From $e_1 = 0$ and $e_3 = 0$ we can find y_2 and z_0, respectively. Substituting y_2 and z_0 in e_5 and e_7, we find that $y_1 = y_0 + 2(C_1c_3 - c_1C_3)/(C_2c_3 - c_2C_3)$ vanishes both equations. So there is a continuum of periodic orbits and no limit cycles. □

Proof. [Proof of Theorem 6.1.3] We consider such a possible limit cycle which intersects at the points $(1, y_0, z_0)$ and $(1, y_3, z_3)$ the plane $x = 1$ and at the points $(-1, y_1, z_1)$ and $(-1, y_2, z_2)$ the plane $x = -1$, with $(y_0, z_0) \neq (y_3, z_3)$ and $(y_1, z_1) \neq (y_2, z_2)$. The vector fields X, Y and Z have the first integrals $F_1(\mathbf{x}), F_2(\mathbf{x})$, $G_1(\mathbf{x}), G_2(\mathbf{x})$ and $H_1(\mathbf{x}), H_2(\mathbf{x})$, respectively.

These four points must satisfy the following systems of equations for the variables (y_0, y_1, y_2, y_3, z_0, z_1, z_2, z_3):

$$
\begin{aligned}
e_1 &= F_1(1, y_3, z_3) - F_1(1, y_0, z_0) = 0,\\
e_2 &= F_2(1, y_3, z_3) - F_2(1, y_0, z_0) = 0,\\
e_3 &= G_1(1, y_0, z_0) - G_1(-1, y_1, z_1) = 0,\\
e_4 &= G_2(1, y_0, z_0) - G_2(-1, y_1, z_1) = 0,\\
e_5 &= H_1(-1, y_1, z_1) - H_1(-1, y_2, z_2) = 0,\\
e_6 &= H_2(-1, y_1, z_1) - H_2(-1, y_2, z_2) = 0,\\
e_7 &= G_1(-1, y_2, z_2) - G_1(1, y_3, z_3) = 0,\\
e_8 &= G_2(-1, y_2, z_2) - G_2(1, y_3, z_3) = 0.
\end{aligned}
$$

Using the even equations we get

$$\begin{aligned} z_1 = &\quad z_0 + \frac{2\gamma_1}{\gamma_3} + \frac{y_0\gamma_2}{\gamma_3} - \frac{y_1\gamma_2}{\gamma_3}, \\ z_2 = &\quad -\frac{C_2 y_2}{C_3} + z_0 + \frac{2\gamma_1}{\gamma_3} + \frac{y_0\gamma_2}{\gamma_3} - \frac{y_1(C_3\gamma_2 - C_2\gamma_3)}{C_3\gamma_3}, \end{aligned}$$

$$\begin{aligned} y_3 = &\quad y_0 - \frac{c_3 y_1(C_3\gamma_2 - C_2\gamma_3)}{C_3(c_3\gamma_2 - c_2\gamma_3)} + \frac{c_3 y_2(C_3\gamma_2 - C_2\gamma_3)}{C_3(c_3\gamma_2 - c_2\gamma_3)}, \\ z_3 = &\quad z_0 + \frac{c2 y_1(C_3\gamma_2 - C_2\gamma_3)}{C_3(c_3\gamma_2 - c_2\gamma_3)} - \frac{c_2 y_2(C_3\gamma_2 - C_2\gamma_3)}{C_3(c_3\gamma_2 - c_2\gamma_3)}. \end{aligned}$$

Again note that we are assuming that all the denominators which appear in the previous expressions of z_1, z_2, y_3 and z_3, are non-zero. That is, we are solving the system $e_1 = 0, \ldots, e_8 = 0$, in the more generic case, i.e. when the mentioned denominators do not vanish, and the denominators which will appear solving the remaining equations $e_1 = e_3 = e_5 = e_7 = 0$ do not vanish.

We substitute the obtained values of y_3, z_1, z_2 and z_3 in the equations $e_k = 0$ for $k = 1,3,5,7$.

EqVar	y_0	y_1	y_2	z_0
e_1	1	1	1	1
e_3	2	2	0	1
e_5	1	1	1	1
e_7	2	2	2	1

Table 6.1: *Maximum exponent for each variable in the polynomials e_k for $k = 1,3,5,7$.*

It remains to solve the equations $e_1 = e_3 = e_5 = e_7 = 0$ with respect to the unknowns y_0, y_1, y_2 and z_0. We do not provide the big explicit expressions of the equations $e_1 = e_3 = e_5 = e_7 = 0$, which are easy to obtain with some algebraic manipulator as Mathematica or Mapple.

The equations $e_1 = 0$ and $e_5 = 0$ are both of degree one, see Table 1. Thus we can find the variables y_0 and y_1 as linear functions of the variables y_2 and of z_0.

Substituting the expressions of y_0 and y_1 into the remaining equations $e_3 = 0$ and $e_7 = 0$ we obtain two polynomial equations of degree two in the variables z_0 and y_2. Again we do not provide the huge explicit expressions of the equations $e_3 = 0$ and $e_7 = 0$ which will need several pages for writing them.

Applying the Bézout Theorem (see [65]) to this system we know that at most there are four real solutions for (y_2, z_0), which can produce four limit cycles substituting these solutions in the previously obtained expressions of $(y_0, y_1, y_3, z_1, z_2, z_3)$. Hence the first part of Theorem 6.1.3 is proved.

In order to complete the proof of Theorem 6.1.3 we provide a discontinuous piecewise differential system in $\mathbb{R}^3$ formed by three centers and separated by two parallel planes.

When we have computed (z_1, z_2, y_3, z_3) from $e_2 = e_4 = e_6 = e_8 = 0$ in the last proof, it remains the equations $e_1 = e_3 = e_5 = e_7 = 0$ for computing (y_0, y_1, y_2, z_0). From the equation $e_1 = 0$ the variable y_2 appears linearly and we obtain $y_2 = P_{y_2}(y_0, y_1, z_0)$. With the equation $e_3 = 0$ we get $z_0 = P_{z_0}(y_0, y_1)$ of degree 2 and with the third $e_5 = 0$ it is gotten $y_1 = P_{y_1}(y_0, z_0)$ of degree 1 for z_0. Then we made the substitution $y_1 = P_{y_1}(y_0, P_{z_0}(y_0, y_1))$ and we can find two solutions $y_1^+ = P^+(y_0)$ and $y_1^- = P^-(y_0)$. Then we should find the last variable y_0 from the equation $e_7 = 0$. With the discriminant of $P^+(y_0)$ we used a numeric method, following the ideas described in [20] with an absolute tolerance of 10^{-15}, for finding the 36 parameters and y_0 which do a positive discriminant. Using the notation of the first part of the proof of Theorem 6.1.3, the center given by the vector field X is obtained for the values of the parameters

$$
\begin{aligned}
&a_1 = 13.708561862548212.., && b_1 = -2.0668139685572826..,\\
&a_2 = -0.46436203202470083.., && b_2 = -2.1162121013313744..,\\
&a_3 = -1.5737561143110694.., && b_3 = -0.30359559321560803..,\\
&a_4 = -5.2597752179200175.., && b_4 = -3.837509139027315..,\\
&c_1 = 1, \quad c_2 = -0.938643702906351.., && c_3 = 1, \quad c_4 = 1.
\end{aligned}
$$

The vector field Y has the form

$$\begin{aligned}
&\alpha_1 = 2, \quad \alpha_2 = -5, && \alpha_3 = -7, \quad \alpha_4 = -11,\\
&\beta_1 = -3, \quad \beta_2 = 1, && \beta_3 = 3, \quad \beta_4 = 1,\\
&\gamma_1 = 0.454545454545454, \quad \gamma_2 = -0.5454545454545444, \ \gamma_3 = 1, \ \gamma_4 = 6.
\end{aligned}$$

And the vector field Z is given by

$$\begin{aligned}
&A_1 = -3.840000000006582, \quad A_2 = 5, \quad A_3 = 0, \quad A_4 = 14,\\
&B_1 = 1, \quad B_2 = 12, && B_3 = 11, \quad B_4 = 14,\\
&C_1 = 2, \quad C_2 = -4, && C_3 = 5, \quad C_4 = -8.
\end{aligned}$$

When we have computed (y_3, z_1, z_2, z_3) from $e_2 = e_4 = e_6 = e_8 = 0$ in the last proof, it remains the equations $e_1 = e_3 = e_5 = e_7 = 0$ for computing (y_0, y_1, y_2, z_0). From the equation $e_1 = 0$ the variable y_2 appears linearly and we obtain $y_2 = P_{y_2}(y_0, y_1, z_0)$. Now from the equation $e_5 = 0$ the variable y_1 appears linearly and we get $y_1 = P_{y_1}(y_0, z_0)$. From the polynomial equations $e_3 = e_7 = 0$ both of degree two, we can obtain the four solutions for (y_0, z_0), and from these four solutions we obtain the intersection points (y_0, z_0, y_1, z_1, y_2, z_2, y_3, z_3) of our limit cycles with the two planes of discontinuity, see Figure 6.1, which are

$$\begin{gathered}
(0.8978733932366719.., -2.2444618685679187.., -0.8476262083331095..,\\
-2.2874616512423445.., 0.885305277605572.., -0.901116462491399..,\\
2.0197502924959307.., -1.1914191816421125..),
\end{gathered}$$

$$\begin{gathered}
(2.618593513041539.., -2.017041157299665.., 1.6304557768236465..,\\
-1.6469344679639704.., -0.25095559475947454.., -3.152063565230467..,\\
1.4005927017518383.., -3.1603099489515696..),
\end{gathered}$$

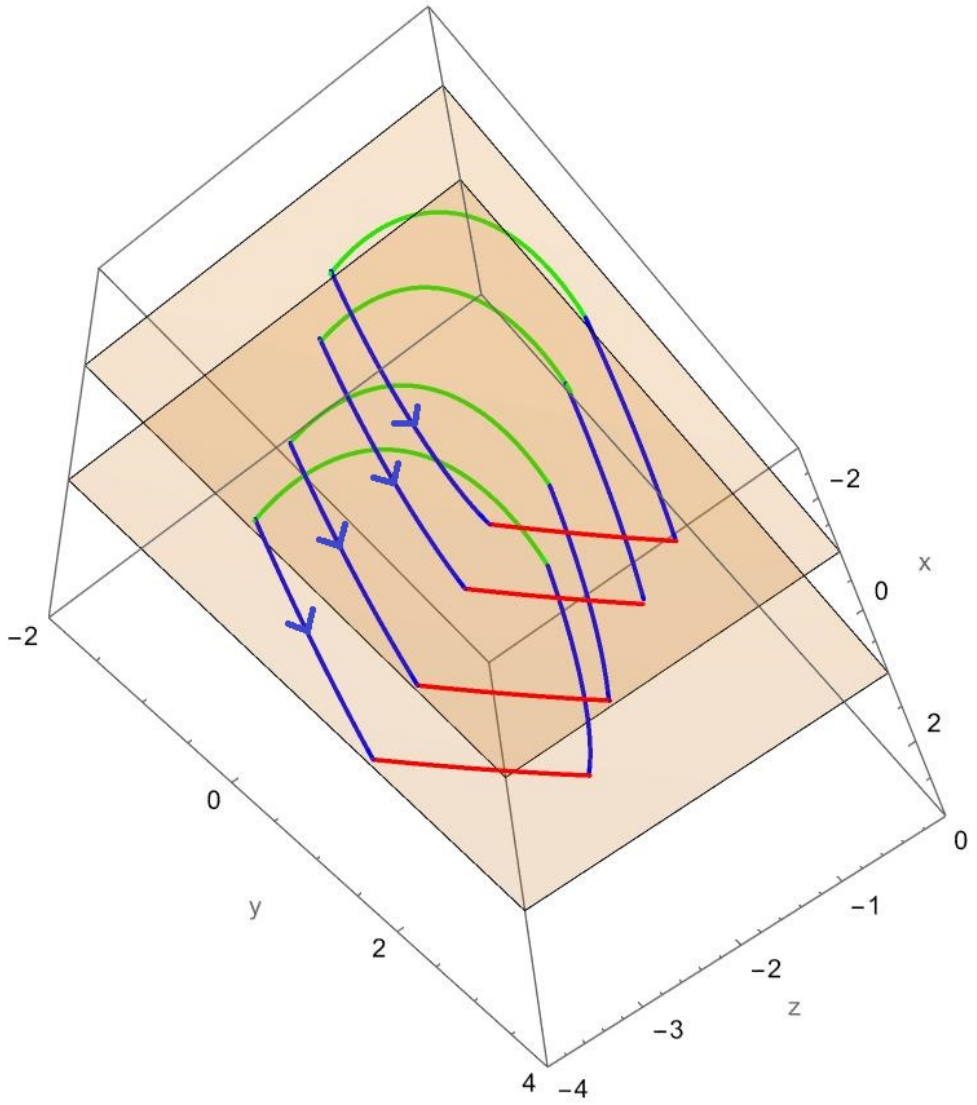

Figure 6.1: *The four limit cycles, vector fields X (red), Y (blue) and Z (green).*

$$(0.5348395678273713..,-1.7034390938102253..,-1.2941046025617466..,$$
$$-1.7919540958406528..,0.47916792990915597..,-0.3733360698639303..,$$
$$1.6828327264792675..,-0.6258825444620513..),$$

$$(1.7558413358089768..,-3.9459570275133773..,0.15273809964405125..,$$
$$-3.911286065421518..,2.3088449504708346..,-2.1864005847600914..,$$
$$3.1516763632780256..,-2.635765268683441..).$$

□

6.3 Conclusions

We have shown that from the four classes of piecewise differential systems in $\mathbb{R}^3$ here studied, generically the only ones having limit cycles are the discontinuous piecewise differential systems in $\mathbb{R}^3$ separated by two parallel planes and formed by three centers having at most four limit cycles, see Theorem 6.1.3.

We remark that the discontinuous piecewise differential systems in $\mathbb{R}^2$ separated by two parallel straight lines and formed by three linear differential centers can have at most one limit cycle, see [54].

Bibliography

[1] ANAGNOST, J. J.; DESOER, C. A. **An elementary proof of the Routh-Hurwitz stability criterion**. *Circuits Systems Signal Process.*, 10(1):101–114, 1991.

[2] ANDRONOV, A. A.; VITT, A. A.; KHAIKIN, S. E. **Theory of oscillators**. Pergamon Press, Oxford-New York-Toronto, Ont., 1966. Translated from the Russian by F. Immirzi; translation edited and abridged by W. Fishwick.

[3] ARNOLD, V. I. **Catastrophe theory**. Springer-Verlag, Berlin, third edition, 1992. Translated from the Russian by G. S. Wassermann, Based on a translation by R. K. Thomas.

[4] ARTÉS, J. C.; LLIBRE, J.; MEDRADO, J. C.; TEIXEIRA, M. A. **Piecewise linear differential systems with two real saddles**. *Math. Comput. Simulation*, 95:13–22, 2014.

[5] BAKHSHALIZADEH, A.; LLIBRE, J. **Limit cycles of piecewise differential equations on the cylinder**. *Bull. Sci. Math.*, 170:Paper No. 103013, 13, 2021.

[6] BEYER, W. **CRC standard mathematical tables**. CRC Press, Boca Ratón, Florida, 28 ed. edition, 1987.

[7] BROGLIATO, B. **Nonsmooth mechanics**. Communications and Control Engineering Series. Springer, [Cham], third edition, 2016. Models, dynamics and control.

[8] BUZZI, C.; PESSOA, C.; TORREGROSA, J. **Piecewise linear perturbations of a linear center**. *Discrete Contin. Dyn. Syst.*, 33(9):3915–3936, 2013.

[9] BUZZI, C. A.; CARVALHO, T.; EUZÉBIO, R. D. **On Poincaré-Bendixson theorem and non-trivial minimal sets in planar nonsmooth vector fields**. *Publ. Mat.*, 62(1):113–131, 2018.

[10] CÂNDIDO, M. R.; LLIBRE, J. **New results on averaging theory and applications**. *Z. Angew. Math. Phys.*, 67(4):Art. 106, 11, 2016.

[11] CASTILLO, J.; LLIBRE, J.; VERDUZCO, F. **The pseudo-Hopf bifurcation for planar discontinuous piecewise linear differential systems**. *Nonlinear Dynam.*, 90(3):1829–1840, 2017.

[12] CRISTIANO, R.; PAGANO, D. J. **Two-parameter boundary equilibrium bifurcations in 3D-Filippov systems**. *J. Nonlinear Sci.*, 29(6):2845–2875, 2019.

[13] DE CARVALHO BRAGA, D.; MELLO, L. F. **Limit cycles in a family of discontinuous piecewise linear differential systems with two zones in the plane**. *Nonlinear Dynam.*, 73(3):1283–1288, 2013.

[14] DI BERNARDO, M.; BUDD, C. J.; CHAMPNEYS, A. R.; KOWALCZYK, P. **Piecewise-smooth dynamical systems**, volume 163 de **Applied Mathematical Sciences**. Springer-Verlag London, Ltd., London, 2008. Theory and applications.

[15] DI BERNARDO, M.; BUDD, C. J.; CHAMPNEYS, A. R.; KOWALCZYK, P. **Piecewise-smooth dynamical systems**, volume 163 de **Applied Mathematical Sciences**. Springer-Verlag London, Ltd., London, 2008. Theory and applications.

[16] DO CARMO, M. P. **Differential geometry of curves & surfaces**. Dover Publications, Inc., Mineola, NY, 2016. Revised & updated second edition of [MR0394451].

[17] DO CARMO, M. P. A. **Geometria Riemanniana**, volume 10 de **Projeto Euclides [Euclid Project]**. Instituto de Matemática Pura e Aplicada, Rio de Janeiro, 1979.

[18] DULAC, H. **Détermination et intégration d'une certaine classe d'équations différentielles ayant pour point singulier un centre**. Gauthier-Villars, 1908.

[19] DUMORTIER, F.; LLIBRE, J.; ARTÉS, J. C. **Qualitative theory of planar differential systems**. Universitext. Springer-Verlag, Berlin, 2006.

[20] ECHEVERRY, L. M.; VILLANUEVA, Y. **Minimizing fuel consumption in orbit transfers using universal variable and particle swarm optimization**. *Revista mexicana de astronomía y astrofísica*, 55:177 – 184, 00 2019.

[21] ESTEBAN, M.; LLIBRE, J.; VALLS, C. **The 16th Hilbert problem for discontinuous piecewise isochronous centers of degree one or two separated by a straight line**. *Chaos*, 31(4):Paper No. 043112, 18, 2021.

[22] EUZÉBIO, R. D.; JUCÁ, J. S. **Limit sets of discontinuous vector fields on two-dimensional manifolds**. *J. Nonlinear Sci.*, 32(1):Paper No. 18, 30, 2022.

[23] EUZÉBIO, R. D.; LLIBRE, J. **On the number of limit cycles in discontinuous piecewise linear differential systems with two pieces separated by a straight line**. *J. Math. Anal. Appl.*, 424(1):475–486, 2015.

[24] EUZÉBIO, R. D.; LLIBRE, J. **Zero-Hopf bifurcation in a Chua system**. *Nonlinear Anal. Real World Appl.*, 37:31–40, 2017.

[25] EUZÉBIO, R. D.; LLIBRE, J.; VIDAL, C. **Zero-Hopf bifurcation in the FitzHugh-Nagumo system**. *Math. Methods Appl. Sci.*, 38(17):4289–4299, 2015.

[26] FILIPPOV, A. F. **Differential equations with discontinuous righthand sides**, volume 18 de **Mathematics and its Applications (Soviet Series)**. Kluwer Academic Publishers Group, Dordrecht, 1988. Translated from the Russian.

[27] FREIRE, E.; ORDÓÑEZ, M.; PONCE, E. **Bifurcations from a center at infinity in 3D piecewise linear systems with two zones**. *Phys. D*, 402:132280, 11, 2020.

[28] FREIRE, E.; PONCE, E.; RODRIGO, F.; TORRES, F. **Bifurcation sets of continuous piecewise linear systems with two zones**. *Internat. J. Bifur. Chaos Appl. Sci. Engrg.*, 8(11):2073–2097, 1998.

[29] FREIRE, E.; PONCE, E.; TORRES, F. **Canonical discontinuous planar piecewise linear systems**. *SIAM J. Appl. Dyn. Syst.*, 11(1):181–211, 2012.

[30] FREIRE, E.; PONCE, E.; TORRES, F. **A general mechanism to generate three limit cycles in planar Filippov systems with two zones**. *Nonlinear Dynam.*, 78(1):251–263, 2014.

[31] GIANNAKOPOULOS, F.; PLIETE, K. **Planar systems of piecewise linear differential equations with a line of discontinuity**. *Nonlinearity*, 14(6):1611–1632, 2001.

[32] GOMIDE, O. M. L.; TEIXEIRA, M. A. **On structural stability of 3D Filippov systems: a semi-local approach**. *Math. Z.*, 294(1-2):419–449, 2020.

[33] GOUVEIA, M. R. A.; LLIBRE, J.; NOVAES, D. D. **On limit cycles bifurcating from the infinity in discontinuous piecewise linear differential systems**. *Appl. Math. Comput.*, 271:365–374, 2015.

[34] HIRSCH, M. W. **Differential topology**, volume 33 de **Graduate Texts in Mathematics**. Springer-Verlag, New York, 1994. Corrected reprint of the 1976 original.

[35] HUAN, S.-M.; YANG, X.-S. **On the number of limit cycles in general planar piecewise linear systems**. *Discrete Contin. Dyn. Syst.*, 32(6):2147–2164, 2012.

[36] HUAN, S.-M.; YANG, X.-S. **Existence of limit cycles in general planar piecewise linear systems of saddle-saddle dynamics**. *Nonlinear Anal.*, 92:82–95, 2013.

[37] HUAN, S.-M.; YANG, X.-S. **On the number of limit cycles in general planar piecewise linear systems of node-node types**. *J. Math. Anal. Appl.*, 411(1):340–353, 2014.

[38] JEFFREY, M. R. **Hidden dynamics**. Springer, Cham, 2018. The mathematics of switches, decisions and other discontinuous behaviour.

[39] JOHNSON, C. R. **Positive definite matrices**. *Amer. Math. Monthly*, 77:259–264, 1970.

[40] KUZNETSOV, N. V.; KUZNETSOVA, O. A.; LEONOV, G. A. **Visualization of four normal size limit cycles in two-dimensional polynomial quadratic system**. *Differ. Equ. Dyn. Syst.*, 21(1-2):29–34, 2013.

[41] LEONOV, G. A.; KUZNETSOV, N. V. **Hidden attractors in dynamical systems. From hidden oscillations in Hilbert-Kolmogorov, Aizerman, and Kalman problems to hidden chaotic attractor in Chua circuits**. *Internat. J. Bifur. Chaos Appl. Sci. Engrg.*, 23(1):1330002, 69, 2013.

[42] LI, L. **Three crossing limit cycles in planar piecewise linear systems with saddle-focus type**. *Electron. J. Qual. Theory Differ. Equ.*, p. No. 70, 14, 2014.

[43] LI, S.; LLIBRE, J. **Phase portraits of continuous piecewise linear Liénard differential systems with three zones**. *Chaos Solitons Fractals*, 120:149–157, 2019.

[44] LI, S.; LLIBRE, J. **Phase portraits of planar piecewise linear refracting systems: focus-saddle case**. *Nonlinear Anal. Real World Appl.*, 56:103153, 11, 2020.

[45] LI, S.; LLIBRE, J. **Phase portraits of planar piecewise linear refracting systems: focus-saddle case**. *Nonlinear Anal. Real World Appl.*, 56:103153, 11, 2020.

[46] LIMA, E. L. **Curso de análise. Vol. 2**, volume 13 de **Projeto Euclides [Euclid Project]**. Instituto de Matemática Pura e Aplicada, Rio de Janeiro, 1981.

[47] LLIBRE, J.; TEIXEIRA, M. A.; TORREGROSA, J. **Lower bounds for the maximum number of limit cycles of discontinuous piecewise linear differential systems with a straight line of separation**. *Internat. J. Bifur. Chaos Appl. Sci. Engrg.*, 23(4):1350066, 10, 2013.

[48] LLIBRE, J.; NOVAES, D. D.; TEIXEIRA, M. A. **Limit cycles bifurcating from the periodic orbits of a discontinuous piecewise linear differentiable center with two zones**. *Internat. J. Bifur. Chaos Appl. Sci. Engrg.*, 25(11):1550144, 11, 2015.

[49] LLIBRE, J.; NOVAES, D. D.; TEIXEIRA, M. A. **Maximum number of limit cycles for certain piecewise linear dynamical systems**. *Nonlinear Dynam.*, 82(3):1159–1175, 2015.

[50] LLIBRE, J.; NOVAES, D. D.; TEIXEIRA, M. A. **On the birth of limit cycles for non-smooth dynamical systems**. *Bull. Sci. Math.*, 139(3):229–244, 2015.

[51] LLIBRE, J.; ORDÓÑEZ, M.; PONCE, E. **On the existence and uniqueness of limit cycles in planar continuous piecewise linear systems without symmetry**. *Nonlinear Anal. Real World Appl.*, 14(5):2002–2012, 2013.

[52] LLIBRE, J.; PONCE, E. **Three nested limit cycles in discontinuous piecewise linear differential systems with two zones**. *Dyn. Contin. Discrete Impuls. Syst. Ser. B Appl. Algorithms*, 19(3):325–335, 2012.

[53] LLIBRE, J.; TEIXEIRA, M. A. **Piecewise linear differential systems without equilibria produce limit cycles?** *Nonlinear Dynam.*, 88(1):157–164, 2017.

[54] LLIBRE, J.; TEIXEIRA, M. A. **Piecewise linear differential systems with only centers can create limit cycles?** *Nonlinear Dynam.*, 91(1):249–255, 2018.

[55] LLIBRE, J.; ZHANG, X. **Limit cycles for discontinuous planar piecewise linear differential systems separated by one straight line and having a center**. *J. Math. Anal. Appl.*, 467(1):537–549, 2018.

[56] MAKARENKOV, O.; LAMB, J. S. W. **Dynamics and bifurcations of nonsmooth systems: a survey**. *Phys. D*, 241(22):1826–1844, 2012.

[57] MARTINET, J. **Sur les singularités des formes différentielles**. *Ann. Inst. Fourier (Grenoble)*, 20(fasc. 1):95–178, 1970.

[58] MARTINS, R. M.; TONON, D. J. **The chaotic behaviour of piecewise smooth differential equations on two-dimensional torus and sphere**. *Dyn. Syst.*, 34(2):356–373, 2019.

[59] PALIS, JR., J.; DE MELO, W. **Introdução aos sistemas dinâmicos**, volume 6 de **Projeto Euclides [Euclid Project]**. Instituto de Matemática Pura e Aplicada, Rio de Janeiro, 1978.

[60] PEIXOTO, M. M. **Structural stability on two-dimensional manifolds**. *Topology*, 1:101–120, 1962.

[61] PEIXOTO, M. M. **Structural stability on two-dimensional manifolds. A further remark**. *Topology*, 2:179–180, 1963.

[62] PERKO, L. **Differential equations and dynamical systems**, volume 7 de **Texts in Applied Mathematics**. Springer-Verlag, New York, third edition, 2001.

[63] POINCARÉ, H. **Mémoire sur les courbes définies par les équations différentielles (i)**. *Journal de Mathématiques Pures et Appliquées*, 7:375–422, 1881.

[64] ROBINSON, C. **Dynamical systems**. Studies in Advanced Mathematics. CRC Press, Boca Raton, FL, 1995. Stability, symbolic dynamics, and chaos.

[65] SHAFAREVICH, I. R. **Basic algebraic geometry**. Springer Study Edition. Springer-Verlag, Berlin-New York, 1977. Translated from the Russian by K. A. Hirsch, Revised printing of Grundlehren der mathematischen Wissenschaften, Vol. 213, 1974.

[66] SIMPSON, D. J. W. **Bifurcations in piecewise-smooth continuous systems**, volume 70 de **World Scientific Series on Nonlinear Science. Series A: Monographs and Treatises**. World Scientific Publishing Co. Pte. Ltd., Hackensack, NJ, 2010.

[67] SOTOMAYOR, J.; TEIXEIRA, M. A. **Regularization of discontinuous vector fields**. In: *International Conference on Differential Equations (Lisboa, 1995)*, p. 207–223. World Sci. Publ., River Edge, NJ, 1998.

[68] SOTOMAYOR, J. **Lições de equações diferenciais ordinárias**, volume 11 de **Projeto Euclides [Euclid Project]**. Instituto de Matemática Pura e Aplicada, Rio de Janeiro, 1979.

[69] SOTOMAYOR, J. **Curvas definidas por equações diferenciais no plano**. 13th Brazilian Mathematics Colloquium. Instituto de Matemática Pura e Aplicada, Conselho Nacional de Desenvolvimento Científico e Tecnológico, Rio de Janeiro, 1981.

[70] SOTOMAYOR, J.; GARCIA, R. **Structural stability of piecewise-linear vector fields**. *J. Differential Equations*, 192(2):553–565, 2003.

[71] TAKENS, F. **Singularities of vector fields**. *Inst. Hautes Études Sci. Publ. Math.*, 43:47–100, 1974.

[72] TANG, Y. **Global dynamics and bifurcation of planar piecewise smooth quadratic quasi-homogeneous differential systems**. *Discrete Contin. Dyn. Syst.*, 38(4):2029–2046, 2018.

[73] VÁRKONYI, P. L.; OR, Y. **Lyapunov stability of a rigid body with two frictional contacts**. *Nonlinear Dynam.*, 88(1):363–393, 2017.

[74] VILLANUEVA, Y.; LLIBRE, J.; EUZÉBIO, R. **Limit cycles of generic piecewise center-type vector fields in $\mathbb{R}^3$ separated by either one plane or by two parallel planes**. *Bull. Sci. Math.*, 179:Paper No. 103173, 14, 2022.

[75] WALCHER, S. **On the Poincaré problem**. *J. Differential Equations*, 166(1):51–78, 2000.

[76] YAKOVENKO, S. **A geometric proof of the Bautin theorem**. In: *Concerning the Hilbert 16th problem*, volume 165 de **Amer. Math. Soc. Transl. Ser. 2**, p. 203–219. Amer. Math. Soc., Providence, RI, 1995.

[77] ZBIB, H. M. **On the mechanics of large inelastic deformations: kinematics and constitutive modeling**. *Acta Mech.*, 96(1-4):119–138, 1993.

APPENDIX A

Conclusions

We have presented a robust global analysis on the dynamics of inelastic piecewise smooth differential equations with some curves and surfaces as discontinuity region, the classification of stability classes and limit sets thought canonical regions was made. Also several theorems about asymptotic stability were analyzed. Finally, we studied and found the Hilbert's number for generic center-type PSVF in $\mathbb{R}^3$. As future work we will extend the classification of canonical regions to $\mathbb{R}^3$, due to Poincaré's compactification and new theories from Lie derivatives. Make the analysis of global dynamics of other kind of differential systems, where can exist different conditions for the tangency points and T-singularities, structural stability and also some applications in weather predictions, epidemiology, electromagnetism and general relativity. The main future goal will be to extend the results of the Chapter 4 to $\mathbb{R}^3$ and then to $\mathbb{R}^n$.

APPENDIX B

Algorithm

The following algorithm was executed in MATHEMATICA and shows step by step the procedures for proving the first part of the Theorem 6.1.1, it is so useful for students who are starting in the theory of PSVF.

Algorithm B.1: Method for limit cycles with a continuous condition

Data: Piecewise Smooth Differential system $N(\mathbf{x})$, see equation (6-3).

Result: Global Limit cycles.

1 Establish the center-type differential system which will be our template.

2 Make two affine transformations over the system for getting the two classical center-type vector fields, the first integrals and complete the PVF.

3 Get some parameters in terms of other using the continuous equations in the plane $x = 0$.

4 Look for the points of the limit cycles using the compatibility equations which come from the first integral at the plane $x = 0$.

B.1 Implementation

(*This differential system in $\mathbb{R}^3$ has a global center at the equilibrium point $(0,0,z_0)$ of each plane $z = z_0$. So all its orbits are periodic except the points of the z - axis which are equilibrium points. We denote this differential system as the periodic system.*)

$xp = -y;\ yp = x;\ zp = 0;$

(*Two independent first integral of the periodic system are*)

$H1 = x^2 + y^2;\ H2 = z;$

(*We will do to this system a general affine change of variables given by*)

$aa = \{x- > a1X + a2Y + a3Z + a4,\ y- > b1X + b2Y + b3Z + b4,\ z- > c1X + c2Y + c3Z + c4\};$

(*with of course*)

$det = a3b2c1 - a2b3c1 - a3b1c2 + a1b3c2 + a2b1c3 - a1b2c3;$

(*is not zero.*)

$Solve[\{x == a1X + a2Y + a3Z + a4,\ y == b1X + b2Y + b3Z + b4,\ z == c1X + c2Y + c3Z + c4\}, \{X, Y, Z\}]$

(*The initial system doing a rescaling of the independent variable after the affine change of variables given by aa becomes*)

$bb = x- > xp, y- > yp, z- > zp;$

$Xp = Collect[(-b3c2x + b2c3x + a3c2y - a2c3y - a3b2z + a2b3z/.bb)/.aa, X, Y, Z, Factor]$

$Yp = Collect[(b3c1x - b1c3x - a3c1y + a1c3y + a3b1z - a1b3z/.bb)/.aa, X, Y, Z, Factor]$

$Zp = Collect[(-b2c1x + b1c2x + a2c1y - a1c2y - a2b1z + a1b2z/.bb)/.aa, X, Y, Z, Factor]$

(*Two independent first integrals of the differential system (Xp, Yp, Zp) are*)

$F1[X_, Y_, Z_] = H1/.aa$

$F2[X_, Y_, Z_] = H2/.aa$

(*The following is the continuous condition for the piecewise differential system*)

$ba = X- > 0, Y- > Y, Z- > Z;$

$Xpp[X_, Y_, Z_] = Xp/.ba$

$Ypp[X_, Y_, Z_] = Yp/.ba$

$Zpp[X_, Y_, Z_] = Zp/.ba$

(*Now we complete the PVF with the other vector field*)

$cc = \{a1- > \alpha 1, a2- > \alpha 2, a3- > \alpha 3, a4- > \alpha 4, b1- > \beta 1, b2- > \beta 2, b3- > \beta 3, b4- > \beta 4, c1- > \gamma 1, c2- > \gamma 2, c3- > \gamma 3, c4- > \gamma 4\};$

$$det1 = det/.cc$$

$$XP = Xp/.cc$$

$$YP = Yp/.cc$$

$$ZP = Zp/.cc$$

(*Two independent first integrals of the differential system (XP, YP, ZP) are*)

$$G1[X,Y,Z] = F1[X,Y,Z]/.cc$$

$$G2[X,Y,Z] = F2[X,Y,Z]/.cc$$

(*We need to put the continuous condition*)

$$XPP[X,Y,Z] = XP/.ba$$

$$YPP[X,Y,Z] = YP/.ba$$

$$ZPP[X,Y,Z] = ZP/.ba$$

(*Thus, we can isolate some parameters using the equations of the continuous condition*)

$$eq1 = Xpp[0,Y0,Z0] - XPP[0,Y0,Z0]$$

$$eq11 = Coefficient[eq1,Y0]$$

$$eq12 = Coefficient[eq1,Z0]$$

$$eq13 = Factor[eq1 - (eq11 * Y0) - (eq12 * Z0)]$$

$$eq2 = Ypp[0,Y0,Z0] - YPP[0,Y0,Z0]$$

$$eq21 = Coefficient[eq2,Y0]$$

$$eq22 = Coefficient[eq2,Z0]$$

$$eq23 = Factor[eq2 - (eq21 * Y0) - (eq22 * Z0)]$$

$$eq3 = Zpp[0,Y0,Z0] - ZPP[0,Y0,Z0]$$

$$eq31 = Coefficient[eq3,Y0]$$

$$eq32 = Coefficient[eq3,Z0]$$

$$eq33 = Factor[eq3 - (eq31 * Y0) - (eq32 * Z0)]$$

(*Then we form the following algebraic system*)

$$eq = \{eq11, eq12, eq13, eq21, eq22, eq23, eq31, eq32, eq33\};$$

(*And we can find seven parameters*)

$$Solve[eq == 0, b4, b1, a1, b2, a2, \alpha 1, \beta 1]$$

(*Finally we have the system of the first integrals at the switching manifold*)

$$e1 = F1[0, Y0, Z0] - F1[0, Y1, Z1]$$

$$e2 = F2[0, Y0, Z0] - F2[0, Y1, Z1]$$

$$e3 = G1[0, Y0, Z0] - G1[0, Y1, Z1]$$

$$e4 = G2[0, Y0, Z0] - G2[0, Y1, Z1]$$

(*therefore we find the unique solution*)

$$Y1 -> Y0,\ Z1 -> Z0.$$